Biology Dissertations
Department of Biology

10-1-2007

Neuronal Growth Cone Dynamics are Regulated by a Nitric Oxide-Initiated Second Messenger Pathway.

Kristy Welshhans

Recommended Citation

NEURONAL GROWTH CONE DYNAMICS ARE REGULATED BY A

NITRIC OXIDE-INITIATED SECOND MESSENGER PATHWAY

by

KRISTY WELSHHANS

Under the direction of Vincent Rehder

ABSTRACT

During development, neurons must find their way to and make connections with their appropriate targets. Growth cones are dynamic, motile structures that are integral to the establishment of appropriate connectivity during this wiring process. As growth cones migrate through their environment, they encounter guidance cues that direct their migration to their appropriate synaptic targets. The gaseous messenger nitric oxide (NO), which diffuses across the plasma membrane to act on intracellular targets, is a signaling molecule that affects growth cone motility. However, most studies have examined the effects of NO on growth cone morphology when applied in large concentrations and to entire cells. In addition, the intracellular second messenger cascade activated by NO to bring about these changes in growth cone morphology is not well understood. Therefore, this dissertation addresses the effects that a spatially- and temporally-restricted application of physiological amounts of NO can have on individual growth cone morphology, on the second messenger pathway that is activated by this application of

NO, and on the calcium cascades that result and ultimately affect growth cone morphology.

Helisoma trivolvis, a pond snail, is an excellent model system for this type of research because it has a well-defined nervous system and cultured neurons form large growth cones. In the present study, local application of NO to *Helisoma trivolvis* B5 neurons results in an increase in filopodial length, a decrease in filopodial number, and an increase in the intracellular calcium concentration ($[Ca^{2+}]_i$). In B5 neurons, the effects of NO on growth cone behavior and $[Ca^{2+}]_i$ are mediated via sGC, protein kinase G, cyclic adenosine diphosphate ribose, and ryanodine receptor-mediated intracellular calcium release. This study demonstrates that neuronal growth cone pathfinding *in vitro* is affected by a single spatially- and temporally-restricted exposure to NO. Furthermore, NO acts via a second messenger cascade, resulting in a calcium increase that leads to cytoskeletal changes. These results suggest that NO may be a signal that promotes appropriate pathfinding and/or target recognition within the developing nervous system. Taken together, these data indicate that NO may be an important messenger during the development of the nervous system *in vivo*.

NEURONAL GROWTH CONE DYNAMICS ARE REGULATED BY A

NITRIC OXIDE-INITIATED SECOND MESSENGER PATHWAY

by

KRISTY WELSHHANS

A Dissertation Submitted in Partial Fulfillment of the Requirements for the Degree of

Doctor of Philosophy

in the College of Arts and Sciences

Georgia State University

2007

NEURONAL GROWTH CONE DYNAMICS ARE REGULATED BY A

NITRIC OXIDE-INITIATED SECOND MESSENGER PATHWAY

by

KRISTY WELSHHANS

Major Professor: Vincent Rehder

Committee: Sarah Pallas

                  William Walthall

Electronic Version Approved:

Office of Graduate Studies

College of Arts and Sciences

Georgia State University

December 2007

Acknowledgements

There are numerous people who have supported me throughout my doctoral work, from scientists and colleagues to family and friends.

First and foremost, I thank my advisor, Dr. Vincent Rehder, for his unwavering support and guidance. My time in your laboratory has transformed me from an unknowing experimenter into a true scientist. I will always look to you as an example of how to be a mentor and a researcher. Thank you so much!

Secondly, I thank my other committee members, Drs. Sarah Pallas and Bill Walthall. Your questions have resulted in my thinking "outside of the box" and allowed me to see the bigger picture in my research. I truly appreciate your guidance throughout the doctoral process.

I also thank my fellow students at Georgia State University. I thank the Rehder lab as a whole, but especially appreciate the friendship of Matt Geddis and Karine Tornieri. Matt, thank you for answering my five million questions and teaching me how to persevere in my early years as a PhD student. Karine, thank you for always being there to listen to me when I needed someone with whom to discuss my latest results or rant to about the current state of affairs. Thank you to Ed Rodgers and Karine Tornieri for taking the time

to eat lunch with me every week. Those lunches provided me with much-needed moments of joviality and friendship.

Finally, I thank my family and friends. My Dad and Mom, Richard & Claudia Welshhans, and sister, Jennifer Welshhans, for always being there for me and believing in me. My friend, Connie Crowe, for having confidence that I could accomplish this goal, but teaching me to have fun along the way. Most importantly, my husband, Aaron Jasnow, who has been there for me in every aspect of this endeavor. We started our journey at the time of your defense, and now we continue it together through mine. I can't imagine making it through these past 5 years without you. You are an inspiration to me, not only as a scientist, but also in your everyday actions. Thank you.

TABLE OF CONTENTS

LIST OF TABLES

Chapter 5

LIST OF FIGURES

LIST OF ABBREVIATIONS

ADF	actin depolymerizing factor
BDNF	brain derived neurotrophic factor
β-gal	β-galactosidase
Ca^{2+}	Calcium
$[Ca^{2+}]_i$	intracellular calcium concentration
Ca^{2+}/CaM	calcium/calmodulin
cADPR	cyclic adenosine diphosphate ribose
CaMKII	Ca^{2+}-calmodulin-dependent protein kinase II
cAMP	cyclic adenosine monophosphate
CICR	calcium-induced calcium release
cGMP	cyclic guanosine monophosphate
CMV	cytomegalovirus
CNG	cyclic nucleotide gated
CNS	central nervous system
CytoB	cytochalasin B
EGFP	enhanced green fluorescent protein
eNOS	endothelial nitric oxide synthase
EGF RTK	epidermal growth factor receptor tyrosine kinase
ER	endoplasmic reticulum
ET	esophageal nerve trunk

GFP	green fluorescent protein
iNOS	inducible nitric oxide synthase
$InsP_3Rs$	inositol triphosphate receptors
KCl	potassium chloride
L-15	Leibovitz's L-15 medium
NGF	nerve growth factor
Nic	nicotinamide
nNOS	neuronal nitric oxide synthase
NOS	nitric oxide synthase
NO	nitric oxide
PDEs	phosphodiesterases
PDEIII	phosphodiesterase III
PI-3K	phosphatidylinositol-3-kinase
PKA	protein kinase A
PKG	protein kinase G
PKI	myristoylated PKA inhibitor 14-22
ROCK	Rho kinase
RyR	ryanodine receptor
sGC	soluble guanylyl cyclase
TG	thapsigargin
TRP	transient receptor potential

Chapter 1: General Introduction

Neuronal development is an essential period encompassing the processes of proliferation, differentiation, neuronal migration, growth cone formation and neurite elongation, and synaptogenesis. During this period, a neuron will establish itself from a precursor cell and then it will form growth cones and extend neurites (as reviewed in Sanes *et al.*, 2000; Escuin & Georges-Labouesse, 2007). The growth cone will pathfind to its target region, identify its appropriate cellular target, and finally, form a synapse on that target. These steps ultimately define the wiring connectivity of the nervous system and as such, a defect in any one of these steps can lead to inappropriate connections or lack of connectivity, both of which can result in a number of disease states (Kenwrick *et al.*, 2000; Fan & Simard, 2002; Antar *et al.*, 2006). Therefore, the study of how neurons find and make connections with their appropriate targets is essential. Although much is known about the extracellular cues that affect growth cone navigation, much less is known about the intracellular pathways that are activated by these cues. Thus, understanding how growth cone behavior is affected by extracellular cues, as well as the intracellular pathways that lead to those changes, is fundamental to elucidating the mechanisms underlying growth cone pathfinding during development.

Growth cones are the essential pathfinding structures of developing neurons.

The growth cone is a unique structure that tips a neurite and allows for proper pathfinding and navigation in the developing and regenerating nervous system. There are a number of factors, or guidance cues, that direct the migration of the growth cone by activating signaling cascades that lead to changes in the cytoskeleton, thereby "guiding" the growth

cone. The initial formation of the neurite and the growth cone and its forward movement is dependent on the presence of substrate-bound factors and soluble trophic factors (da Silva & Dotti, 2002; Escuin & Georges-Labouesse, 2007). In *Helisoma trivolvis*, it has been shown that the ability to form growth cones is an intrinsic property of the neuron, because a growth cone will form on the axon stump of a neuron placed into conditioned medium deprived-culture, however, the growth cone will not exhibit neurite extension (Williams & Cohan, 1994). This study suggests that the formation of the growth cone is an intrinsic property of the neuron; however, growth factors are required for neuritogenesis and growth cone motility.

The neuronal growth cone

Growth cones are motile, pathfinding structures that are essential for sensing and responding to various cues that neurons encounter in their environment. Growth cones were first described and drawn in detail by Ramón y Cajal in 1899 (Ramón y Cajal, 1899, as translated by Pasik & Pasik, 1999). He even had the foresight to anticipate that these growth cones would have "exquisite chemical sensitivity" (Ramón y Cajal, 1899, as translated by Pasik & Pasik, 1999). From extensive research encompassing numerous studies, we are now fully aware that the appropriate wiring of the nervous system is dependent on the growth cone and its ability to sense and respond to the chemicals cues that are found within the growth cone's surrounding environment.

There are three major components of the growth cone (Figure 1.1): the central domain, which is the thickened central region made up of mainly microtubules;
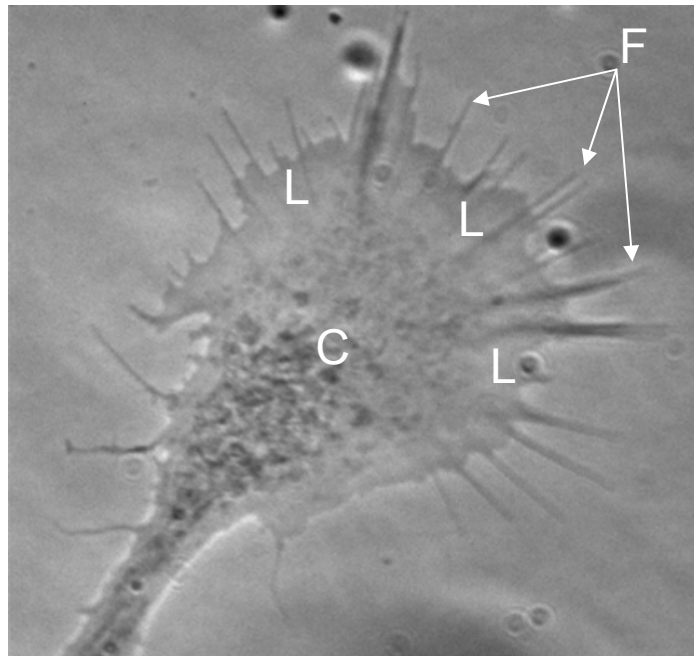
Figure 1.1: The neuronal growth cone. Phase contrast image of a *Helisoma trivolvis* B5 growth cone. There are 3 major components to the growth cone: the central domain (indicated with a "C"), the lamellipodial region ("L"), and filopodia ("F"; the arrows point to representative filopodia).

the lamellipodia, which is the peripheral region that surrounds the central domain and contains an actin meshwork; and filopodia, which are the finger-like extensions that extend out from the central domain and through the lamellipodia and are composed of actin bundles (Suter & Forscher, 2000; Bamburg, 2003). Filopodia have been shown to be autonomous units that contain ion channels, as well as receptors for various guidance molecules (Davenport *et al.*, 1993; Kater & Rehder, 1995; Gomes *et al.*, 2006). These receptors allow for detection of cues in advance of the growth cone proper, which further allows for highly regulated directional pathfinding.

Growth cone guidance

Growth cones will change the length and number of their filopodia in response to various guidance cues that they encounter during pathfinding (for review see Huber *et al.*, 2003). When a growth cone changes the length of its filopodia, we term this a change in the "sensory radius" of the growth cone. The sensory radius is the area within which a growth cone can detect cues at any given point in time. For example, if a filopodia encounters a repulsive cue, it may shorten its filopodia on the side where it senses the cue, which results in a decrease in the sensory radius of the growth cone. Likewise, the opposite is also true, growth cones will increase the length of their filopodia in order to be able to sense and respond to cues in a much larger area, which results in an increase in the sensory radius of the growth cone. Changes in the sensory radius of the growth cone translate into behaviors that are necessary for the growth cone to pathfind appropriately and make connections with its correct target.

There are numerous guidance cues that have been demonstrated to affect neuronal pathfinding both *in vitro* and *in vivo*. These guidance cues fall into two main categories: bound factors, such as cell adhesion molecules, and diffusible molecules, such as trophic factors. Cell adhesion molecules include the integrin, cadherin, and immunoglobulin families and they mediate interactions either with the extracellular matrix or with other cells (Huber *et al.*, 2003; Escuin & Georges-Labouesse, 2007). One cell adhesion molecule, L1, is involved in the processes of fasciculation, neuritogenesis, and axon outgrowth (as reviewed in Kenwrick *et al.*, 2000; Kiryushko *et al.*, 2004; Maness & Schachner, 2007). In addition, mutations in the gene encoding L1 can result in mental retardation and hydrocephalus, thus highlighting the essential role of guidance cues for the appropriate wiring of the nervous system.

Some common and well-studied trophic molecules are the netrins, semaphorins, and nerve growth factor (NGF). These chemotrophic factors can serve as attractants or repellants depending on their type. Furthermore, in some cases the intracellular messengers present in the affected growth cone determine the response of the growth cone to the trophic factor. For example, netrin-1 has been shown to serve as either an attractive or a repulsive guidance cue, dependent on the ratio of cyclic nucleotide signaling (cAMP to cGMP) within the growth cone (Nishiyama *et al.*, 2003). A high cAMP/cGMP ratio results in attractive turning due to signaling through the netrin-1 receptor, DCC, and calcium influx through L-type calcium channels, whereas a low cAMP/cGMP ratio results in repulsive turning due to blockage of this calcium influx. Semaphorins are a large family of molecules that can also have varied effects on growth

cone dynamics. For example, Sema3A is an inhibitor of neurite outgrowth and often causes growth cone collapse in a variety of cell types, whereas Sema3C acts as an attractive cue (for review see Goshima *et al.*, 2002). NGF is a neurotrophin that signals via p75 and TrkA receptors, and has been shown to act as a chemoattractant (for review see Huber *et al.*, 2003). Additionally, there are numerous other guidance cues that influence growth cone pathfinding, including brain derived neurotrophic factor, myelin associated glycoprotein, ephrins, and a variety of cell adhesion molecules (Huber *et al.*, 2003; Henley & Poo, 2004; Wen & Zheng, 2006).

It is important to note that the effect of guidance cues on growth cone motility is not limited simply to attraction and repulsion of growing neurites. Growth factors can also have a variety of other effects on the growth cone cytoskeleton, including branching, fasciculation and growth cone collapse. Furthermore, these effects directly affect the wiring of the nervous system. For example, an increase or decrease in axonal branching can directly alter the number of synapses formed within an area. Netrin-1 and a semaphorin, Sema3A, regulate the branching of cortical axons, resulting in an increase or decrease in branching, respectively (Dent *et al.*, 2004). Fasciculation is a process that results in the appropriate pathfinding of the neurites from "follower" neurons. Semaphorins play an essential role in the fasciculation of axons, in that overexpression of Sema1a in *Drosophila* leads to hyper-fasciculation of photoreceptor axons, whereas loss of Sema3A signaling in mouse lateral motor column spinal neurons leads to defasciculation (Huber *et al.*, 2005; Cafferty *et al.*, 2006). Growth cone collapse is necessary to prevent growth cones from entering inappropriate tissues or tissue regions;

additionally, growth cone collapse serves as a mechanism to allow for the formation of a single terminal growth cone (Knobel *et al.*, 1999). Complete collapse of growth cones is mediated via a number of signaling molecules, including Slit2, ephrinA5, Sema3A and nitric oxide (Luo *et al.*, 1993; Ernst *et al.*, 2000; Trimm & Rehder, 2004; Wong *et al.*, 2004). Overall, these studies demonstrate that guidance cue-induced changes in specific facets of growth cone motility can regulate numerous aspects of neuronal connectivity.

Environmental cues that growth cones encounter during development are translated into cytoskeletal changes via second messenger cascades.

When a growth cone encounters a guidance cue during migration, that cue will bind to a receptor and activate a signaling cascade that ultimately results in changes in the growth cone cytoskeleton. There are numerous second messengers that play roles in this signaling cascade; however, they all ultimately appear to converge on the two major cytoskeletal polymeric proteins in the growth cone, actin and tubulin. There are a number of common and well-studied intracellular pathways that lead to changes in the cytoskeleton. For example, some of the most common guidance cues, the neurotrophins (such as NGF and brain derived neurotrophic factor) bind to tyrosine kinase receptors. After these neurotrophins bind to either p75 or Trk receptors, they activate intracellular signaling cascades, including molecules such as PI-3K and the Rho GTPases, which include Rac1, Cdc42, and RhoA (Dontchev & Letourneau, 2003; Huber *et al.*, 2003). Another common guidance cue, semaphorin 3A, affects growth cone motility by binding to neuropilin-1/plexin-A1 and activating a signaling cascade involving the Rho GTPase,

Rac1 (Vastrik *et al.*, 1999; Turner *et al.*, 2004; Woo & Gomez, 2006). Subsequently, these Rho GTPases affect cytoskeletal dynamics by being integral members of a signaling cascade that leads to direct regulation of actin dynamics through proteins such as cofilin, myosin, and the Arp2/3 complex (for review see Huber *et al.*, 2003).

Regulation of growth cone guidance by calcium

One extremely important second messenger that is involved in the regulation of growth cone morphology in a variety of species is calcium. The intracellular calcium concentration within cells can be modulated through two major pathways, either calcium influx across the plasma membrane or calcium release from intracellular calcium stores (Berridge *et al.*, 2003). Calcium influx across the plasma membrane of growth cones is thought to be mainly carried either through L-type voltage gated calcium channels or transient receptor potential (TRP) channels. L-type voltage gated calcium channels are present in growth cone membranes and have been demonstrated to regulate growth cone motility, including outgrowth rate and turning (Ohbayashi *et al.*, 1998; Nishiyama *et al.*, 2003; Tang *et al.*, 2003). Calcium influx through a particular type of TRP channel, TRPC, has been shown to regulate growth cone turning and morphology (Greka *et al.*, 2003; Li *et al.*, 2005; Shim *et al.*, 2005; Wang & Poo, 2005).

The major pool of stored intracellular calcium is in the endoplasmic reticulum (ER), in which calcium is weakly buffered by proteins such as calreticulin and calsequestrin (Berridge *et al.*, 2003; Verkhratsky, 2005). However, calcium stores also exist in other intracellular compartments, such as the mitochondria and nucleus (Rizzuto

et al., 2000; Carafoli, 2004; Marchenko & Thomas, 2006). Calcium release from intracellular calcium stores occurs through two main receptor-mediated channels, inositol triphosphate receptors (InsP$_3$Rs) and ryanodine receptors (RyRs) (Berridge *et al.*, 2003; Verkhratsky, 2005). InsP$_3$Rs are activated by binding of the second messenger IP$_3$. IP$_3$ is formed via a signaling cascade that involves activation of phospholipase C by G-proteins or receptor tyrosine kinases. Phospholipase C subsequently cleaves phosphatidylinositol 4,5 bisphosphate into diacylglycerol and IP$_3$. IP$_3$ will then bind to InsP$_3$Rs on the endoplasmic membrane and result in the release of calcium from intracellular stores. Ryanodine receptors (RyRs) are activated by the binding of calcium, and therefore, are usually thought of as mediators of calcium-induced calcium release (CICR). CICR is the mechanism through which a calcium elevation within the cytosol (e.g. IP$_3$ binding to InsP$_3$Rs) leads to a further calcium elevation via activation of other calcium release channels (e.g. calcium binding to RyRs). Cyclic adenosine diphosphate ribose (cADPR) is an additional second messenger molecule that facilitates release of calcium through the RyR. cADPR can cause release of calcium directly in some cell types (Koshiyama *et al.*, 1991; Thorn *et al.*, 1994; Mothet *et al.*, 1998), whereas it potentiates calcium release initiated through other sources in other cell types (De Flora *et al.*, 1996; Hashii *et al.*, 2000). These studies suggest that calcium release from intracellular stores can occur in multiple ways and help shape the calcium dynamics that occur within the cell.

The level of calcium within growth cones directly modulates their behavior. For example, the length of filopodia can be correlated with the intracellular calcium concentration within *Helisoma* growth cones (Rehder & Kater, 1992). The resting

calcium concentration within *Helisoma* neurons is around 100 nM, and interestingly, an increase in calcium as small as 50 nM within *Helisoma* growth cones results in a significant increase in filopodial length, as well as a significant decrease in filopodial number. Additionally, neurite outgrowth in *Helisoma* is dependent on the intracellular calcium concentration, as high concentrations of calcium influx blockers suppress outgrowth, whereas low concentrations enhance the outgrowth rate (Mattson & Kater, 1987). This study and others have demonstrated that there is an optimal concentration of intracellular calcium that promotes growth cone motility, and increases or decreases from this concentration range lead to reduction or suppression of neurite outgrowth (Kater & Mills, 1991).

Growth cone steering or turning has been shown to be directly related to the gradient of calcium that is set up within the growth cone by external guidance cues. For example, local application of netrin-1 to one side of a growth cone results in a transient gradient of calcium within the growth cone that is higher on the side facing the netrin-1 source; this calcium gradient then leads to attractive turning (Hong *et al.*, 2000). Downstream of calcium, there are a number of effector proteins that have been identified in growth cones as being involved in calcium signaling. Calmodulin and Ca^{2+}-calmodulin-dependent protein kinase II (CaMKII), two effectors that are activated by calcium, are essential for proper growth cone navigation and motility (VanBerkum & Goodman, 1995; Kuhn *et al.*, 1998; Wen *et al.*, 2004). There are numerous other effectors of calcium signaling, including calcineurin, protein kinase C, and myosin II (for review see Henley & Poo, 2004). Taken together, these studies demonstrate that calcium

regulates many aspects of growth cone motility, thereby defining calcium as an integral molecule involved in the formation of connectivity within the nervous system.

Second messenger signaling leads to changes in growth cone morphology and motility

Importantly, all of the aforementioned second messengers converge on downstream targets that regulate actin and microtubules within growth cones. Local changes in filopodia are mediated mainly through changes in actin whereas changes in outgrowth and extension rates are mediated mainly via microtubules; however, the interaction between the two is also important for overall motility (Kalil & Dent, 2005). Therefore, different external guidance cues and their subsequent intracellular signaling pathways lead to various effects on the growth cone due to their action on different cytoskeletal proteins. Although many of these cytoskeletal binding proteins have not been well studied in the growth cone, there is a basis of knowledge about a few actin-binding proteins and microtubule-associated proteins. One major actin-binding protein is actin depolymerizing factor (ADF)/cofilin, which severs and depolymerizes f-actin filaments (for review see Sarmiere & Bamburg, 2004). Interestingly calcium also plays a role in the positive regulation of ADF/cofilin, because calcium/calmodulin activates calcineurin, which is a protein phosphatase that subsequently activates ADF/cofilin (Henley & Poo, 2004). There are also microtubule-associated proteins, such as microtubule-associated protein 2 and Tau, that are regulated by calcium via CaMKII and lead to the stabilization of microtubules (for review see Dehmelt & Halpain, 2004). In addition, microtubules within growth cones can be stabilized by microtubule-associated plus end tracking

proteins, such as CLASP (Lee *et al.*, 2004; Kalil & Dent, 2005). Although it is not completely understood how actin and microtubules within growth cones are regulated and interact with one another, it is known that they are the components that directly translate the intracellular second messenger cascades into cytoskeletal changes. Furthermore, it is these changes in the cytoskeleton that direct growth cones to their appropriate targets and thereby create appropriate connectivity within the nervous system.

The gaseous messenger, nitric oxide, acts as an intercellular messenger during development.

Nitric oxide (NO) is a gas that is produced through the conversion of L-arginine to L-citrulline. The enzyme responsible for this conversion is nitric oxide synthase (NOS), and this enzyme requires the presence of calcium/calmodulin (for review see Alderton *et al.*, 2001). There are three known types of NOS: inducible NOS (iNOS), endothelial NOS (eNOS) and neuronal NOS (nNOS). iNOS is usually found in the immune system, whereas eNOS is found mainly in vascular epithelium, but now has also been found in a number of other cell types, including the nervous system (as reviewed in Li *et al.*, 2002; Mungrue *et al.*, 2003). nNOS is the major form found in the nervous system (as reviewed in Dawson *et al.*, 1998; Alderton *et al.*, 2001).

Modes of action of nitric oxide

There are two widely accepted modes of action of NO, one, the activation of soluble guanylyl cyclase (sGC) and two, s-nitrosylation of proteins (Ahern *et al.*, 2002). In the first mode, NO has been shown to directly bind to the heme group of sGC, which leads to its activation. sGC then converts GTP to cGMP. This pathway can then go on to regulate numerous cellular processes though three major players: phosphodiesterases (PDEs), cyclic nucleotide gated ion channels (CNG) and/or protein kinase G (PKG). In the second mode of action, NO can s-nitrosylate proteins. S-nitrosylation occurs when NO binds to the thiol group on a cysteine, and a s-nitrosothiol results (for review see Hess *et al.*, 2005). Recently, S-nitrosylation has been shown to be a common occurrence that can regulate the function of many proteins, including protein kinases, transcription factors and ion channels. In addition, s-nitrosylation has also been shown to affect filopodial motility of rat retinal ganglion cells (Cheung *et al.*, 2000).

Importance of nitric oxide during development

NOS is essential to proper development of a variety of organisms. In mice, a double knockout of any two NOS isoforms results in significantly decreased viability (Tranguch & Huet-Hudson, 2003). A study in *Drosophila* demonstrates that knocking out NOS (there is only a single isoform of NOS in this species) results in death early in development (Regulski *et al.*, 2004). It is thought that in mammals, NOS knockouts do not reveal the true deficiencies that would follow from total loss of NOS because the

isoform that remains after knockout is upregulated and can compensate somewhat for the loss of the other isoforms.

NO has been shown to have a variety of effects on growth cone and neurite motility *in vitro*, which emphasizes its importance during development. In salamander cone photoreceptors, exogenous application of NO results in an increase of neuritic sprouting, whereas in rod photoreceptors, NO inhibits this sprouting (Zhang *et al.*, 2005). In relation to growth cones, exogenous application of nitric oxide causes collapse of rat dorsal root ganglion neurons, *Xenopus* retinal ganglion neurons, and chick dorsal root ganglion neurons (Hess *et al.*, 1993; Renteria & Constantine-Paton, 1996; Ernst *et al.*, 2000). NO has also been shown to be involved in eliminating a transient ipsilateral retinotectal projection and refining the contralateral retinotectal projection in the chick visual system (Wu *et al.*, 1994; Wu *et al.*, 2001). The importance of NO for proper connectivity has been shown in *Drosophila* and in grasshoppers. If the production of NO is inhibited in *Drosophila* photoreceptors, retinal patterning is disrupted (Gibbs & Truman, 1998). In the grasshopper, inhibition of NOS blocks the migration of a population of midgut neurons (Haase & Bicker, 2003). Overall, these studies demonstrate the importance of NO for regulating a number of essential processes during development.

Previous studies from the Rehder lab have laid the foundation for the current set of experiments. In *Helisoma*, global application of NO donors to B5 neurons results in an increase in filopodial length, a decrease in filopodial number, a decrease in the neurite outgrowth rate and an increase in the intracellular calcium concentration (Van Wagenen & Rehder, 1999; Trimm & Rehder, 2004). In addition, these effects were shown to be

mediated via sGC. Furthermore, it was demonstrated that these effects were specific to the B5 neuron, because the application of NO donors to another *Helisoma* neuron, B19, had no effect on filopodial motility or the intracellular calcium concentration (Van Wagenen & Rehder, 2001). This disparity is due to differences in receptors for NO within these neurons. Using immunocytochemistry, this study demonstrated that the B5 neuron stains for one of the major targets of NO, sGC, whereas the B19 neuron does not.

A study in *Helisoma* has also demonstrated that global application of nitric oxide leads to a slow-down in neurite outgrowth of B5 neurons, showing that NO is a "stop and search" signal for pathfinding growth cones (Trimm & Rehder, 2004). In *Helisoma* B5 neurons, NO binds to sGC and this results in the production of cGMP. Interestingly, the Trimm & Rehder study demonstrated that growth cone dynamics can be correlated with the amount of cGMP within the growth cone. That is, there is an optimal concentration of cGMP within the growth cone that leads to normal outgrowth, whereas decreases from that level slow outgrowth and increases lead to the "stop and search" signal. This "stop and search" behavior may be essential to obtaining appropriate connectivity in *Helisoma*, because it could regulate growth cone morphology *in vivo* when the growth cone is either at a decision point or within the target region.

Helisoma trivolvis as a model system for studying processes that occur during development and regeneration.

Molluscan model systems have helped shape our understanding of nervous system development and function. For example, the squid giant axon provided the first

intracellular recordings from neurons and allowed for an understanding of the ionic basis of the action potential (Sattelle & Buckingham, 2006). The neural basis for a variety of behaviors, as well as information on learning and memory, has come from studies in *Aplysia* (Elliott & Susswein, 2002; Sattelle & Buckingham, 2006). This dissertation employs the pond snail, *Helisoma trivolvis*, as a model system for studying growth cone behavior. Molluscan nervous systems are composed of ganglia, which are collections of neurons that control various functions. In *Helisoma*, the major ganglion of interest for the present investigation is the buccal ganglion, which controls feeding in these animals (Figure 1.2). There are two neurons in particular that have been well-studied, termed B5 and B19. The B5 neuron has two projections, both of which exit out of the esophageal nerve trunk (for review see Berdan *et al.*, 1989). From there, the major projection exits out of the gastric nerve to innervate the muscle of the esophagus whereas the minor projection exits the dorsobuccal nerve to innervate the buccal mass (Murphy & Kater, 1980a; Berdan *et al.*, 1990). The buccal mass is a muscle structure involved in many feeding-related behaviors. The B5 neuron is a cholinergic motorneuron and is responsive to exogenous application of glutamate (Haydon, 1988; Berdan *et al.*, 1989; Haydon & Zoran, 1989). The major projection of the B19 neuron innervates the buccal mass, specifically the supralateral radular tensor muscles within that structure (Kater, 1974; Berdan *et al.*, 1989). The B19 neuron is a cholinergic motorneuron that shows changes in growth cone morphology in response to serotonin and dopamine (Haydon *et al.*, 1984; McCobb *et al.*, 1988; Berdan *et al.*, 1989; Zoran *et al.*, 1989). Additionally, when B5 and
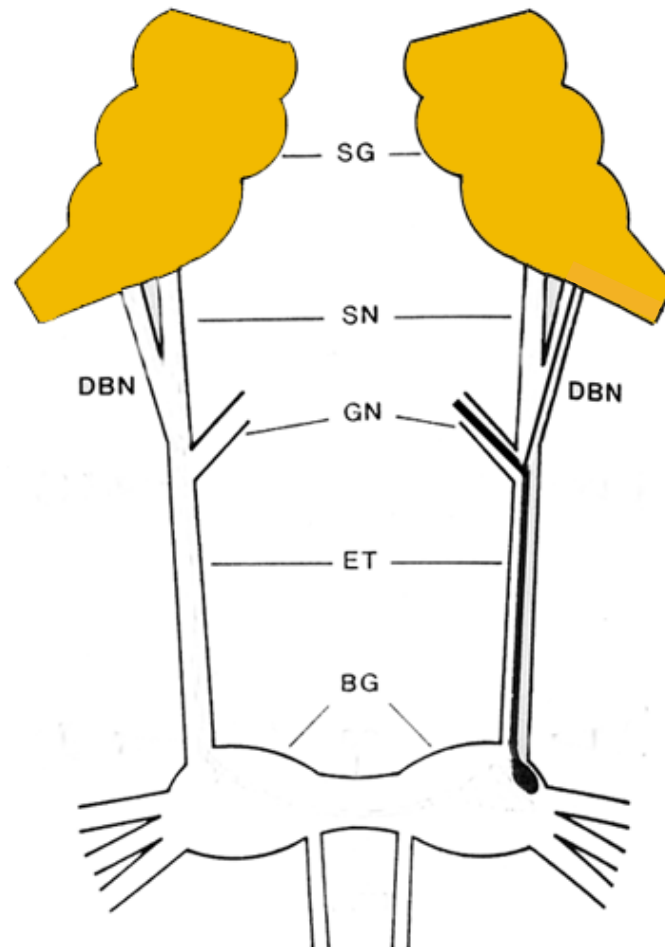
Figure 1.2: The buccal ganglion of *Helisoma trivolvis*. The projection of the B5 neuron exits the buccal ganglion (BG) through the esophageal nerve trunk (ET) and splits into two projections. The major projection exits the gastric nerve (GN) to innervate the esophagus and the minor projection exits the dorsobuccal nerve (DBN) to innervate the buccal mass. The buccal mass is a muscle structure that controls many feeding-related behaviors. Modified from Kruk and Bulloch 1992. SG: salivary gland; SN: salivary nerve

B19 neurons are placed into isolated cell culture, they differ in growth cone dynamics and morphology (Haydon *et al.*, 1985). B5 neurons have more filopodia per growth cone, advance faster over the substrate, and show more extensive outgrowth than B19 neurons. However, the filopodia on B19 neurons are significantly longer than those on B5 neurons. The varied dynamics and morphology displayed by these two neurons may be due to differences in their intracellular composition, as well as the behavior they would display on their trajectory to reach their respective targets *in vivo*.

Molluscan nervous systems lend themselves to our line of research for a number of reasons. First of all, the neurons found in these ganglia are quite large: the soma of the B5 neuron is around 50-75 μm in diameter (Berdan *et al.*, 1989). In addition, these neurons are easily identifiable, based on their size, coloring and placement within the ganglion. Therefore, repeated experimentation can be done on an identified neuron, which reduces variability between experiments and assures that the neuron will always have the same properties (i.e. neurotransmitters, second messengers). Additionally, these neurons of interest can be removed individually from the ganglion and placed into cell culture, which allows for complete control over the neuron's environment.

Another advantageous feature of molluscan nervous systems is that the central nervous system will regenerate following injury. This has been demonstrated quite clearly in *Helisoma*, because when the esophageal trunk nerve is crushed, both the B4 and the B5 neurons will reinnervate their original targets within 5-7 days (Murphy & Kater, 1978; 1980b; a). Although this functional regeneration has been demonstrated to take place both *in vivo* and in organ culture, regeneration of growth cones is also seen *in*

vitro. If growth cones in culture are transected, they will reform growth cones within 10 to 45 minutes, providing an *in vitro* model system with which to study regeneration (Rehder *et al.*, 1992). Overall, *Helisoma* is a beneficial model system for studying processes that take place during permissive regeneration because this regeneration will take place both *in vivo* and *in vitro* following injury. Furthermore, the processes that take place during permissive regeneration in *Helisoma* can be contrasted with and applied to research performed within the mammalian central nervous system, which does not regenerate following injury.

Perhaps most importantly, the size and morphology of the growth cones formed from *Helisoma* neurons lend themselves to a detailed study of growth cone behavior. Importantly, the growth cones that form at the tips of neurites from *Helisoma* neurons cultured in conditioned medium are large (ranging in size from 10-50 microns) and contain many filopodia, allowing for exceptional visualization of changes in growth cone morphology, and particularly, filopodial behavior. Furthermore, invertebrate and vertebrate growth cones are similar in terms of the effects of guidance molecules on motility, some of the intracellular signaling pathways that control motility, and their cytoskeletal composition. Growth factors are molecules found in both invertebrates and vertebrates and are necessary for neurite outgrowth. Growth cones from *Helisoma* will form without the presence of growth factors (at the tip of an axon stump), but they will not exhibit outgrowth (Williams & Cohan, 1994). Outgrowth in *Helisoma* neurons requires conditioned medium, created by incubating the central ganglia from *Helisoma* in defined medium (Leibovitz's L-15 medium), to extend multiple neurites and exhibit

neurite outgrowth (Wong *et al.*, 1981; Wong *et al.*, 1984). However, the specific factors that are released by the central ganglia and promote outgrowth are not well-defined. The only factor yet identified as playing a role in promoting neurite outgrowth from *Helisoma* neurons is a described as a "laminin-like" 300 kD protein (Miller & Hadley, 1991). Due to its overall simplicity, regenerative ability, and growth cone characteristics, *Helisoma* lends itself to the study of developmental processes that take place during the wiring and rewiring of the nervous system.

Specific aims of dissertation

This dissertation employs *Helisoma trivolvis* as a model system to examine the effects of a gaseous messenger, nitric oxide, on growth cone dynamics. Furthermore, this dissertation identifies the intracellular signaling cascade that mediates the effects of nitric oxide on growth cone motility. Three major questions are addressed in these studies.

Specific Aim 1: How does a spatially- and temporally-restricted application of nitric oxide affect growth cone morphology and calcium?

Global application of NO to *Helisoma* B5 neurons results in an increase in filopodial length, a decrease in filopodial number, an increase in the intracellular calcium concentration and a decrease in the neurite outgrowth rate (Van Wagenen & Rehder, 1999; Trimm & Rehder, 2004). These data suggest that NO can cause changes in growth cone morphology and in the intracellular calcium concentration, but do not provide information about the location of the action of NO or to the amount of NO required to

cause changes in growth cone morphology. Therefore, the present study tests the hypothesis that NO is acting at the growth cone proper and that a very spatially- and temporally-limited application of NO can affect growth cone morphology and the intracellular calcium concentration.

Specific Aim 2: What is the downstream pathway through which nitric oxide exerts its effects on growth cone morphology?

Global application of NO acts via sGC to result in changes in growth cone morphology and outgrowth rates of *Helisoma* B5 neurons (Van Wagenen & Rehder, 1999; 2001; Trimm & Rehder, 2004). These data suggest the NO directly binds to and activates sGC, initiating a second messenger cascade that results in the changes in growth cone morphology and the intracellular calcium concentration. However, the NO-activated second messengers involved in the regulation of *Helisoma* B5 growth cone morphology have not been characterized. Therefore, the present study tests the hypothesis that local application of NO mediates its effects on growth cone morphology and calcium via a second messenger cascade involving cGMP, PKG and cADPR.

Specific Aim 3: How do intracellular and extracellular calcium cascades contribute to the nitric oxide-induced calcium dynamics?

Global application of NO is known to cause an increase in the intracellular calcium concentration in *Helisoma* B5 growth cones (Van Wagenen & Rehder, 1999; 2001; Trimm & Rehder, 2004). However, it not known whether the increase in the intracellular

calcium concentration results from release from intracellular stores, influx across the plasma membrane or a combination of both of these processes. Therefore, the present study tests the hypothesis that local application of NO results in increase in the intracellular calcium concentration via release from intracellular calcium stores, as well as calcium influx across the plasma membrane.

Overall, this dissertation addresses the location of action of NO that results in changes in growth cone morphology; the spatial and temporal requirements for NO to exert its effects on growth cone morphology and calcium; the downstream pathways through which local application of NO exerts its effects on growth cone morphology and calcium; and the intracellular and extracellular calcium cascades that are activated by local NO application. Therefore, these experiments provide a mechanism whereby NO can directly and locally affect the motility of a pathfinding growth cone. Furthermore, this dissertation implicates nitric oxide as an integral player in the formation of the connectivity of the nervous system during development.

Chapter 2: Local activation of the nitric oxide/cyclic guanosine monophosphate pathway in growth cones regulates filopodial length via protein kinase G, cyclic adenosine diphosphate ribose, and intracellular calcium release.

This chapter has been published as:

Welshhans, K and Rehder V. Local activation of the nitric oxide/cyclic guanosine monophosphate pathway in growth cones regulates filopodial length via protein kinase G, cyclic adenosine diphosphate ribose, and intracellular calcium release. Eur. J. Neurosci. 22(12): 3006-16, 2005.

Abstract

Nitric oxide (NO) is a gaseous messenger that has been shown to affect growth cone motility and neurite outgrowth in several model systems, but how NO brings about its effects is not understood. We have previously demonstrated that global and long-term application of NO to *Helisoma trivolvis* B5 neurons results in a transient increase in filopodial length, a decrease in filopodial number and a decrease in neurite outgrowth, all of which is mediated via soluble guanylyl cyclase (sGC) and involves an increase in the intracellular calcium concentration (Van Wagenen and Rehder (1999) *J. Neurobiol.*, 39, 168-185 and Trimm and Rehder (2004) *Eur. J. Neurosci.*, 19, 809-818). The goal of the current study was twofold: to investigate the effects of short-term NO exposure on individual growth cones and to further elucidate the downstream pathway through which NO exerts its effects. Local application of the NO donor, NOC-7, for 10-20 ms via puffer micropipette resulted in a transient increase in filopodial length and a small decrease in filopodial number. We show evidence that these effects of NO are mediated via sGC, protein kinase G (PKG), and cyclic ADP ribose (cADPR), resulting in the release of calcium from intracellular stores, most likely of the ryanodine-sensitive type. These results suggest that growth cones expressing sGC are highly sensitive to local and short-term exposure to NO, which they may experience during pathfinding, and that the stereotyped response of transient filopodial elongation seen in B5 neurons in response to NO requires intracellular calcium release.

Introduction

Nitric oxide (NO) is a gaseous signaling molecule that has been reported to regulate a number of processes during neuronal development, including differentiation, cell motility, neuronal pathfinding, and synaptic pruning (Peunova & Enikolopov, 1995; Ball & Truman, 1998; Gibbs & Truman, 1998; Cramer & Sur, 1999; Ernst *et al.*, 1999; Phung *et al.*, 1999; Ernst *et al.*, 2000; Rialas *et al.*, 2000; Wu *et al.*, 2001; Bicker, 2005). Neuronal growth cones, which form the motile tips of advancing neurites, are important for neurite outgrowth and the fan of filopodia extending from the growth cone has been shown to be necessary for neuronal pathfinding (Marsh & Letourneau, 1984; Bentley & Toroian-Raymond, 1986; McCaig, 1989; Chien *et al.*, 1993; Kater & Rehder, 1995). Several studies have reported that NO affects neurite outgrowth and growth cone motility. As demonstrated in experiments *in vitro*, growth cones of several neuronal types, such as from rat dorsal root ganglion, *Xenopus* and chick retinal ganglion cells, and *Helisoma* buccal ganglion collapse in response to high concentrations of NO (Hess *et al.*, 1993; Renteria & Constantine-Paton, 1996; Ernst *et al.*, 2000; Trimm & Rehder, 2004). In addition, NO has been reported to cause both increases (Hindley *et al.*, 1997; Yamazaki *et al.*, 2001) and decreases (Hess *et al.*, 1993; Ernst *et al.*, 2000; Trimm & Rehder, 2004) in neurite outgrowth in various cell types. Such experiments are typically performed by adding NO donors to the neuronal cultures and by monitoring growth cone motility over time. A disadvantage of this approach is that the entire neuron is exposed to NO and that the exposure is often maintained for considerable amounts of time. To more clearly determine whether the effects of NO observed on growth cone motility were

mediated by NO acting at the growth cone proper or elsewhere, and to determine the temporal requirements of NO stimulation necessary to affect growth cone morphology, we administered NO locally to growth cones and varied the duration of stimulation.

The canonical target of NO is the enzyme soluble guanylyl cyclase (sGC), whose activation leads to an increase in cyclic guanosine monophosphate (cGMP). Experiments on identified B5 neurons from the buccal ganglion of the gastropod *Helisoma trivolvis* suggest that NO acts via sGC, cGMP, and an increase in the intracellular Ca^{2+} concentration ($[Ca^{2+}]_i$). This increase in $[Ca^{2+}]_i$ results in an increase in filopodial length, a decrease in filopodial number and a reduction in neurite outgrowth rate (Van Wagenen & Rehder, 1999; Trimm & Rehder, 2004). How the increase in cGMP is linked to the increase in $[Ca^{2+}]_i$ is presently unclear.

We now report that NO acts locally at the growth cone and provide evidence that the NO-induced changes in growth cone morphology are produced via the activation of sGC, cGMP, PKG, cADPR, and calcium release from intracellular stores. The results support the hypothesis that sGC expressing growth cones can be influenced by transient NO release along their path and that NO might influence pathfinding by regulating the growth cone's sensory radius and its rate of advance.

Materials and Methods

Helisoma neuronal culture

Identified B5 and B19 neurons were individually removed from the buccal ganglion of *Helisoma trivolvis* and plated into 35mm culture dishes (Falcon 1008) that have the bottoms removed and replaced with poly-L-lysine (hydrobromide, MW 70,000-150,000; Sigma, St. Louis, MO) coated glass coverslips. Each dish contained 2 ml of conditioned medium, which was created by incubating Helisoma brains (2 brains per 1 ml) for 3-4 days in Leibovitz L-15 (L-15). L-15 is made by dilution and supplementation of standard L-15 (Invitrogen; Carlsbad,CA) to result in the following concentrations: 46 mM NaCl, 1.8 mM KCl, 1.5 mM $MgCl_2$, 4.1 mM $CaCl_2$, 10 mM HEPES, 50 μg gentamycin/ml, 0.15 mg glutamate/ml in distilled water (pH = 7.3). Following plating, neurons were allowed to grow at room temperature for 24-72 hours. Neurons were used for experimentation when they had extended neurites that were tipped with motile growth cones that had extended at least one cell body diameter away from the soma.

Image acquisition and analysis

Growth cones were viewed using the 100x oil immersion objective on either a Zeiss Axiovert 135 microsope (Thornwood, NY) or an ausJENA Sedival microscope. Images were acquired using a cooled CCD camera (CH250, Photometrics, Tucson, AZ) or a CCD C72 camera (MIT Dage, Michigan City, IN), digitized on a frame grabber (Scion LG-3; Scanalytics, Fairfax, VA) and stored on Macintosh computers (Apple Computer Inc.; Cupertino, CA). Phase contrast- and fluorescent images were captured before (-5

and 0 min) and at defined times after (2, 5, 10, 15, 20, and 30 minutes) NOC-7 application. If pharmacological inhibitors were used in combination with NOC-7 application, the inhibitor was bath-applied by removing 200 µl of conditioned medium, dissolving the inhibitor in it, adding the solution back to the dish and then incubating neurons for 20 minutes prior to the start of the experiment.

Filopodial length and number were analyzed with "Scion Image" software (Scion Corporation; Frederick, Maryland) on a Dell Inspiron 600m computer (Round Rock, TX). Filopodial length was measured from the base of a filopodium (the location where the end of the filopodium meets the central domain) to its distal tip. This assessment of filopodial length has the advantage of being independent of extensions and retractions of the overlying lamellipodium, which could otherwise result in the erroneous measurement of filopodial length. In the figures, changes in filopodial length and number are expressed as a percent change normalized to the time point t = 0 (just before drug addition). This normalization step is necessary because individual growth cone vary in size and overall filopodial length and number. Statistical analysis was performed with the software package SuperANOVA (Abacus Concepts; Cary, NC). Significance between conditions was determined by using a repeated measures ANOVA. Fisher's protected LSD test was employed as the post-hoc test of statistical significance. Growth cones were excluded from statistical analysis if they deviated more than two standard deviations from the mean. Significance between conditions is designated as follows: $*p \leq 0.05$; $**p \leq 0.01$; $***p \leq 0.001$.

Local nitric oxide application

The NO donor, NOC-7 (Calbiochem; San Diego, CA), was made up in sodium hydroxide (100 mM) at a stock concentration of 100 mM. In order to locally apply NOC-7, micropipettes were pulled on a microelectrode puller (Fredrick Haer and Co., Bowdinham, ME). They were then filled with fast green and NOC-7, diluted in L-15, to result in final concentrations of 2% and 100 µM respectively. The micropipette was then placed approximately 15-20 µm away from the growth cone and NOC-7 was applied with a Picospritzer (General Valve Corp., Fairfield, NJ) delivering pulses of 8-10 psi. In the standard stimulation protocol, NOC-7 (100 µM in the pipette) was applied locally to a single growth cone for 10 ms. This event was repeated once with 1 second in between puffs. This stimulation paradigm (10 ms, 2 puffs) was used throughout the paper except where indicated otherwise. Typically, cultured neurons extend several neurites that are tipped by growth cones. One growth cone was chosen randomly to be exposed to NO (experimental condition), whereas the other growth cones on the cell were used as controls (not exposed to NO) and labeled as "Control" in the figures. In cases where an inhibitor was used in combination with NOC-7 application, the control is labeled "(Inhibitor Name) Control" (e.g. "ODQ Control"). An additional control group (labeled as "NaOH Control") involved the administration of vehicle alone (a diluted sodium hydroxide solution (100 µM) and fast green) onto individual growth cones.

Pharmacological agents

1H-[1,2,4]Oxadiazolo[4,3-a]quinoxalin-1-one (ODQ; sGC inhibitor), KT5823 (specific PKG inhibitor), and 8-Br-cADPR (cADPR inhibitor) were dissolved in dimethylsulfoxide (DMSO; Sigma) to result in stock concentrations of 20 mM, 2 mM, and 10 mM, respectively. Nicotinamide (Nic; ADP-ribosyl cyclase inhibitor) was dissolved in water to result in a stock concentration of 5 M. Thapsigargin (TG; a Ca^{2+}/ATPase inhibitor) was dissolved in ethanol to result in a stock concentration of 10 mM. All pharmacological agents were obtained from Calbiochem, except for 8-Br-cADPR, which was obtained from Sigma. Pharmacological agents were added to the medium 20 minutes prior to the start of the experiment, by removing 200 µl of conditioned medium from the dish, mixing the drug in this volume, and then adding it back to the dish. These drugs were tested by themselves for effects on filopodia length and number (in figures as "Inhibitor Name", e.g. "5 mM Nic") before being used in combination with NOC-7 application (for controls also see (Van Wagenen & Rehder, 1999).

Calcium imaging

Cells were injected with 10 mM fura-2 pentapotassium salt (Molecular Probes; Eugene, OR) and allowed to sit for 20-35 minutes to give the dye time to diffuse. Images were acquired using 340 ± 10nm and 380 ± 10nm excitation filters (Chroma Technology; Rockingham, VT) mounted in a filter wheel (Empix Imaging; Mississauga, ON, Canada) and a 495 nm emission filter. The system was calibrated using the Calcium Calibration buffer Kit II (Molecular Probes) and intracellular calcium concentrations were calculated

using the Ratio software program (developed by and a gift of S.B. Kater). The intracellular calcium concentration within a growth cone was determined by placing a box into the center of each growth cone and by calculating the ratio of emission signals at 340 and 380 nm after background subtraction according to Grynkiewicz *et al.* (1985) using the formula: $[Ca^{2+}] = K_d[(R-R_{min})/(R_{max}- R)] \times [F_o/F_s]$ as described previously (Rehder & Cheng, 1998). Growth cones were excluded from analysis if their baseline levels of $[Ca^{2+}]_i$ exceeded 200 nM.

Results

We have previously demonstrated that bath application of NOC-7 (100 µM) results in a decrease in neurite outgrowth, increase in filopodial length and decrease in filopodial number (Trimm & Rehder, 2004). In the present experiments, NOC-7 application was spatially restricted to a single growth cone to directly test the effect of nitric oxide (NO) on this structure. NOC-7 (50 or 100 µM) was applied through a micropipette and driven by a picospritzer that delivered pressure pulses of 10 ms duration. This approach allowed us to not only spatially restrict our application to a single growth cone, but also allowed for various amounts of NOC-7 to be applied by varying either the concentration of NOC-7 in the pipette or the pulse duration on the picospritzer. In these experiments, we directly test the effects of local application of NO on filopodial behavior and elucidate the pathway through which these effects are mediated.

Local application of NOC-7 to B5 neurons, but not B19 neurons, results in a dose-dependent, spatially-restricted increase in filopodial length and intracellular calcium

Our first experiment tested the ability to spatially restrict the application of drugs to single growth cones. To determine the region that would be reached by pressure ejection, a micropipette was loaded with a concentrated solution of fast green (2%). The tip of a micropipette was placed 15-20 µm from the growth cone and the duration of the pressure 'puff' was varied until the resulting plume of the dye would reach the growth cone to be stimulated. We next examined the effects of a local application of the NO donor, NOC-7, on filopodial length and number in *Helisoma* B5 neurons. In these experiments,

pretreatment images were acquired at -5 and 0 minutes prior to application of the NO

donor. Immediately following t = 0 min, NOC-7 (100 μM in the pipette) was locally

applied to a single growth cone (standard stimulus paradigm, see 'Methods' for details).

Local NOC-7 application using this stimulation paradigm resulted in an increase in

filopodial length, which was evident in phase contrast images when comparing the time

point prior to application (Figure 2.1A) to 10 minutes following NOC-7 application

(Figure 2.1B). In fact, this effect was already evident in the first image taken at 2 minutes

after NOC-7 addition (Figure 2.1C). Filopodial elongation was transient, in that filopodial

length reached a maximum of 23 ± 6% at 10 minutes following NOC-7 application and

returned to pre-treatment values within 30 minutes of application ($p \leq 0.001$ as compared

to control; Figure 2.1C). This response was spatially restricted to the stimulated growth

cone, as evidenced by the fact that control growth cones (growth cones on the same cell,

but not puffed with NOC-7) did not show a change in filopodial length. In addition, local

NOC-7 application resulted in a small, significant decrease in filopodial number, which

reached -13 ± 6% at 10 minutes following NOC-7 application and returned to

pretreatment values within 30 minutes of application ($p \leq 0.05$ as compared to control;

Figure 2.1D). A vehicle control in which growth cones were puffed with the NOC-7

solvent (NaOH) had no significant effect on filopodial length or number (data not

shown), demonstrating that the filopodial effects observed were caused by NOC-7 and

not by the solvent or the pressure pulse of the puff.

In order to test whether the effects of NO were dose-dependent, a lower

concentration of NOC-7 (50 μM) was employed. When 50 μM NOC-7 was locally

Figure 2.1: Local application of the NO donor, NOC-7, results in a dose-dependent increase in filopodial length and a transient increase in [Ca^{2+}]$_i$. (A, B) Phase contrast images of a B5 growth cone prior to (A) and 10 minutes following local application of 100 μM NOC-7 (B). Note filopodial elongation and some retraction of the lamellipodium. Scale: 10 μm. **(C)** Local application of 100 μM NOC-7 resulted in transient filopodial elongation, which reached a maximum of 23 ± 6% at 10 minutes following application and returned to pretreatment values within 30 minutes. Control growth cones (growth cones on the same cell, but not puffed with NOC-7) showed no change in filopodial length over time, demonstrating that application of NOC-7 was localized. Growth cones that were treated with 100 μM NOC-7 showed a significant increase in filopodial length as compared to control growth cones (ANOVA repeated measures, $p \leq 0.001$). Local application of a lower concentration of NOC-7 (50 μM) resulted in transient filopodial elongation, which reached a maximum of 14 ± 3% at 5 minutes following treatment and returned to pre-treatment values by 20 minutes ($p \leq 0.05$ as compared to control). **(D)** Local application of 100 μM NOC-7 resulted in a small decrease in filopodial number, as compared to control growth cones ($p \leq 0.05$). Local application of a lower concentration of NOC-7 (50 μM) did not result in a change in filopodial number ($p = 0.65$ as compared to control). **(E)** Local application of 100 μM NOC-7 to B5 growth cones resulted in a transient increase in intracellular calcium that reached a maximum of 168 ± 16 nM at 2 minutes following application, and returned to pretreatment values within 20 minutes ($p \leq 0.01$ as compared to control). The number of growth cones studied per condition is given as 'n' and the level of significance compared to the control group is indicated in parentheses following the experimental condition as described in 'Methods'.
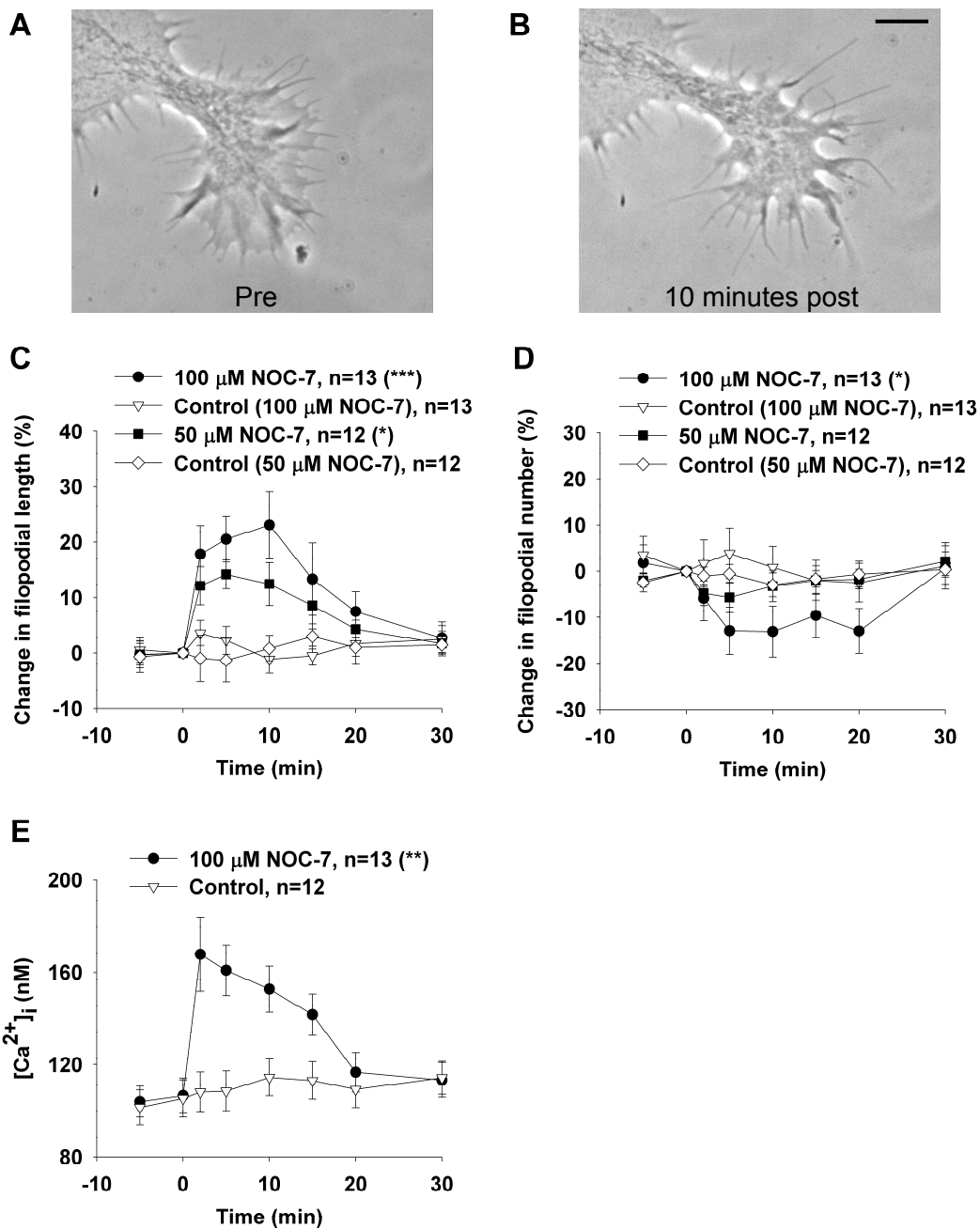
applied, a transient increase in filopodial length resulted, reaching a maximum of 14 ± 3% at 5 minutes following NOC-7 application and returning to pre-treatment values within 20 minutes of application ($p \leq 0.05$ as compared to control; Figure 2.1C). However, local NOC-7 (50 µM) application had no effect on filopodial number ($p = 0.65$ as compared to control; Figure 2.1D). To further investigate the dose-dependency of NO, the concentration of NO in the pipette was doubled (to 200 µM) or the duration of individual pressure pulses was doubled or quadrupled. These stimulation conditions resulted in an increase in filopodial length and decrease in filopodial number (data not shown) that was similar to that seen with the standard stimulation protocol used above (Figure 2.1C, D). Therefore, there may be a 'ceiling' effect that is reached with a single, local NOC-7 application by micropipette and all experiments from here on employ the standard stimulation paradigm (100 µM NOC-7).

Previous work has also demonstrated that growth cones respond with an increase in intracellular calcium ($[Ca^{2+}]_i$) to a global and sustained application of NO (Van Wagenen *et al.*, 1999; Van Wagenen & Rehder, 2001; Trimm & Rehder, 2004). Therefore, we tested next whether the short-term stimulation of individual growth cones would result in $[Ca^{2+}]_i$ changes in the exposed cell. When 100 µM NOC-7 was locally applied to B5 growth cones, $[Ca^{2+}]_i$ increased significantly, reaching a maximum of 168 ± 16 nM at 2 minutes following NOC-7 application, and returning to pretreatment levels within 20 minutes ($p \leq 0.01$; Figure 2.1E). Control growth cones (located on other neurites of the same cell but not exposed to NO) did not show a change in $[Ca^{2+}]_i$, suggesting that the increase in $[Ca^{2+}]_i$ remained local to the stimulated growth cone.

We next tested whether local application of NO to another identified neuron, B19, would have a similar effect on filopodial length and number. When B19 growth cones were exposed to 100 μM NOC-7, they did not respond with a change in filopodial length or number (Figure 2.2A, B; $p = 0.10$ for length and $p = 0.59$ for number). This result supported previous findings that NO was acting through sGC to bring about changes in filopodial length. As demonstrated previously, B5 neurons show immunoreactivity to soluble guanylyl cyclase (sGC), the target of NO, whereas B19 neurons show little to no staining for sGC (Van Wagenen & Rehder, 2001). Accordingly, when B19 growth cones were exposed to 100 μM NOC-7, there was also no change in $[Ca^{2+}]_i$ ($p = 0.83$; Figure 2.2C).

The effects of NO on filopodial dynamics are mediated via the sGC/PKG pathway

NO binds to the heme group of sGC and directly activates the enzyme (Craven & DeRubertis, 1978) to produce cGMP (Arnold *et al.*, 1977). To test more directly whether sGC was involved in the pathway mediating the effects of NO on filopodial dynamics, we next employed a specific inhibitor of sGC, ODQ. Whereas ODQ (20 μM) had no significant effect on filopodial length and number when applied by itself, preincubation with 20 μM ODQ for 25 minutes completely blocked the effect on filopodial length normally seen when 100 μM NOC-7 was applied onto B5 growth cones ($p \leq 0.01$ as compared to 100 μM NOC-7 alone; Figure 2.3A). In addition, preincubation with ODQ also eliminated the small NO-induced decrease in filopodial number ($p \leq 0.01$ as compared to 100 μM NOC-7 alone; Figure 2.3B).

Figure 2.2: Local application of 100 µM NOC-7 to B19 neurons has no effect on filopodial dynamics or [Ca^{2+}]$_i$. (A, B) Local application of 100 µM NOC-7 did not result in a change in filopodial length or number of B19 neurons. Neither control growth cones (on the same cell as treated growth cones, but not puffed with NOC-7) nor NaOH control growth cones (puffed with NaOH as a solvent control) showed a significant change in filopodial length or number. **(C)** Local application of 100 µM NOC-7 to B19 growth cones did not result in a significant change in intracellular calcium (p = 0.83).

A

B

C
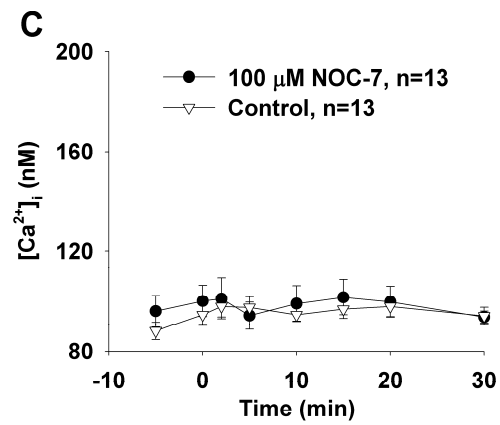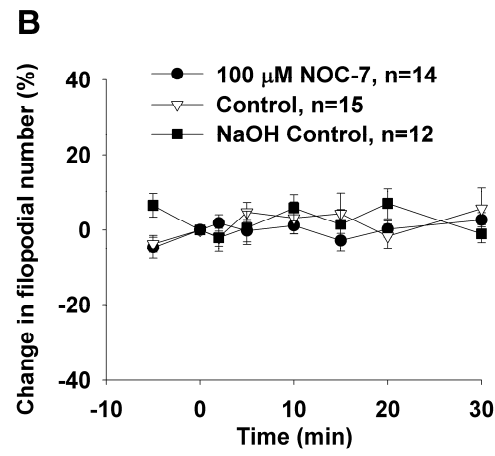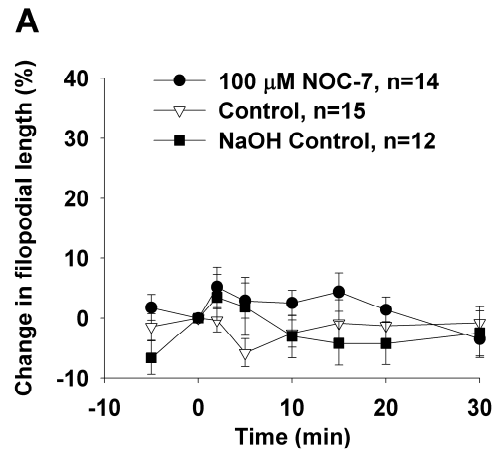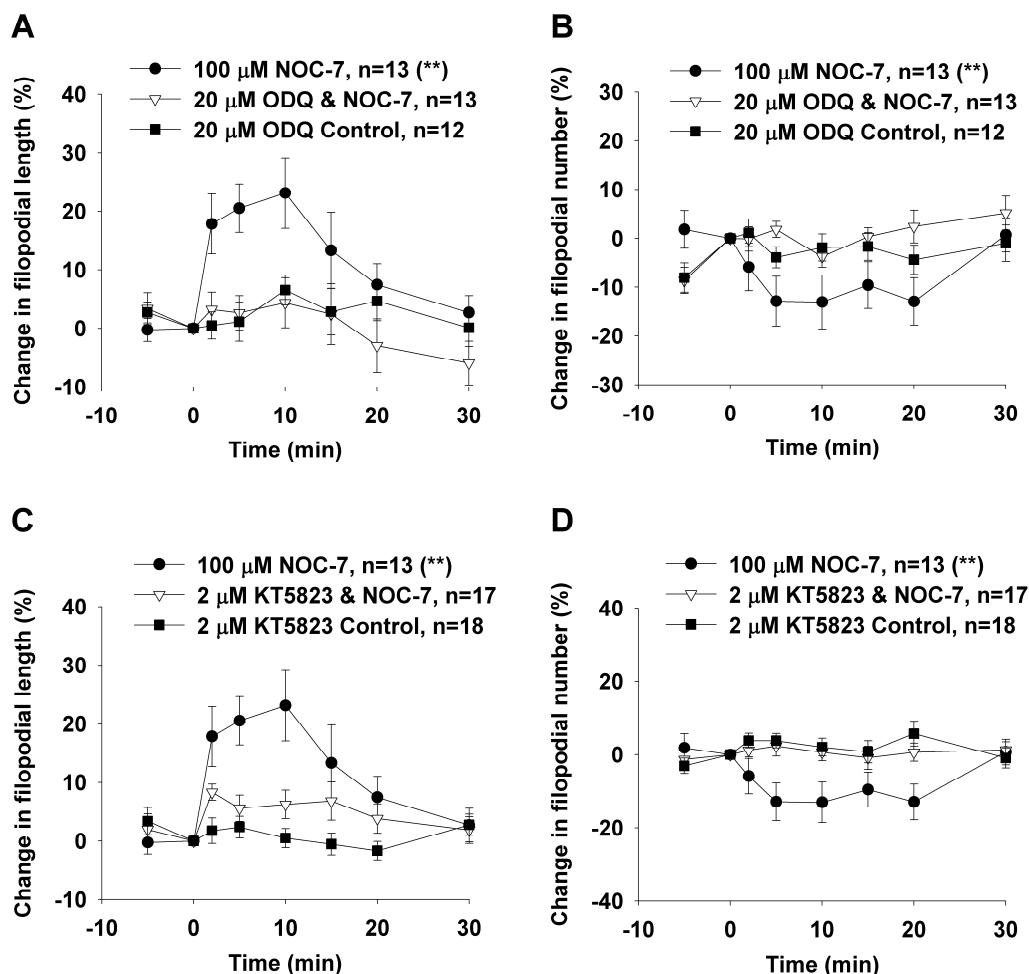
Figure 2.3: The NO-induced increase in filopodial length on B5 neurons occurs via sGC and PKG. (A) Pretreatment for 25 minutes with a sGC inhibitor (20 μM ODQ) followed by local application of 100 μM NOC-7 abolished the NO-induced increase in filopodial length (p ≤ 0.01 as compared to 100 μM NOC-7 alone), whereas ODQ by itself had no effect. Note that in this figure, the NOC-7 data from Figure 1C & 1D have been overlaid in each graph for ease of comparison. **(B)** Pretreatment with 20 μM ODQ, followed by local 100 μM NOC-7 treatment also abolished the small decrease in filopodial number that is usually seen following NO application (p ≤ 0.01 as compared to 100 μM NOC-7 alone). **(C)** Pretreatment with a specific PKG inhibitor, 2 μM KT5823, for 25 minutes, followed by 100 μM NOC-7 application significantly reduced the NO-induced increase in filopodial length (p ≤ 0.01 as compared to 100 μM NOC-7 alone). **(D)** Pretreatment with 2 μM KT5823 for 25 minutes, followed by 100 μM NOC-7 application abolished the NO-induced decrease in filopodial number (p ≤ 0.01 as compared to 100 μM NOC-7 alone).

After having determined that NO exerts its effects via sGC, we next investigated how cGMP might bring about its effects on filopodial length and number by investigating a major target of cGMP, namely protein kinase G (PKG). To investigate a potential role of PKG in NO signaling, we tested the effects of NO on filopodial parameters in the presence of a PKG inhibitor. Interestingly, a 25 minute preincubation with the specific PKG inhibitor KT5823 (2 μM) significantly inhibited the filopodial elongation normally seen when single growth cones were exposed to 100 μM NOC-7 ($p \leq 0.01$ as compared to 100 μM NOC-7 alone; Figure 2.3C). In addition, preincubation with 2 μM KT5823 followed by local 100 μM NOC-7 application also abolished the NO-induced decrease in filopodial number ($p \leq 0.01$ as compared to 100 μM NOC-7 alone; Figure 2.3D). These results suggest that NO affects filopodial length and number through a pathway involving sGC and PKG.

NO exerts its effects on filopodial dynamics via cADPR and intracellular calcium release
One downstream target of PKG is cyclic adenosine diphosphate ribose (cADPR), which is known to cause release of Ca^{2+} from ryanodine receptor (RyR) sensitive internal stores (Higashida *et al.*, 2001; Lee, 2001). Because we have shown that an increase in $[Ca^{2+}]_i$ is involved in the NO signaling pathway (Figure 2.1E and Van Wagenen & Rehder, 1999; Trimm & Rehder, 2004), we next used an inhibitor of the production of cADPR, nicotinamide (Nic), in combination with NOC-7 application. Nicotinamide has been shown to inhibit the production of cADPR through inhibition of the enzyme necessary for its synthesis, ADP-ribosyl cyclase (Sethi *et al.*, 1996). Pretreatment for 25 minutes with

the cADPR inhibitor, 5 mM Nic, followed by 100 μM NOC-7 application significantly reduced the NO-induced filopodial elongation ($p \leq 0.05$ as compared to 100 μM NOC-7 alone; Figure 2.4A). In addition, pretreatment with 5 mM Nic, followed by 100 μM NOC-7 application slightly reduced the NO-induced decrease in filopodial number ($p = 0.31$; Figure 2.4B). These results suggest that the NO-induced increase in filopodial length involves cADPR.

In order to confirm these results, we employed a second inhibitor of cADPR, 8-Br-cADPR. 8-Br-cADPR is a competitive inhibitor of cADPR that acts by occupying the binding site on the receptor (Walseth & Lee, 1993). Pretreatment for 25 minutes with 8-Br-cADPR (10 μM) followed by local 100 μM NOC-7 application abolished the NO-induced filopodial elongation ($p \leq 0.01$ as compared to 100 μM NOC-7 alone; Figure 2.4C). Additionally, 8-Br-cADPR blocked the NO-induced decrease in filopodial number ($p \leq 0.001$ as compared to 100 μM NOC-7 alone; Figure 2.4D). The finding that both inhibitors of cADPR blocked the NO induced effects on filopodial length and number suggests that NO acted through cADPR.

Because cADPR is known to activate calcium release from intracellular stores, we next tested whether the NO-induced increase in $[Ca^{2+}]_i$ was also blocked by pretreatment with the cADPR inhibitor, nicotinamide (Nic). Indeed, pretreatment with 5 mM Nic, followed by the application of 100 μM NOC-7 abolished the NO-induced transient increase in $[Ca^{2+}]_i$ (Figure 2.5; $p \leq 0.05$ when comparing the first 20 minutes of Nic & NOC-7 treatment to 100 μM NOC-7 alone), strongly suggesting that the NO-induced
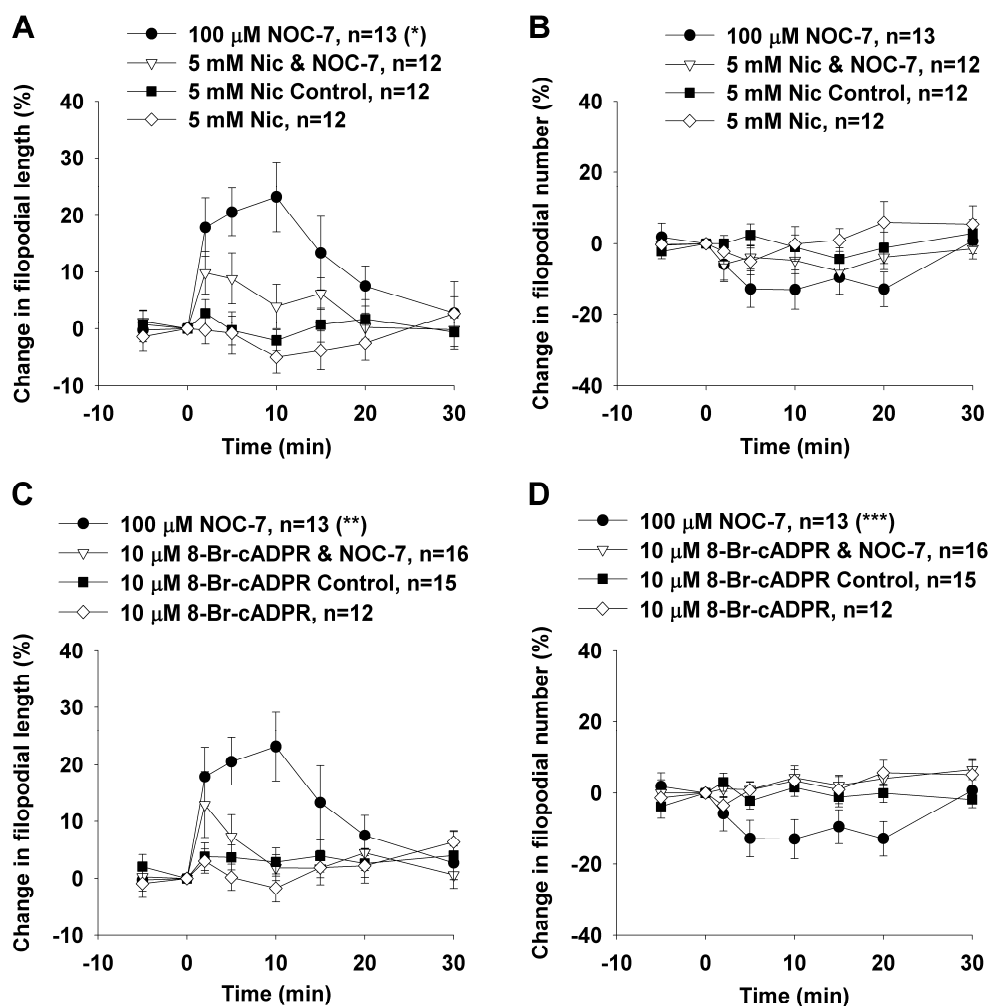
Figure 2.4: The NO-induced increase in filopodial length is mediated via cADPR. **(A)** Pretreatment with a cADPR inhibitor, 5 mM nicotinamide (Nic), for 25 minutes, followed by local application of 100 µM NOC-7 significantly reduced the NO-induced increase in filopodial length ($p \leq 0.05$ as compared to 100 µM NOC-7 alone). Note that 5 mM Nic by itself did not have an effect on filopodial length. The NOC-7 data from Figure 1C & 1D has been overlaid in each graph for ease of comparison. **(B)** Pretreatment with 5 mM Nic followed by local 100 µM NOC-7 application nominally reduced the NO-induced decrease in filopodial number but this effect was not statistically significant ($p = 0.31$ as compared to 100 µM NOC-7 alone). Note that 5 mM Nic alone did not have an effect on filopodial number. **(C)** Pretreatment with another cADPR inhibitor, 10 µM 8-Br-cADPR, for 25 minutes, followed by local application of 100 µM NOC-7 significantly reduced the NO-induced increase in filopodial length ($p \leq 0.01$ as compared to 100 µM NOC-7 alone). 10 µM 8-Br-cADPR alone had no effect on filopodial length. **(D)** Pretreatment with 10 µM 8-Br-cADPR followed by local 100 µM NOC-7 application abolished the NO-induced decrease in filopodial number ($p \leq 0.001$ as compared to 100 µM NOC-7 alone).
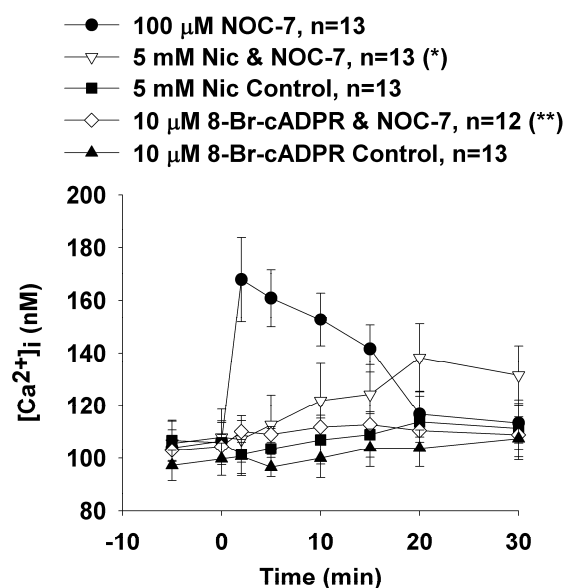
Figure 2.5: The NO-induced increase in $[Ca^{2+}]_i$ is mediated via cADPR.
Pretreatment with the cADPR inhibitor, 5 mM nicotinamide (Nic), for 25 minutes, followed by local application of 100 µM NOC-7 significantly reduced the NO-induced increase in intracellular calcium ($p \leq 0.05$ when comparing the first 20 minutes of Nic & NOC-7 treatment to 100 µM NOC-7 alone). Pretreatment with another cADPR inhibitor, 10 µM 8-Br-cADPR, followed by local application of 100 µM NOC-7 abolished the NO-induced increase in intracellular calcium ($p \leq 0.01$ as compared to 100 µM NOC-7 alone).

transient increase in $[Ca^{2+}]_i$ is mediated through cADPR. Although growth cones treated with Nic & NOC-7 displayed a slow increase in calcium (Figure 2.5), there was no significant difference between any post treatment time point when compared to the pre (0 minute) time point. In order to confirm that cADPR was responsible for the NO-induced increase in calcium, a second cADPR inhibitor was employed, 10 µM 8-Br-cADPR, which also blocked the NO-induced increase in $[Ca^{2+}]_i$ (Figure 2.5; $p \leq 0.01$ as compared to NOC-7 alone). Taken together, these results suggest that the NO-induced increase in $[Ca^{2+}]_i$ is linked to a release mechanism involving cADPR.

If the release of $[Ca^{2+}]_i$ from intracellular stores was necessary for NO to affect filopodial length and number, it would be expected that NO should not be able to exert its effects when intracellular stores of calcium are depleted. Thapsigargin blocks the Ca^{2+}-ATPases in the endoplasmic reticulum (Thastrup *et al.*, 1990) and thereby assists in the emptying of ryanodine-sensitive stores. Whereas 100 nM thapsigargin (TG) by itself had no significant effect on either filopodial parameters or levels of $[Ca^{2+}]_i$, pretreatment with TG significantly inhibited the NO-induced increase in filopodial length (Figure 2.6A; $p \leq$ 0.05 when comparing NOC-7 alone to the combined TG and NOC-7 treatment). Although pretreatment with TG did slightly reduce the NO-induced decrease in filopodial number, this effect was not significant (Figure 2.6B; $p = 0.19$ when comparing NOC-7 alone to the combined TG and NOC-7 treatment). Preincubation with TG also abolished the NO-induced increase in $[Ca^{2+}]_i$ (Figure 2.6C; $p \leq 0.001$ when comparing NOC-7 alone to the combined TG and NOC-7 treatment). These results suggest that intracellular calcium stores are necessary for the NO-induced changes in filopodial length.

Figure 2.6: Depleting intracellular calcium stores with thapsigargin blocks the NO-induced increase in filopodial length and $[Ca^{2+}]_i$. **(A)** Intracellular calcium stores were depleted by treating cells for 30 minutes with a Ca^{2+}/ATPase inhibitor, 100 nM thapsigargin (TG). Pretreatment with 100 nM TG abolished the NO-induced (100 µM NOC-7) increase in filopodial length ($p \leq 0.05$ when comparing 100 µM NOC-7 alone to the combined 100 nM TG & NOC-7 treatment). Note that this treatment by itself had no effect on filopodial length. **(B)** Pretreatment with 100 nM TG, followed by local application of 100 µM NOC-7 nominally reduced the NO-induced decrease in filopodial number ($p = 0.19$ when comparing 100 µM NOC-7 alone to the combined 100 nM TG & NOC-7 treatment). Treatment with 100 nM TG by itself had no effect on filopodial number. **(C)** Pretreatment for 30 minutes with 100 nM TG blocked the NO-induced increase in $[Ca^{2+}]_i$ that is normally seen following local NOC-7 application ($p \leq 0.001$ when comparing 100 µM NOC-7 alone to the combined 100 nM & NOC-7 treatment).
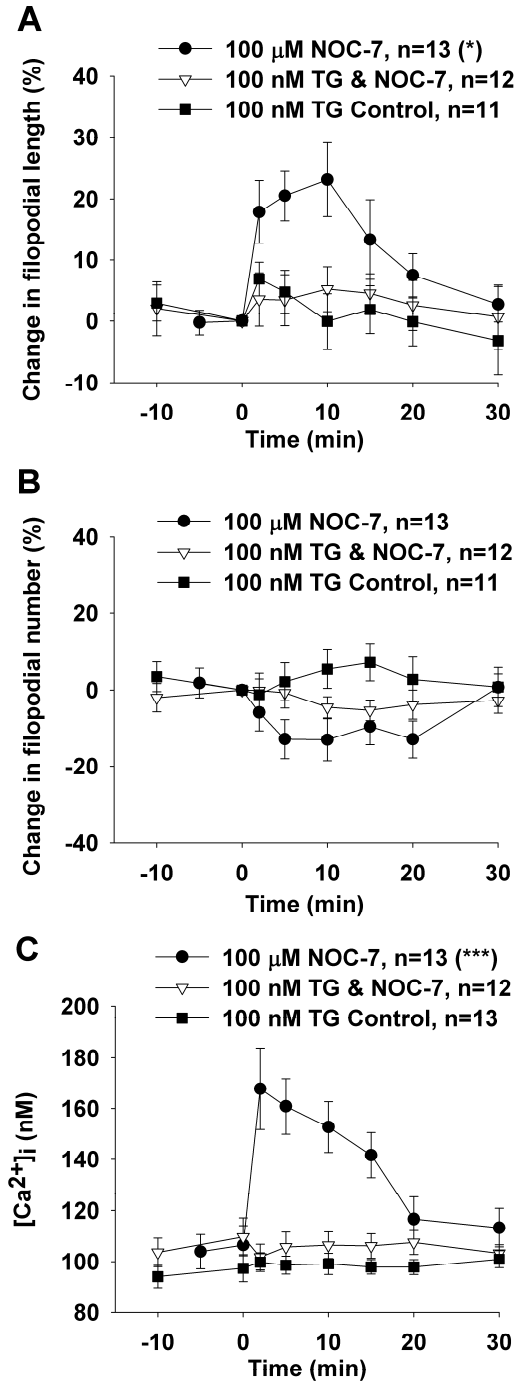
Discussion

Nitric oxide serves a wide range of functions, including the regulation of neuronal differentiation, proliferation and survival (Peunova & Enikolopov, 1995; Ball & Truman, 1998; Gibbs & Truman, 1998; Cramer & Sur, 1999; Ernst *et al.*, 1999; Phung *et al.*, 1999; Ernst *et al.*, 2000; Rialas *et al.*, 2000; Wu *et al.*, 2001; Contestabile & Ciani, 2004; Bicker, 2005). The importance of NO for development was demonstrated most clearly in Drosophila, where knocking out the only NO producing isoform of the enzyme NO synthase (NOS) resulted in a lethal phenotype early in development (Regulski *et al.*, 2004). Less dramatic effects are seen in other systems in response to knockouts or pharmacological blockade of particular NOS isoforms, presumably due to the presence of other isoforms that might compensate for the absence or blockade of one isoform (Huang *et al.*, 1993; Mashimo & Goyal, 1999; Packer *et al.*, 2003).

During neural development axons elongate and are guided by growth cones to their target areas, where they synapse onto appropriate postsynaptic cells. Although NO has been shown to affect neuritogenesis and neuronal outgrowth both *in vivo* and *in vitro* (Truman *et al.*, 1996; Hindley *et al.*, 1997; Mize & Lo, 2000; Rialas *et al.*, 2000; Seidel & Bicker, 2000; Tsukada *et al.*, 2002; Trimm & Rehder, 2004; Yamazaki *et al.*, 2004; Bicker, 2005; Zhang *et al.*, 2005), its role is best established as a retrograde signaling molecule at synapses, where it appears to be involved in synaptogenesis as well as in synaptic plasticity in the adult (Garthwaite *et al.*, 1988; Garthwaite & Boulton, 1995; Contestabile, 2000; Bon & Garthwaite, 2002; Nikonenko *et al.*, 2003). Less is known about a role for NO during cell migration and axonal pathfinding, although there is good

evidence that NOS is expressed early enough in development to overlap with axon pathfinding and synaptogenesis in several model systems (Truman *et al.*, 1996; Bicker, 1998; Grueber & Truman, 1999; Villani, 1999; Gibson & Nighorn, 2000; Bicker, 2005). Recent evidence from the enteric nervous system of the embryonic grasshopper suggests that NO is produced in a subset of midgut cells. These cells line the path of neurons that migrate along the gut and inhibition of NOS in this system results in a slow down in the migration rates of these neurons (Haase & Bicker, 2003). This finding suggests that NO production along the path of migrating neurons can modulate their rate of advance. NO has also been shown to regulate cell migration in cerebellar granule cells in slice culture, because inhibition of NOS was shown to block migration (Tanaka *et al.*, 1994). Moreover, simulation of NO release by applying the NO donor NOC-7 to migrating *Helisoma* B5 neurons *in vitro* resulted in a slow down of neurite advance, which was dose-dependent and mediated via sGC (Trimm & Rehder, 2004). In other neuronal cell types, NO has been reported to cause both increases (Hindley *et al.*, 1997; Yamazaki *et al.*, 2001) and decreases (Hess *et al.*, 1993; Ernst *et al.*, 2000; Trimm & Rehder, 2004) in neurite outgrowth. Addition of high concentrations of NO-donors to neuronal cultures from rat dorsal root ganglion, *Xenopus* retinal ganglion cells, chick retinal ganglion cells, and *Helisoma* buccal ganglion was shown to result in growth cone collapse (Hess *et al.*, 1993; Renteria & Constantine-Paton, 1996; Ernst *et al.*, 2000; Trimm & Rehder, 2004). Although these differences in cellular responses may reflect cell type specificity, it is also possible that they are due to differences in the concentrations and types of NO donors used. A study on *Helisoma* neurons indeed suggests that NO can have dose-dependent

effects and proposes a view that outgrowth is regulated by the concentration of cGMP in the cell (Trimm & Rehder, 2004). In B5 neurons, high concentrations of cGMP shift a growth cone from an 'optimal' growth rate to slower growth or even collapse, whereas lowered concentrations of cGMP also result in slower outgrowth.

NO acts at the growth cone proper

Effects of NO on physiological processes are often tested by adding NO donors to an entire preparation, which has the disadvantage that the location of NO action is difficult to discern. Moreover, temporal and spatial information provided in a NO signal cannot be investigated. Studies on single cells in culture have the advantage that effects of NO can be investigated on a single cell level, but addition of NO donors to the culture medium still gives NO access to the entire neuron. We reported previously that filopodia of B5 neurons start to elongate their filopodia within a minute of exposure to NO (Van Wagenen & Rehder, 1999). This rapid response supported the interpretation that NO acted locally at the growth cone. We have now confirmed this notion by applying small amounts of NO directly to single growth cones. Whereas growth cones stimulated directly responded with a stereotypical elongation of filopodia and a small reduction in filopodial numbers, other growth cones from the same cell and growing in the vicinity of the stimulated growth cone showed no response. Thus, not only was the application of NO-donor localized and NO did not spread to other growth cones, we could also rule out an indirect effect of NO communicated from the stimulated growth cone to other growth cones throughout the cell. Interestingly, the effects of NO were less pronounced and

shorter in duration when compared to earlier studies in which NO donors were applied to the entire dish for 30 minutes or more (Van Wagenen & Rehder, 1999; 2001). The finding that 10 ms puffs of NO donor caused a significant effect on filopodial length and number in B5 but not B19 neurons, suggests that neurons can be sensitive to short transients of NO release. The finding that the effects on $[Ca^{2+}]_i$ and filopodial elongation in response to NO exposure in the range of seconds lasted for about 20 minutes suggests that NO initiates intracellular signaling events that long outlast the initial stimulus. Moreover, the similarity in time courses of the Ca^{2+} and filopodial responses (compare Figures 2.1C and 2.1E) indicate that calcium levels have to be restored to baseline levels for filopodial elongation to return to pretreatment levels. Although we do not know the maximal concentration of NO donor at the growth cone, nor the effective time course of NO release from NOC-7, modeling studies suggest that the presence of NO at the growth cone will be very limited due to rapid diffusion and short half life (Wood & Garthwaite, 1994; Philippides *et al.*, 2000).

NOC-7 application led to a dose-dependent response on filopodial length and number. Interestingly we noticed an apparent 'ceiling effect' such that longer exposures and exposures using higher concentrations of NOC-7 did not lead to stronger effects. The reason for this upper limit on filopodial elongation is presently unclear, but might reside in limiting amounts of g-actin available for addition at filopodial tips. The stronger elongation observed after long-term exposure to NO seen in earlier experiments (Van Wagenen *et al.*, 1999; Van Wagenen & Rehder, 1999) was paralleled by a larger reduction in the number of filopodia, and the breakdown of f-actin resulting from

reabsorbing filopodia into the growth cone may be required to provide additional g-actin for further polymerization.

NO acts through the sGC/PKG/cADPR pathway

The main target of NO is the enzyme soluble guanylyl cyclase (sGC) (Pyriochou & Papapetropoulos, 2005) and effects of NO signaling through cGMP on neurite outgrowth and pathfinding have been reported in several model systems (Hindley *et al.*, 1997; Gibbs & Truman, 1998; Seidel & Bicker, 2000; Haase & Bicker, 2003; Bicker, 2005). We suggest that NO affects growth cone motility via sGC, because the effects of the NO-donor are blocked when this enzyme is inhibited with ODQ. Moreover, the fact that NO did not affect growth cone motility in B19 neurons further supports this notion. This use of B19 neurons as a 'negative control' resulted from a previous report in which we demonstrated immunohistochemically that growth cones of B5 neurons are sGC-positive, whereas those of B19 neurons are sGC-negative (Van Wagenen & Rehder, 2001). The expression of sGC has been shown to be developmentally regulated in other systems (Truman *et al.*, 1996; Gibbs *et al.*, 2001; Haase & Bicker, 2003; Ding *et al.*, 2005), providing for a mechanism that would allow a cell to change its sensitivity to NO or 'tune in' or 'tune out' of NO signaling altogether. Whether such changes in expression levels of sGC are found during different developmental stages in B5 and B19 neurons, and whether they are correlated with neuronal pathfinding is presently unknown. The activity of sGC can also be controlled by other mechanisms, including elevations in $[Ca^{2+}]_i$ that have been shown to desensitize sGC (Bellamy *et al.*, 2000; Garthwaite, 2005). Thus, the

increase in $[Ca^{2+}]_i$ seen upon long term exposure to NO donors could have desensitized the enzyme and thereby resulted in a reduction in cGMP production in growth cones, potentially explaining the observation that levels of $[Ca^{2+}]_i$ and filopodial responses returned towards baseline during prolonged stimulation with NO donors in previous studies (Van Wagenen & Rehder, 1999; 2001).

The enzyme sGC produces cGMP, which has been previously identified in regulating neurite outgrowth and growth cone turning (Gundersen & Barrett, 1980; Hindley *et al.*, 1997; Song *et al.*, 1998; Mizuhashi *et al.*, 2001; Trimm & Rehder, 2004; Bicker, 2005). cGMP is known to act through three major targets: it activates or inhibits several phosphodiesterases (PDEs), activates cyclic nucleotide gated (CNG) ion channels, and activates protein kinase G (PKG) (Fain *et al.*, 2001; Barnstable *et al.*, 2004; Contestabile & Ciani, 2004). Here we provide evidence that cGMP regulates filopodial length and number through PKG, because the effect of NO was fully inhibited in the presence of the PKG inhibitor KT5823. Moreover, we show that the effect of NO was blocked when cADP ribose was inhibited with either nicotinamide or 8-Br-cADPR. These findings suggest that cGMP activates PKG, and that PKG, by activating ADP ribosyl cyclase directly or indirectly, leads to an increase in the concentration of cADP ribose (Figure 2.7). According to our model, cADP ribose would then trigger the release of Ca^{2+} from ryanodine–sensitive Ca^{2+} stores, identifying the ER as an important source of the Ca^{2+} increase seen in response to NO. This conclusion was further supported by our results that the effects of NO on both $[Ca^{2+}]_i$ and filopodial motility were blocked by
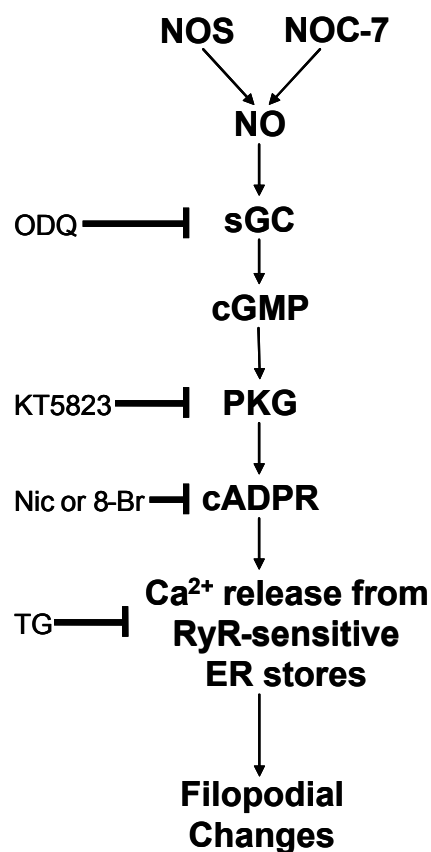
Figure 2.7: Summary of the pathway by which NO is suggested to affect filopodial dynamics. NO is produced by isoforms of nitric oxide synthases (NOS) but is here applied externally via the NO donor, NOC-7. NO binds to the heme group of sGC and activates it to produce cGMP. cGMP then activates PKG, which activates ADP-ribosyl cyclase to produce cyclic adenosine diphosphate ribose (cADPR). cADPR in turn causes release of Ca^{2+} from ryanodine-sensitive Ca^{2+}-stores located in the endoplasmic reticulum. The following pharmacological agents were employed in this study: ODQ (sGC inhibitor), KT5823 (PKG inhibitor), Nic (ADP-ribosyl cyclase inhibitor), 8-Br-cADPR (cADPR inhibitor), and thapsigargin (ER Ca^{2+}/ATPase inhibitor).

thapsigargin, an inhibitor of Ca^{2+}-ATPases located in the ER membrane (Lytton *et al.*, 1991). Thus, when Ca^{2+} re-uptake into the ER was prevented and stores became depleted of Ca^{2+}, the effects of NO on filopodial length were abolished.

NO has been demonstrated to increase $[Ca^{2+}]_i$ via cADPR in sea urchin eggs (Dargie *et al.*, 1990) and this release was later shown to be mediated by the ryanodine receptor (Willmott *et al.*, 1996a). cADPR has also been demonstrated to increase $[Ca^{2+}]_i$ via the ryanodine receptor in neurons (Hua *et al.*, 1994; Verkhratsky & Shmigol, 1996; Guse, 2004) and in addition, has also been described to modulate the interaction of Ca^{2+} release and Ca^{2+} influx (Empson & Galione, 1997; Hashii *et al.*, 2000). Ca^{2+} release from intracellular stores can result in calcium-induced calcium release (CICR) which is thought to explain the regenerative Ca^{2+} transients seen in many cell types, and both the ryanodine and IP$_3$ receptors have been shown to undergo CICR (Endo *et al.*, 1970; Finch *et al.*, 1991). The long-lasting elevation of $[Ca^{2+}]_i$ in B5 growth cones in response to stimulation with NO could be a result of CICR, but may also require Ca^{2+} influx across the plasma membrane. The importance of Ca^{2+} influx for filopodial regulation has been reported previously for B5 neurons (Van Wagenen & Rehder, 1999) and possible interactions between Ca^{2+} release channels in the ER and Ca^{2+} influx will be the focus of future studies. Because the degree of store filling is important for the resulting Ca^{2+} signal (Berridge, 1995; 2005), one might expect that the effect of NO will depend on this parameter and thereby might reflect the cell's recent stimulation 'history'.

Role of filopodial length and number in determining the growth cone 'action radius'

Filopodia are undergoing continued cycles of extension and retraction and are important for growth cone steering (Marsh & Letourneau, 1984; Bentley & Toroian-Raymond, 1986; McCaig, 1989; Chien *et al.*, 1993; Kater & Rehder, 1995). With receptors embedded in their membranes, filopodia serve to survey the environment ahead of the growth cone and changes in their length or number will alter the radius of the survey area. Our results of rapid filopodial elongation coupled with modest reduction in filopodial number support previous findings that suggest that NO could serve as a 'slow down and search' signal for a navigating growth cone (Trimm & Rehder, 2004).

As mentioned above, the short application of 100 μM NOC-7 caused a smaller effect on filopodial elongation and number as compared to long-term addition used in earlier experiments. This was especially true for the number of filopodia, which was reduced by $13 \pm 6\%$ in this report, but saw maximal reduction of up to $28 \pm 6\%$ in earlier studies (Van Wagenen & Rehder, 1999; 2001). Interestingly, lower concentrations of NOC-7 (50 μM) had no effect on number, while still causing significant elongation. Thus localized stimulation by NO for short periods can cause filopodial elongation without concomitant filopodial loss, resulting in a transient enlargement of the growth cone's sensory span. It is presently unknown whether this mechanism is used for axonal guidance in the developing nervous system *in situ*, but there is good evidence for a role of NO during synaptogenesis and synaptic remodeling, events during which growth cones undergo changes in their rate of advance and/or remodel their shape to adjust to new functions (Williams *et al.*, 1994; Wu *et al.*, 1994; Cogen & Cohen-Cory, 2000;

Contestabile, 2000; Godfrey & Schwarte, 2003; Nikonenko *et al.*, 2003; Sunico *et al.*, 2005).

Conclusions

In this paper we provide evidence that NO affects the neuronal cytoskeleton of identified *Helisoma* neurons in a stereotypical fashion by acting via sGC, PKG, and cADP ribose to release Ca^{2+} from ryanodine sensitive stores. To our knowledge, this is the first report on primary neurons in which NO is demonstrated to cause the release of Ca^{2+} from intracellular stores via this pathway. Moreover, by stimulating single growth cones and by limiting the exposure to NO donors to fractions of seconds, we demonstrate that NO can act at the growth cone locally and that very brief exposures to NO are effective in regulating growth cone morphology. These results suggest that transient release of NO by cells lining the path of a navigating growth cone or its target region would have a significant effect on growth cone shape and could function as a signal to affect growth cone motility during pathfinding.

Chapter 3.1: Nitric oxide regulates filopodial dynamics via ryanodine receptor-mediated calcium release

This chapter has been published as:

Welshhans K and Rehder V. Nitric oxide regulates growth cone filopodial dynamics via ryanodine receptor-mediated calcium release. European Journal of Neuroscience. In press.

Abstract

Nitric oxide (NO) is a gaseous intercellular messenger involved in numerous processes during development, including wiring of the nervous system. Neuronal growth cones are responsible for establishing the correct connectivity in the nervous system, but how NO might affect neuronal pathfinding is not fully understood. We have demonstrated in a previous study that local application of a nitric oxide donor, NOC-7, via micropipette onto individual growth cones from *Helisoma trivolvis* B5 neurons results in an increase in filopodial length, decrease in filopodial number and an increase in the intracellular calcium concentration ($[Ca^{2+}]_i$). Moreover, these NO-induced effects were demonstrated to be mediated via an intracellular cascade involving soluble guanylyl cyclase, protein kinase G (PKG), and cyclic adenosine diphosphate ribose (cADPR). We now demonstrate that the increase in the $[Ca^{2+}]_i$ that results from local NO application is mediated via release from ryanodine receptor (RyR)-sensitive intracellular stores. We also show that PKG and RyRs are localized within growth cones and microinjection of cADPR mimics the effects of NO, providing further support that the NO-induced effects are mediated via cADPR. Lastly, we provide evidence that calcium influx across the plasma membrane is a necessary component of the NO-induced calcium increase, however, this calcium influx is secondary to the RyR-induced calcium release from intracellular stores. This study details a signaling pathway by which NO can cause changes in growth cone morphology and thus provides a mechanism by which NO could affect neuronal wiring by acting locally on individual growth cones during the pathfinding process.

Introduction

Nitric oxide (NO) is a gaseous messenger that has multiple functions during development, including regulation of proliferation, differentiation, pathfinding and synaptic pruning (Ernst *et al.*, 1999; Cogen & Cohen-Cory, 2000; Contestabile & Ciani, 2004; Matarredona *et al.*, 2005; Bicker, 2006; Villalobo, 2006). The signaling pathways through which NO brings about these various effects are only partially understood. We are employing a cell culture approach, using identified neurons from the pond snail *Helisoma trivolvis*, to study how NO affects neuronal motility, with a particular focus on the effects of NO on growth cone dynamics. Growth cones are the motile tips of advancing neuronal processes, such as axons and dendrites, and play a crucial role in neuronal pathfinding and synaptogenesis. NO affects several aspects of neurite outgrowth and targeting (Cheung *et al.*, 2000; Ernst *et al.*, 2000; Haase & Bicker, 2003; Zhang *et al.*, 2005; Bicker, 2006), making the growth cone a highly sensitive assay system to investigate NO signaling. Previous studies from this lab demonstrated that the application of NO donors, such as SIN-1 and NOC-7, to a particular type of neuron (B5) grown in cell culture resulted in a transient increase in filopodial length, a decrease in filopodial number and a slow down in neurite outgrowth (Van Wagenen & Rehder, 1999; Trimm & Rehder, 2004; Welshhans & Rehder, 2005). These effects are elicited by an NO-induced transient increase in the intracellular calcium concentration ($[Ca^{2+}]_i$) and amount to what we have termed growth cone "slow down and search behavior." Using a puffer-pipette approach we subsequently demonstrated that the effects on growth cone morphology and calcium were mediated at and limited to the stimulated growth cone (Welshhans &

Rehder, 2005). Using pharmacological tools, we determined that NO causes these changes in growth cone morphology via an intracellular cascade involving soluble guanylyl cyclase (sGC), cyclic guanosine monophosphate (cGMP), protein kinase G (PKG), and cyclic adenosine diphosphate ribose (cADPR).

The goal of the present study was to further extend the investigation of the NO signaling pathway downstream of cADPR in order to link the effect of NO to the increase in $[Ca^{2+}]_i$, which is a necessary step in the NO-induced changes in growth cone motility. We here report that NO acts via cADPR and ryanodine receptor-mediated intracellular calcium release to cause the transient increase in $[Ca^{2+}]_i$ and changes in growth cone morphology. The calcium release from intracellular stores then results in calcium influx across the plasma membrane, which contributes to the transient intracellular calcium increase seen after stimulation of growth cones with NO. Taken together, this study demonstrates that NO can directly affect growth cone motility of sGC-containing neurons through a transient elevation of $[Ca^{2+}]_i$ from ryanodine sensitive stores, making NO an effective signaling molecule at the growth cone level. Thus, growth cones from NO-sensitive neurons could be affected during neuronal pathfinding or synaptogenesis by individual cells or tissues that release NO in the vicinity of a growth cone's migratory path.

Materials & Methods

Helisoma trivolvis neuronal culture

Identified, individual B5 neurons from the buccal ganglion of *Helisoma trivolvis* were removed and plated into Falcon petri dishes (1008; Becton Dickinson Labware, Franklin Lakes NJ) as previously described (Rehder & Kater, 1992; Rehder & Cheng, 1998). To prepare these dishes for plating, a hole was drilled out of the bottom and replaced with a poly-L-lysine (hydrobromide, MW 70,000-150,000; Sigma, St. Louis MO) coated glass coverslip. Conditioned medium (2 mL) was placed into each dish, which was created by incubating 2 brains per 1 mL of L-15 medium (Leibovitz L-15; Invitrogen, Carlsbad CA) for 3-4 days (Wong *et al.*, 1981; Wong *et al.*, 1984). L-15 for *Helisoma* cell culture was made by using standard L-15 and then diluting and supplementing it in distilled water to result in the following final concentrations: 46 mM NaCl; 1.8 mM KCl; 1.5 mM $MgCl_2$; 4.1 mM $CaCl_2$; 10 mM HEPES; 50 µg/mL gentamycin; 0.15 mg/mL L-glutamine. The final solution was adjusted to pH 7.3. Once neurons were plated, they were allowed 24-48 hours to extend growth cones. In order for a neuron to be used for experimentation, the growth cone had to have extended a distance equal to at least one cell body away from the neuronal soma.

Image acquisition and analysis

Growth cones were viewed using a 100x oil immersion objective (UPlan Fl N; Olympus, Melville NY) on an Olympus IX70 inverted microscope equipped with phase contrast optics. Fluorescent images were acquired using illumination from a high pressure

mercury (HBO) burner (Olympus) that was controlled by a Lamba 10-2 programmable filterwheel (Sutter Instrument Corporation, Novato CA). Images were acquired using a Photometrics C350 cooled CCD camera (Tucson AZ) in combination with MetaMorph software (Universal Imaging Corporation, Dowington PA) and stored on a Universal Imaging Corporation PC. This setup was located on a vibration isolation table (TMC, Peabody MA).

Phase contrast and fluorescent images were acquired at defined time points both before (-5 and 0 minutes) and after (2, 5, 10, 15, 20, 30 minutes) treatment with pharmacological agents. Filopodial length and number were analyzed with ImageJ (NIH) software on a Dell Inspiron 600m computer (Round Rock TX). Filopodial length was analyzed by measuring from the filopodial tip to the central domain of the growth cone. This measuring procedure allows for accurate measurement of filopodial length, independent of changes in lamellipodial size. Changes in filopodial length and number were normalized to $t = 0$ minutes and expressed as a percent change from that value.

Fluorescent images were analyzed with MetaMorph software. Fluorescence values for each growth cone were determined by placing a box over the growth cone at each time point and recording the averaged fluorescent value over that area. Background values were also taken for each image by placing a box outside, but near, the growth cone and recording the averaged fluorescence value over this area. Final values of fluorescence for each growth cone were determined by subtracting the background value from the growth cone value. Data is expressed in the graphs as growth cone fluorescence minus

background fluorescence divided by the fluorescence at t = 0 minutes (which is also background subtracted).

A repeated measures analysis of variance (ANOVA) was used for testing for overall statistical significance between conditions (SuperANOVA software; Abacus Concepts, Cary NC). Fisher's protected LSD was employed as the post-hoc test for determining statistical significance. A Student's t-test was employed for testing for statistical significance between individual time points with the software program Excel (Microsoft, Redmond WA). Significance between conditions is designated as follows: * $p \leq 0.05$, ** $p \leq 0.01$, *** $p \leq 0.001$.

Local application of nitric oxide

Nitric oxide was locally applied with a micropipette that was pulled on a micropipette puller (Fredrick Haer and Company, Bowdinham ME). The NO donor, NOC-7 (Calbiochem, San Diego CA), was dissolved in sodium hydroxide (100 mM) at a stock concentration of 100 mM. When NOC-7 was to be locally applied, this solution was mixed and diluted with L-15 and fast green to result in a final concentrations of 2% fast green and 100 μM NOC-7. Local application of NOC-7 was performed with a Picospritzer (General Valve Corporation, Fairfield NJ). NOC-7 was applied to each growth cone immediately following the t = 0 minute time point with a single burst for a duration of either 80 or 400 ms. All experiments were performed with an 80 ms burst duration, except the lanthanum experiment that used a 400 ms burst duration. The burst duration was modified between experiments to accommodate a variation in the size of the

micropipette tip that resulted from the reconfiguration of the micropipette puller. However, both burst durations produced a similar size cloud of NOC-7, as well as producing results that were not significantly different from one another. In order to control for any potential mechanical effect that fluid movement or the solvent may have on growth cone motility or $[Ca^{2+}]_i$, sodium hydroxide and fast green alone were locally applied in appropriate concentrations. These treatments had no effect on filopodial length, number or the intracellular calcium concentration.

Because a single cell normally extends many neurites and growth cones, some growth cones could be exposed to the pharmacological agent and NO donor, whereas others on the same cell could be exposed to only the pharmacological agent. Therefore, in the figures, the growth cones that were exposed to both NOC-7 and the pharmacological agent are labeled "Inhibitor Name & NOC-7" (e.g. Ryanodine & NOC-7). Other growth cones on the same cell were exposed to the pharmacological agent, but not NOC-7, and are thus labeled "Inhibitor Name Control" (e.g. Ryanodine Control).

Pharmacological agents

3-(2-Hydroxy-1-methyl-2-nitrosohydrazino)-N-methyl-1-propanamine   (NOC-7,   NO donor), cyclic Adenosine Diphosphate Ribose (cADPR), Ryanodine (9,21-dehydro, inhibitor of ryanodine receptor-mediated calcium release), and Dantrolene (sodium salt, inhibitor of ryanodine receptor-mediated calcium release) were all purchased from Calbiochem (San Diego CA). Lanthanum chloride heptahydrate was purchased from Sigma. NOC-7 and Dantrolene were made up in 100 mM sodium hydroxide to result in

stock concentrations of 100 mM and 40 mM, respectively. cADPR and lanthanum chloride were made up in water at stock concentration of 1 mM and 50 mM, respectively. Ryanodine was made up in dimethylsulfoxide (Sigma) at a stock concentration of 100 mM.

When pharmacological agents were used in combination with local NOC-7 application, they were added to the dish 30 minutes prior to the start of the experiment, except for lanthanum chloride that was added to the dish 2 minutes prior to NOC-7 application. Pharmacological agents were added by removing 200 µl of the conditioned medium from the dish, mixing the drug in that volume and then adding it back to the dish. All pharmacological agents were tested by themselves for possible effects on growth cone morphology or $[Ca^{2+}]_i$ before being used in the NOC-7 paradigm.

Calcium Imaging

Growth cone calcium imaging was done by injecting B5 neurons with the cell impermeant calcium indicator dye, Oregon Green 488 BAPTA-1, hexapotassium salt (Molecular Probes, Carlsbad CA). Oregon Green was made up at a stock concentration of 10 mM in 40 mM HEPES. Prior to injection, this solution was diluted in distilled water and resulted in a final concentration of 2.5 mM (10 mM HEPES) in the pipette. Images were acquired with a filter wheel, at an excitation of 490 nm and emission of 528 ± 25 nm. Following injection, cells were allowed 20-30 minutes for the dye to diffuse prior to the start of the experiment.

Immunocytochemistry for PKG and RyR

Once *Helisoma* B5 neurons had extended neurites tipped with growth cones, they were fixed and stained for either PKG or RyR, based on a protocol described in Cohan *et al.* (2001). Briefly, neurons were fixed in 0.1% Glutaraldehyde and 4% Paraformaldehyde (Electron Microscopy Sciences, Hatfield PA; in Small's buffer) for 5 minutes, washed twice with Small's buffer (5 min each), lysed in 0.1% Triton-X 100 (Sigma) for 5 minutes, washed twice with Small's buffer (5 min each), incubated in 100 mM glycine for 10 minutes, washed twice with Small's buffer (5 min each), and then blocked with Blotto (nonfat instant dry milk, 0.05% Tween in PBS) for 30 minutes. They were then incubated in primary antibody for 1 hour at 37º, washed 3 times in PBS-BSA buffer (PBS and 0.05% BSA; 5 min each wash), incubated in secondary antibody for 30 minutes at 37º, washed twice in PBS-BSA buffer (5 min each) and then coverslipped with Slow Fade (Molecular Probes).

PKG was localized with a polyclonal antibody for PKG-1α (Assay Designs, Ann Arbor, MI) at a dilution of 1:500, and the secondary antibody employed was Alexa Fluor 488 goat-anti-rabbit (Invitrogen) at a dilution of 1:400. RyR was localized with a monoclonal antibody for the RyR (Clone 34C; Affinity BioReagents, Golden, CO) at a dilution of 1:20 and the secondary antibody employed was Alexa Fluor 488 goat-anti-mouse (Invitrogen) at a dilution of 1:100. Images were acquired using the Olympus microscope setup as described above in combination with a filter set that had an excitation of 490 nm and emission of 528 ± 25 nm. No staining was observed in control experiments in which the primary antibody was omitted. Experimental and control dishes

were run in parallel during the immunocytochemistry procedure and identical camera parameters were used to capture the fluorescence images of experimental and control growth cones. Immunostaining experiments were repeated a minimum of three times and similar results were obtained in all dishes.

Results

We have previously demonstrated that local application of NOC-7 (100 µM) to individual B5 growth cones causes an elevation in the intracellular calcium concentration ($[Ca^{2+}]_i$) that results in an increase in filopodial length and a decrease in filopodial number (Welshhans & Rehder, 2005). We have further shown that these effects are mediated via a NO-activated second messenger pathway involving soluble guanylyl cyclase (sGC), protein kinase G (PKG), and cyclic adenosine diphosphate ribose (cADPR). In the present set of experiments, we have determined the signaling pathway activated downstream of cADPR and investigated how intracellular calcium stores and calcium influx across the plasma membrane contribute to the regulation of filopodial dynamics.

Local application of NOC-7 to B5 growth cones results in an increase in filopodial length and $[Ca^{2+}]_i$

To apply NO to individual growth cones, a micropipette was loaded with 100 µM NOC-7 and 2% fast green and this solution was locally applied to growth cones through the use of a Picospritzer (see Welshhans and Rehder, 2005 and Materials & Methods for details). Local application of 100 µM NOC-7 resulted in a transient increase in filopodial length, reaching a maximum of 26 ± 6% at 2 minutes following treatment (Figure 3.1B & 3.1C). This effect was significant (p ≤ 0.001) when compared to two types of controls. In each experiment, some growth cones were randomly chosen as 'experimental' growth cones,

Figure 3.1: Local application of 100 µM NOC-7 results in a transient increase in filopodial length, decrease in filopodial number and increase in the $[Ca^{2+}]_i$. (A,B) Phase contrast images of a growth cone immediately prior to (A) and 5 minutes following (B) local 100 µM NOC-7 application. Note the filopodial elongation around the entire growth cone. Scale bar: 10 µm. **(C)** Local application of 100 µM NOC-7 in a puff lasting 80 ms resulted in a transient increase in filopodial length that reached a maximum of 26 ± 6% 2 minutes following treatment and returned to pretreatment values within 30 minutes. Control growth cones (growth cones on the same cell, but not exposed to NOC-7) did not show an increase in filopodial length. Growth cones exposed to a vehicle control (NaOH Control) also did not shown a change in filopodial length. The increase in filopodial length resulting from the 100 µM NOC-7 application was significantly different as compared to both controls ($p \leq 0.001$ each). **(D)** Local application of 100 µM NOC-7 resulted in a decrease in filopodial number that was significantly different from control growth cones ($p \leq 0.001$). **(E)** Local application of 100 µM NOC-7 resulted in a transient increase in the $[Ca^{2+}]_i$ that was significantly different from control growth cones ($p \leq 0.001$). Note that application of a vehicle control (NaOH control) did not result in a change in the $[Ca^{2+}]_i$.
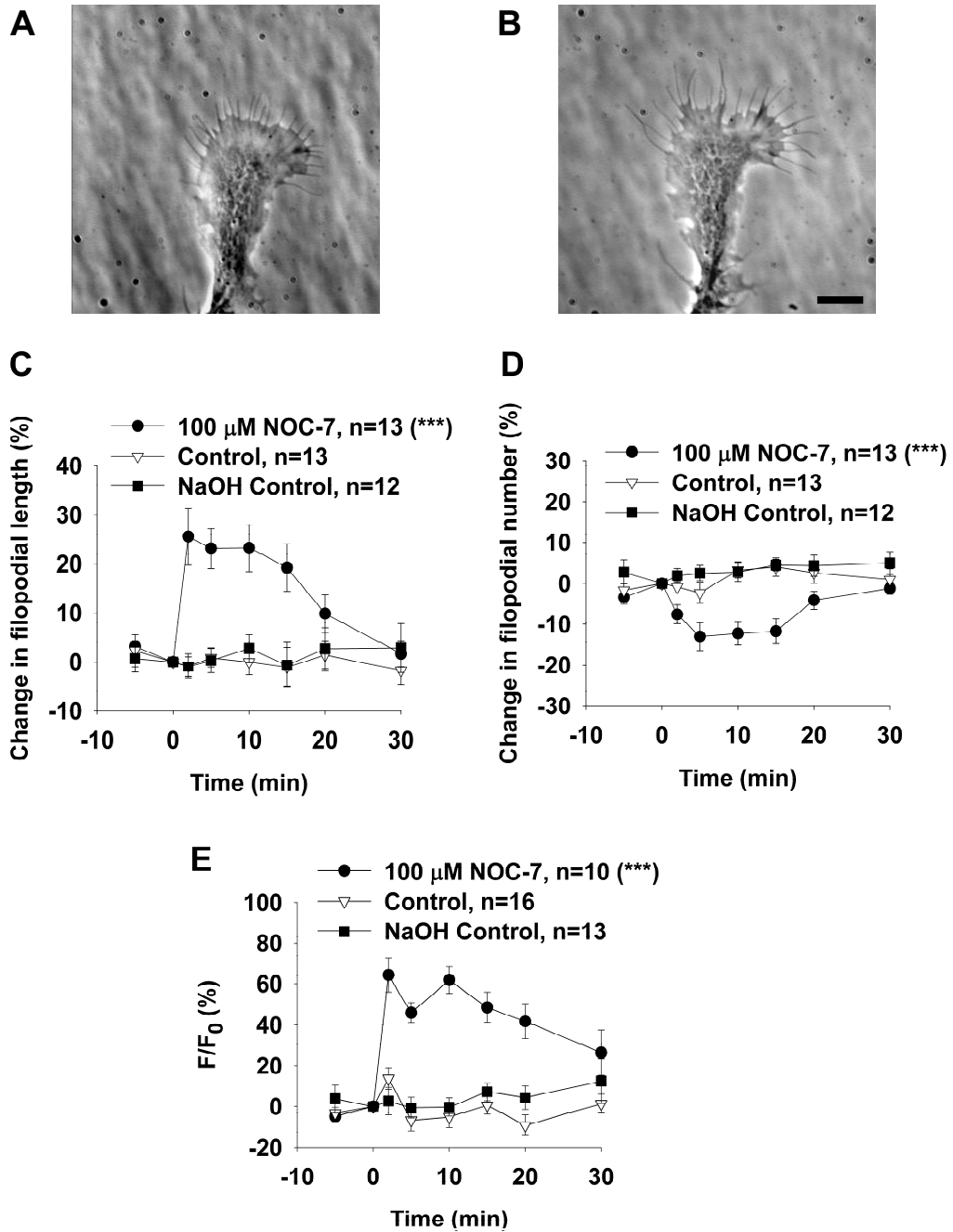
whereas other growth cones on the same neuron were designated as 'control' growth cones. 'Control' growth cones, which were located at distances greater than six to seven growth cone diameters from the 'experimental' growth cones, were used to assess whether the effect of a local NOC-7 application would remain confined to the stimulated growth cone. The second type of control was a 'vehicle only' control that tested for the effect of fluid application onto growth cones and contained the vehicle (sodium hydroxide (NaOH) and fast green in appropriate concentrations) without NOC-7 (termed "NaOH Control"). These experiments demonstrated that the local application of NOC-7 had an effect that was restricted to the stimulated growth cone and that the effect was NO-specific. Local application of 100 μM NOC-7 also resulted in a significant decrease in filopodial number, reaching -13 ± 3% at 5 minutes following treatment ($p \leq 0.001$ as compared to Control & NaOH Control; Figure 3.1D). Local application of NOC-7 (100 μM) also had effects on the $[Ca^{2+}]_i$, as determined by calcium imaging using the calcium indicator dye Oregon Green. Note that the calcium concentration is expressed as a relative percent change of fluorescence, normalized to $t = 0$ minutes (see Materials & Methods for further details). Following NOC-7 application, the Oregon Green fluorescence significantly increased by 64 ± 8% as compared to pre-treatment values ($p \leq 0.001$ as compared to Control & NaOH Control; Figure 3.1E). Note that the increase in $[Ca^{2+}]_i$ was limited to the stimulated growth cone and that other growth cones on the same cell that were not exposed to NO were unaffected ("Control"). In addition, the vehicle only control ("NaOH Control") also had no effect on $[Ca^{2+}]_i$.

Injection of cADPR mimics the effects of local NOC-7 application

We had suggested previously that the effect of NO on filopodial dynamics might involve release of calcium from intracellular stores by demonstrating that inhibition of the intracellular messenger cADPR blocked the NO-induced effects on filopodial length and $[Ca^{2+}]_i$ (Welshhans & Rehder, 2005). cADPR is an intracellular messenger that is known to act downstream of PKG and affect the release of calcium from intracellular stores (Galione *et al.*, 1993; Willmott *et al.*, 1996a; Lee, 2001). To extend our previous findings and further investigate the signaling pathway employed by NO to cause changes in the growth cone cytoskeleton, we next tested the hypothesis that if cADPR is activated downstream of NO application, then an experimental elevation of cADPR should mimic the effect of NO itself. The concentration of cADPR in B5 neurons was elevated by pressure-injection of cADPR (100 μM in the pipette) into the soma through a micropipette. Injection of cADPR resulted in an increase in filopodial length, reaching 44 ± 6% at 5 minutes following treatment (Figure 3.2A). This effect was significant (p ≤ 0.001) when compared to a control injection of vehicle (water) alone. 100 μM cADPR injections also resulted in a significant decrease in filopodial number (p ≤ 0.01 as compared to water control; Figure 3.2B). In addition to the effects on morphology, the $[Ca^{2+}]_i$ was also affected by cADPR. Injection of cADPR resulted in a significant (82 ± 19%) increase in Oregon Green fluorescence (p ≤ 0.001 as compared to water control; Figure 3.2C). Our findings that injection of cADPR reproduced the effects of NO application, together with previous results demonstrating that inhibition of cADPR

Figure 3.2: Injection of cADPR into B5 neurons results in an increase in filopodial length, decrease in filopodial number, and increase in the $[Ca^{2+}]_i$. (A) Injection of 100 µM cADPR resulted in a significant increase in filopodial length, reaching a maximum of $44 \pm 6\%$ 5 minutes following injection ($p \leq 0.001$ as compared to water control). Injection of a vehicle control (Water Control) did not have an effect on filopodial length. **(B)** Injection of 100 µM cADPR resulted in a transient, significant decrease in filopodial number ($p \leq 0.01$ as compared to water control). **(C)** Injection of 100 µM cADPR resulted in a significant increase in the $[Ca^{2+}]_i$ ($p \leq 0.001$ as compared to water control).
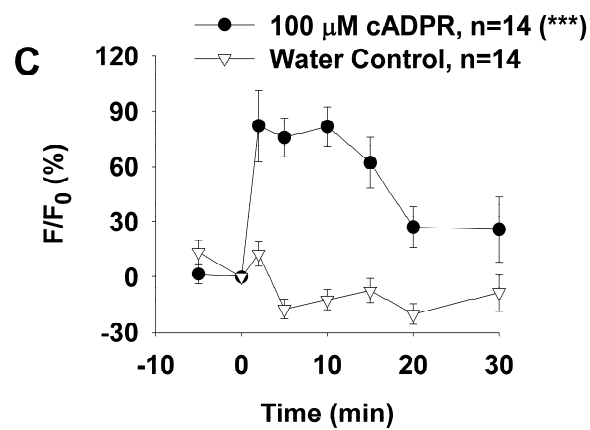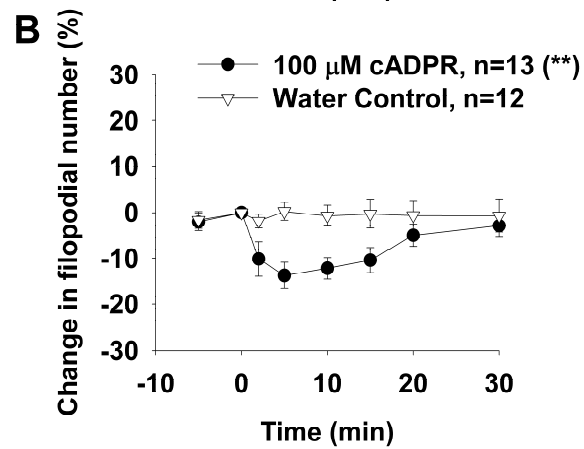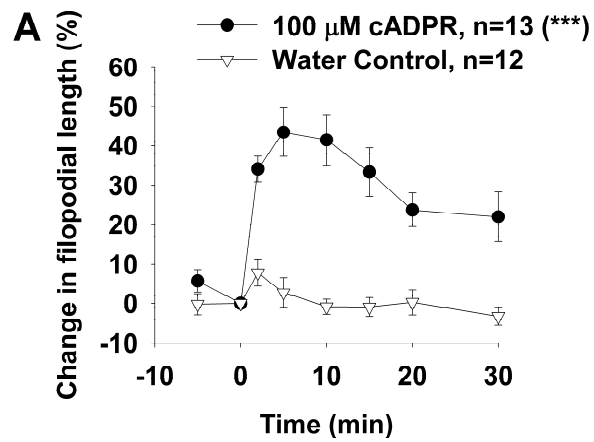
negates the effect of NO, thus supported our hypothesis that NO acts via cADPR to cause changes in growth cone morphology and $[Ca^{2+}]_i$.

Localization of PKG and ryanodine receptors in Helisoma B5 growth cones

We had demonstrated in a previous report (Van Wagenen & Rehder, 2001) that *Helisoma* B5 growth cones stain strongly for sGC, the immediate target of NO. Because we determined previously that NO was acting via sGC and PKG to mediate these NO-induced effects (Welshhans & Rehder, 2005), we sought to confirm these findings by localizing PKG in *Helisoma* B5 neurons. We performed immunocytochemistry with a polyclonal antibody against PKG-1α and examined staining within B5 growth cones. PKG has been cloned in another mollusc, *Aplysia*, and this antibody recognizes PKG in the nervous system of that species (Sung *et al.*, 2004). In the current study, PKG staining was seen in B5 neurons within the central domain of the growth cone (Figure 3.3B). Additionally, there was light staining for PKG within the lamellipodial region of the growth cone, but no staining was detectable in filopodia.

Because we had demonstrated that cADPR was a necessary component of this NO-induced pathway and its known function is to mediate release of calcium through the ryanodine receptor (RyR), we next employed immunocytochemistry to determine if RyRs were present within B5 growth cones as well. We employed a monoclonal antibody against the RyR (Clone 34C) and found that B5 growth cones stain heavily for RyRs (Figure 3.3E). Similar to that seen with the PKG antibody, and as expected, punctate staining was heaviest within the central domain of the growth cone, lighter within the
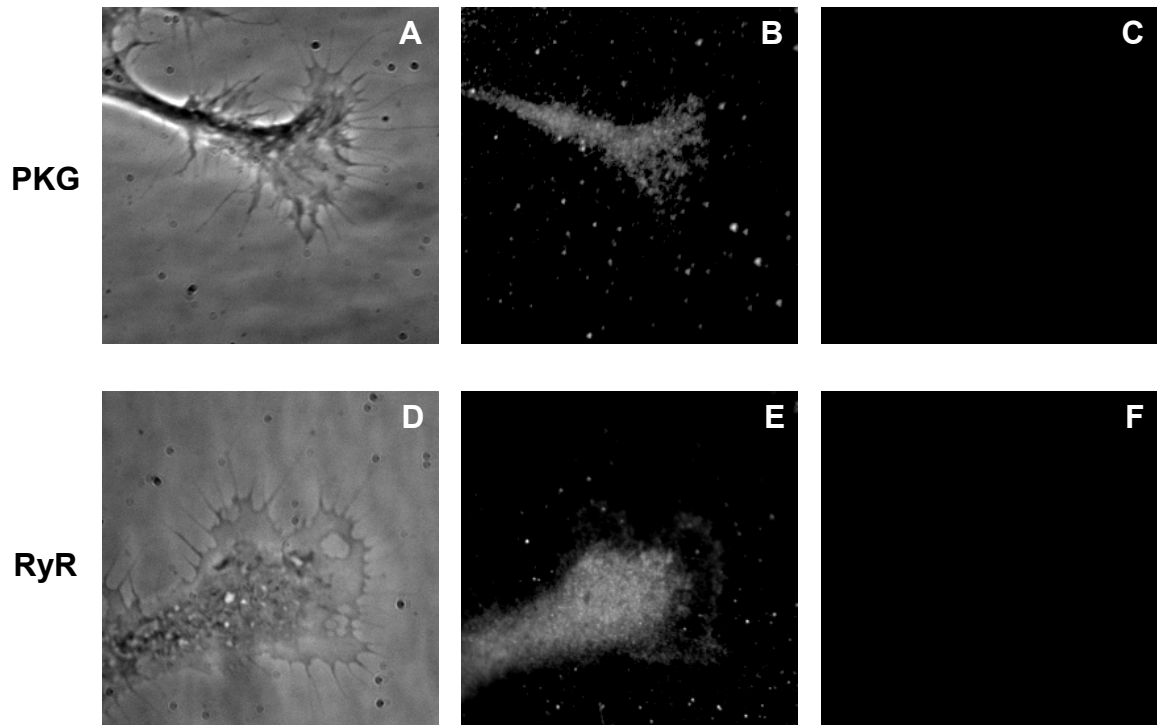
Figure 3.3: Protein Kinase G (PKG) and Ryanodine Receptors (RyRs) are localized in *Helisoma* B5 growth cones. Representative immunostained images of B5 growth cones show localization of staining for PKG **(B)** and RyRs **(E)**. The corresponding phase contrast images are shown in A & D, respectively. Note that the immunostaining for both PKG and RyRs is highest within the central domain of the growth cone, reduced within the lamellipodial region and not visible within filopodia. Omission of the primary antibody resulted in a loss of staining **(C, F)**. Scale bar: 10 μm.

lamellipodial region and not seen in filopodia. Note that omission of the primary antibody in both of these experiments (PKG and RyR) resulted in a loss of staining (Figure 3.3C & 3.3F).

Effects of nitric oxide on filopodial dynamics and $[Ca^{2+}]_i$ require ryanodine receptor-mediated intracellular calcium release

With the demonstration that RyRs are present in B5 growth cones and the knowledge that cADPR can cause intracellular calcium release through the RyR (Lee, 2001; Guse, 2005), we employed a pharmacological approach to determine if the RyR was involved in the NO-induced pathway that results in changes in growth cone morphology and $[Ca^{2+}]_i$. To test if the NO donor, NOC-7, indeed acted by releasing calcium via the RyR, neurons were preincubated with the ryanodine receptor blocker, ryanodine, and subsequently stimulated with NOC-7. We chose to use a high concentration (100 µM) of ryanodine (Ry) at which it has been shown to keep the channel in a closed state (Xu *et al.*, 1998; Verkhratsky, 2005). Following a 30 minute pretreatment with ryanodine, NOC-7 was locally applied onto individual growth cones. Pretreatment with ryanodine significantly blocked the NO-induced increase in filopodial length ($p \leq 0.001$ as compared to 100 µM NOC-7 alone; Figure 3.4A), strongly suggesting that the NO-induced increase in filopodial length was mediated via calcium release through the ryanodine receptor. In addition, pretreatment with ryanodine blocked the NO-induced decrease in filopodial number ($p \leq 0.01$ as compared to 100 µM NOC-7 alone; Figure 3.4B). Pretreatment with ryanodine also fully blocked the NO-induced increase in the $[Ca^{2+}]_i$ ($p \leq 0.001$ as

Figure 3.4: Inhibition of the ryanodine receptor with ryanodine blocks the NO-induced increase in filopodial length, decrease in filopodial number and increase in the $[Ca^{2+}]_i$. (A) Pretreatment with 100 μM ryanodine (Ry) blocked the NOC-7-induced increase in filopodial length (p ≤ 0.001 as compared to 100 μM NOC-7 alone). Treatment with 100 μM ryanodine alone had no effect on filopodial length. **(B)** The NOC-7 induced decrease in filopodial number was significantly inhibited by pretreatment with 100 μM ryanodine (p ≤ 0.01 as compared to 100 μM NOC-7 alone). **(C)** Pretreatment with 100 μM ryanodine significantly inhibited the NOC-7-induced increase in $[Ca^{2+}]_i$ (p ≤ 0.001 as compared to 100 μM NOC-7 alone). However, treatment with ryanodine at this concentration caused a slow decrease in calcium over the 30 minute time course (see 100 μM Ry & NOC-7 and Ry Control).
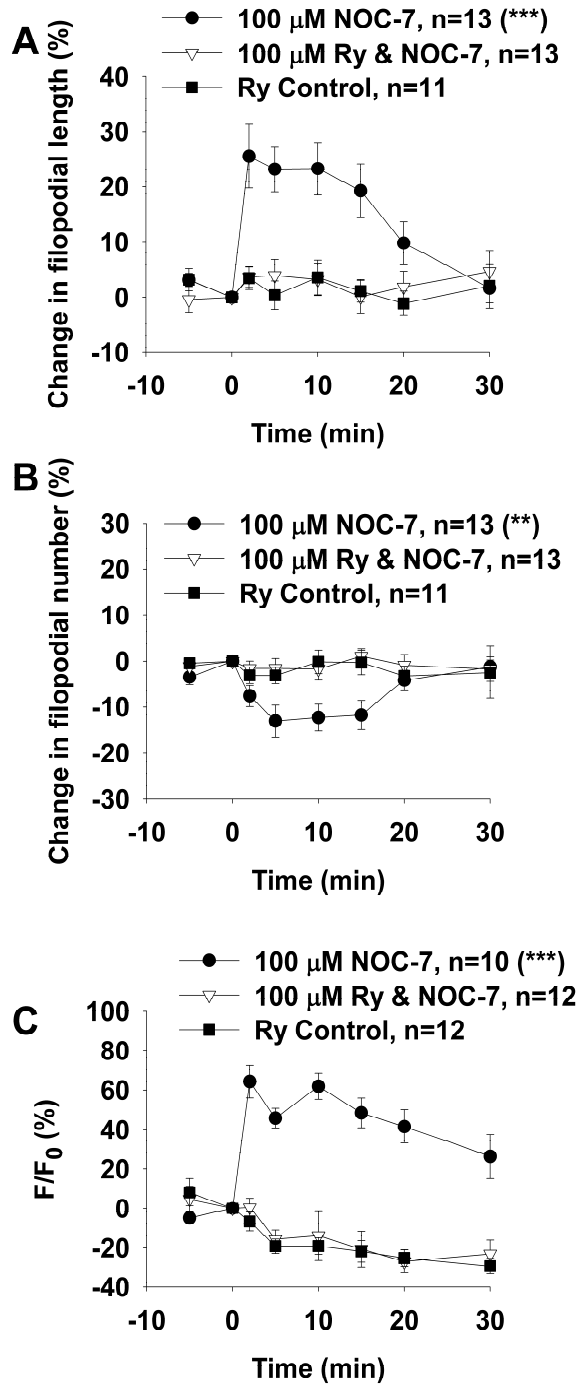
compared to 100 μM NOC-7 alone; Figure 3.4C). We noted, however, that the $[Ca^{2+}]_i$ slowly decreased in all ryanodine-treated growth cones (control and treated) over the 30 minute time course of this experiment, indicating a potential side effect of the drug.

Therefore, we next wanted to independently confirm our results obtained with ryanodine by using a second pharmacological inhibitor of ryanodine receptor-mediated calcium release, dantrolene. Dantrolene is thought to act as an inhibitor of the ryanodine receptor by decreasing the open-time probability of the RyR channel (Verkhratsky, 2005). Pretreatment with dantrolene (40 μM) significantly blocked the NO-induced increase in filopodial length and decrease in filopodial number ($p \leq 0.001$ as compared to 100 μM NOC-7 alone for both length and number; Figure 3.5A,B). Additionally, dantrolene pretreatment blocked the NO-induced increase in the $[Ca^{2+}]_i$ ($p \leq 0.001$; Figure 3.5C). Importantly, in these experiments we did not observe a slow decrease in $[Ca^{2+}]_i$, as was seen with ryanodine treatment (Figure 3.4C & 3.5C). The fact that we obtained the same results using two different ryanodine receptor blockers strongly supported the hypothesis that the NO-induced increase in the $[Ca^{2+}]_i$ occurs via RyR-mediated intracellular calcium release.

Nitric oxide's effect on the $[Ca^{2+}]_i$ requires calcium influx across the plasma membrane
Because application of NOC-7 resulted in a relative large increase in the $[Ca^{2+}]_i$ that outlasts the initial application of the NO donor, we next sought to investigate whether the increase in $[Ca^{2+}]_i$ was solely due to release from intracellular stores of calcium, or if influx of calcium across the plasma membrane might contribute to the long-lasting

Figure 3.5: RyR-mediated calcium release is necessary for the NO-induced increase in filopodial length, decrease in filopodial number and increase in the $[Ca^{2+}]_i$. (A,B) Pretreatment with 40 µM dantrolene blocked the NOC-7-induced increase in filopodial length (p ≤ 0.001 as compared to 100 µM NOC-7 alone) as well as the decrease in filopodial number (p ≤ 0.001 as compared to 100 µM NOC-7 alone). Treatment with 40 µM dantrolene alone did not have an effect on filopodial length or number. **(C)** The NOC-7-induced increase in $[Ca^{2+}]_i$ was significantly inhibited by pretreatment with 40 µM dantrolene (p ≤ 0.001 as compared to 100 µM NOC-7 alone). Note that treatment with dantrolene alone (Dantrolene Control) did not have an effect on the $[Ca^{2+}]_i$.

A

B

C
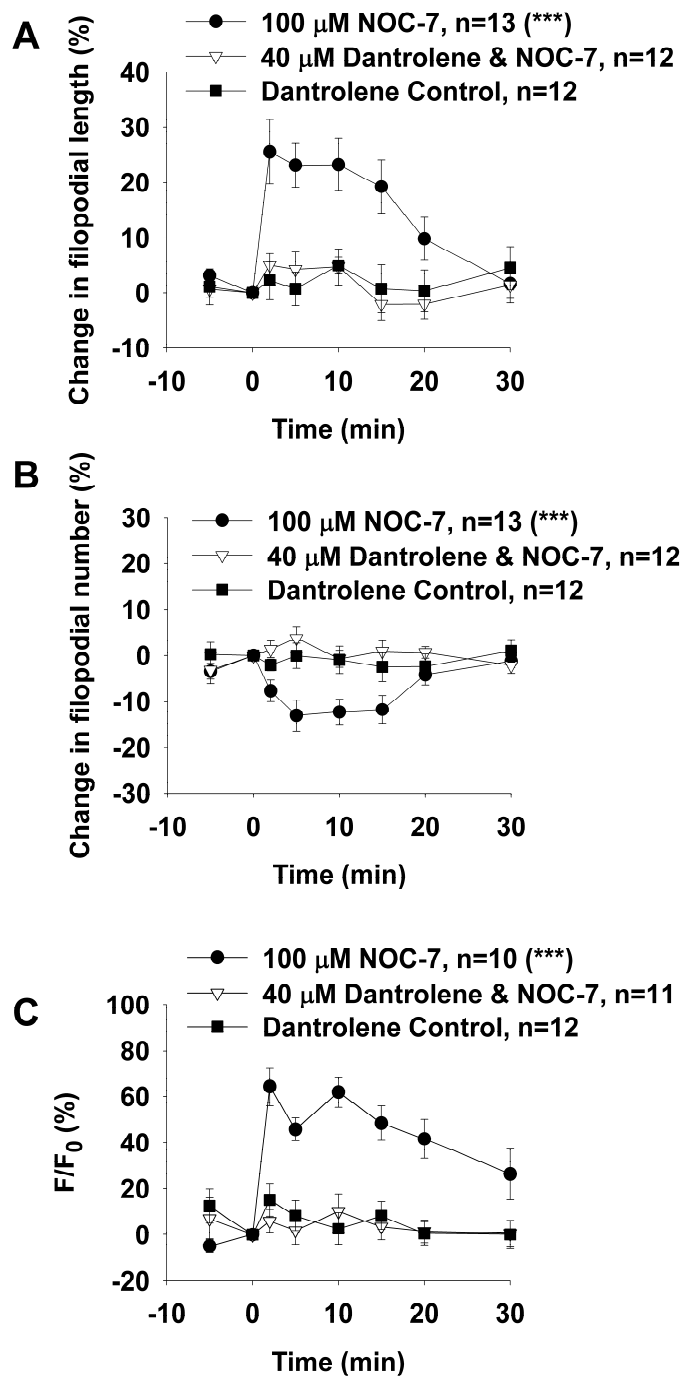
increase in $[Ca^{2+}]_i$ elicited by NO. Due to the absence of specific calcium channel blockers for this preparation, lanthanum chloride, a general blocker of calcium influx across the plasma membrane, was employed to test this possibility (Weiss, 1974; Hagiwara & Byerly, 1981). Lanthanum chloride blocks calcium permeable channels through competitive binding to calcium binding sites and then does not dissociate as easily from those sites as calcium (Weiss, 1974; Lansman, 1990). We used 50 μM lanthanum chloride, a concentration that has been employed previously in the *Helisoma* model system to block calcium transients and that was shown not to affect the distribution of f-actin within the growth cone (Williams & Cohan, 1995). When cells were treated with 50 μM lanthanum chloride ($LaCl_3$) immediately prior to local NO application, the NO-induced increase in $[Ca^{2+}]_i$ was significantly reduced ($p \leq 0.05$ as compared to NOC-7 alone; Figure 3.6A). This result suggested that influx of calcium through plasma membrane channels does contribute significantly to the NO-induced increase in $[Ca^{2+}]_i$. Interestingly, there was no overall significant difference between the $LaCl_3$ & NOC-7 and the $LaCl_3$ Control conditions, suggesting that $LaCl_3$ at this concentration was inhibiting calcium influx efficiently. Comparing individual time points between the $LaCl_3$ & NOC-7 and the $LaCl_3$ Control conditions, the $[Ca^{2+}]_i$ was only significantly different at the earliest time point measured (2 minutes; $p \leq 0.05$) suggesting that the underlying increase in $[Ca^{2+}]_i$ is likely due to release of calcium from intracellular stores that is not blocked by $LaCl_3$.

We next investigated the effect of the calcium channel blocker $LaCl_3$ on the NO-induced changes in growth cone morphology. When B5 neurons were treated with a local
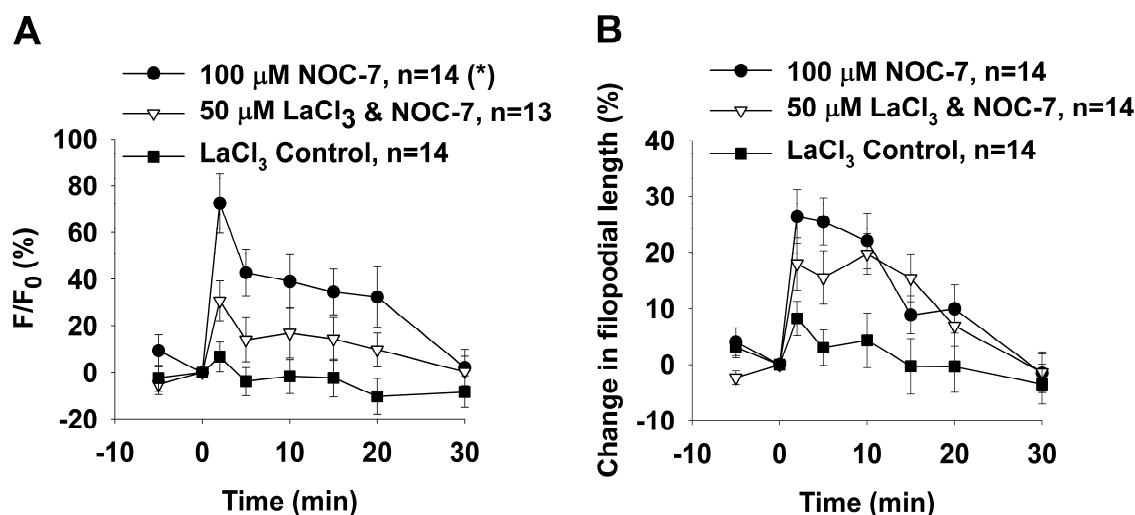
Figure 3.6: Calcium influx across the plasma membrane is a necessary component of the NO-induced increase in $[Ca^{2+}]_i$. **(A)** Addition of 50 µM lanthanum chloride (LaCl$_3$), followed by local NOC-7 application, significantly reduced the increase in the $[Ca^{2+}]_i$ seen upon local NOC-7 application alone ($p \leq 0.05$). There was no overall significant effect between LaCl$_3$ and NOC-7 versus LaCl$_3$ Control using ANOVA ($p = 0.10$), suggesting that calcium influx is responsible for a significant part of the increase in the $[Ca^{2+}]_i$ in response to NOC-7. However, in comparing individual time points, there was a significant difference in the $[Ca^{2+}]_i$ between the LaCl$_3$ and NOC-7 and the LaCl$_3$ Control conditions at the 2 minute time point only ($p \leq 0.05$), suggesting that this remaining increase in the $[Ca^{2+}]_i$ in the presence of LaCl$_3$ could be the calcium release from intracellular stores. **(B)** Inhibition of calcium influx across the plasma membrane with 50 µM LaCl$_3$ immediately followed by local NOC-7 application, resulted in only a small, non-significant reduction in the increase in filopodial length, as compared to NOC-7 treatment alone ($p = 0.54$). Note that treatment with LaCl$_3$ alone (LaCl$_3$ Control) also resulted in a small, but significant increase in filopodial length at t = 2 min ($p \leq 0.05$, LaCl$_3$ Control at t = 2 min as compared to LaCl$_3$ Control at t = 0 min).

NOC-7 application in the presence of 50 µM lanthanum chloride, the filopodial elongation normally seen with NOC-7 treatment was only nominally, but not significantly reduced (Figure 3.6B). Even taking into account that $LaCl_3$ by itself resulted in an increase in filopodial length at the 2 minute time point, and correcting for it in the NOC-7 & $LaCl_3$ condition (data not shown), it appeared that the $LaCl_3$ blockade of calcium influx had little effect on overall filopodial elongation beyond a possible delay for the first 5 minutes of exposure to NO. The finding that the rise in $[Ca^{2+}]_i$ was significantly inhibited in response to NO when calcium influx was blocked by $LaCl_3$, yet filopodial elongation appeared almost unaffected, suggested that relatively small elevations in calcium are sufficient to elicit significant filopodial elongation.

Discussion

Nitric oxide (NO) plays an essential role in the development of the nervous system in numerous species including molluscs, insects, chicks and mice (Wu *et al.*, 2001; Haase & Bicker, 2003; Chen *et al.*, 2004; Bicker, 2006; Currie *et al.*, 2006; Gifondorwa & Leise, 2006; Mejia-Garcia & Paes-de-Carvalho, 2007). Specifically, NO has been shown to regulate the developmental processes of neuronal proliferation, survival, and differentiation (Peunova & Enikolopov, 1995; Cheng *et al.*, 2003; Contestabile & Ciani, 2004; Zhang *et al.*, 2004). Experiments resulting in the loss of the enzyme responsible for NO synthesis, nitric oxide synthase (NOS), have demonstrated the essential role of NO for proper development. Knocking out NOS results in deleterious effects, ranging from premature death in *Drosophila*, in which there is only one isoform of NOS, to decreased viability in mice (when two isoforms were knocked out) (Tranguch & Huet-Hudson, 2003; Regulski *et al.*, 2004).

During development, NO is important in the formation of neuronal connections, including the processes of both neuritogenesis and neuronal migration. There are multiple *in vitro* studies that have demonstrated the importance of NO for growth cone motility and pathfinding. For example, in the pond snail *Helisoma,* application of exogenous NO to B5 neurons results in an increase in filopodial length and a dose-dependent decrease in the neurite outgrowth rate (Van Wagenen & Rehder, 1999; Trimm & Rehder, 2004). In chick retinal neurons, application of exogenous NO results in growth cone collapse (Ernst *et al.*, 2000). Additionally, in salamander photoreceptors, NO has been shown to regulate neuritic growth differentially in cone and rod cells (Zhang *et al.*, 2005). In cone cells,

exogenous NO results in an increase in the sprouting of neurites, whereas in rod cells, NO inhibits this growth. NO has also been shown to be an essential regulator of migration *in vivo*. In the grasshopper, a group of neurons in the midgut follow a specific migration route that is dependent on the presence of endogenous NO (Haase & Bicker, 2003). Collectively, these studies suggest a fundamental role for nitric oxide in the regulation of neuronal pathfinding.

NO is produced by nitric oxide synthases, which catalyze the conversion of L-arginine and oxygen to L-citrulline and NO. There are now 2 major pathways through which NO is thought to act, S-nitrosylation and/or binding to and activation of soluble guanylyl cyclase (sGC). In the former pathway, proteins are S-nitrosylated when NO binds to the thiol group of cysteine, resulting in an S-nitrosothiol (Stamler *et al.*, 1992; Hess *et al.*, 2005). Many proteins, including some ion channels and transcription factors, are subject to S-nitrosylation, which can result in a change in their functional activity (Hess *et al.*, 2005). In the latter pathway, NO binds directly to the heme group of sGC and activates it, resulting in the conversion of guanosine triphosphate to cyclic guanosine monophosphate (cGMP). There are then 3 major targets of cGMP: protein kinase G (PKG), phosphodiesterases and cyclic nucleotide gated ion channels. In a previous study, we were able to inhibit all effects of NO described in this study by inhibiting either sGC or PKG, indicating that, at least in *Helisoma* B5 neurons, NO acts via sGC and PKG to affect filopodial motility (Welshhans & Rehder, 2005).

Nitric oxide acts via cADPR and ryanodine receptor-mediated intracellular calcium release

One target of PKG is ADP-ribosyl cyclase, which is the enzyme responsible for the production of cyclic adenosine diphosphate ribose (cADPR) (Galione *et al.*, 1993; Willmott *et al.*, 1996a; Lee, 2001). We have demonstrated in a previous study that pharmacological inhibition of either ADP-ribosyl cyclase or cADPR significantly blocks the NO-induced increase in filopodial length as well as the increase in intracellular calcium (Welshhans & Rehder, 2005). We have now further extended this study to demonstrate that injection of cADPR directly into the B5 neuron also results in an increase in filopodial length and $[Ca^{2+}]_i$, mimicking the effect of NO treatment. There are multiple studies in which cADPR has been injected into various neuronal cell types, but the outcomes have been variable. Injection of cADPR into *Aplysia* buccal neurons results in an increase in the intracellular calcium concentration in both the soma as well as the neurites (Mothet *et al.*, 1998). However, injection into various mammalian neurons usually does not cause an increase in calcium on its own, but it does potentiate calcium release initiated by other methods (De Flora *et al.*, 1996; Hashii *et al.*, 2000). Therefore, a species-specific difference may exist in the response of neurons to direct injection of cADPR, suggesting that cADPR may serve a different role in different neurons.

The pathway of NO that leads to the downstream activation of PKG, cADPR and intracellular calcium release has been well-documented in sea urchin eggs, but little is known about this pathway in neurons. Exogenous application of NO or cADPR onto sea urchin egg homogenates results in an increase in $[Ca^{2+}]_i$ (Willmott *et al.*, 1996a) and there

is evidence that PC12-16A cells also respond to exogenous application of NO or cADPR with an increase in $[Ca^{2+}]_i$ (Clementi *et al.*, 1996). A more recent report has indicated that this pathway also exists in the vertebrate brain, specifically involving GABAergic neurons within the rat nucleus tractus solitarii (Wang *et al.*, 2006). We here report that NO affects growth cone morphology in *Helisoma* B5 neurons via a pathway involving sGC, cADPR, and ryanodine receptor-mediated intracellular calcium release, suggesting that this pathway may exist in neurons in a more widespread fashion than previously realized. It is important to note that this is, to our knowledge, the first report of the presence of this signaling pathway in growth cones.

cADPR has been linked to the modulation of the ryanodine receptor, however, it is unknown whether cADPR exerts its action on the ryanodine receptor directly and/or via an intermediate binding protein (Higashida *et al.*, 2001; Guse, 2005). It is interesting to note that a study employing sea urchin egg homogenates demonstrated that calmodulin was necessary for the binding of cADPR to its receptor (Thomas *et al.*, 2001). This is in line with a previous finding from our lab that NO's action on growth cone morphology required the presence of calmodulin (Van Wagenen & Rehder, 1999). In the current study, inhibition of the ryanodine receptor prior to NOC-7 application significantly blocked the NO-induced changes in growth cone morphology and $[Ca^{2+}]_i$, supporting the following pathway for the action of NO: NO, sGC, cGMP, PKG, cADPR, calcium release from ryanodine receptor controlled calcium stores (Figure 3.7). These results suggest, for the first time, that nitric oxide activates the sGC-PKG-cADPR-RyR pathway
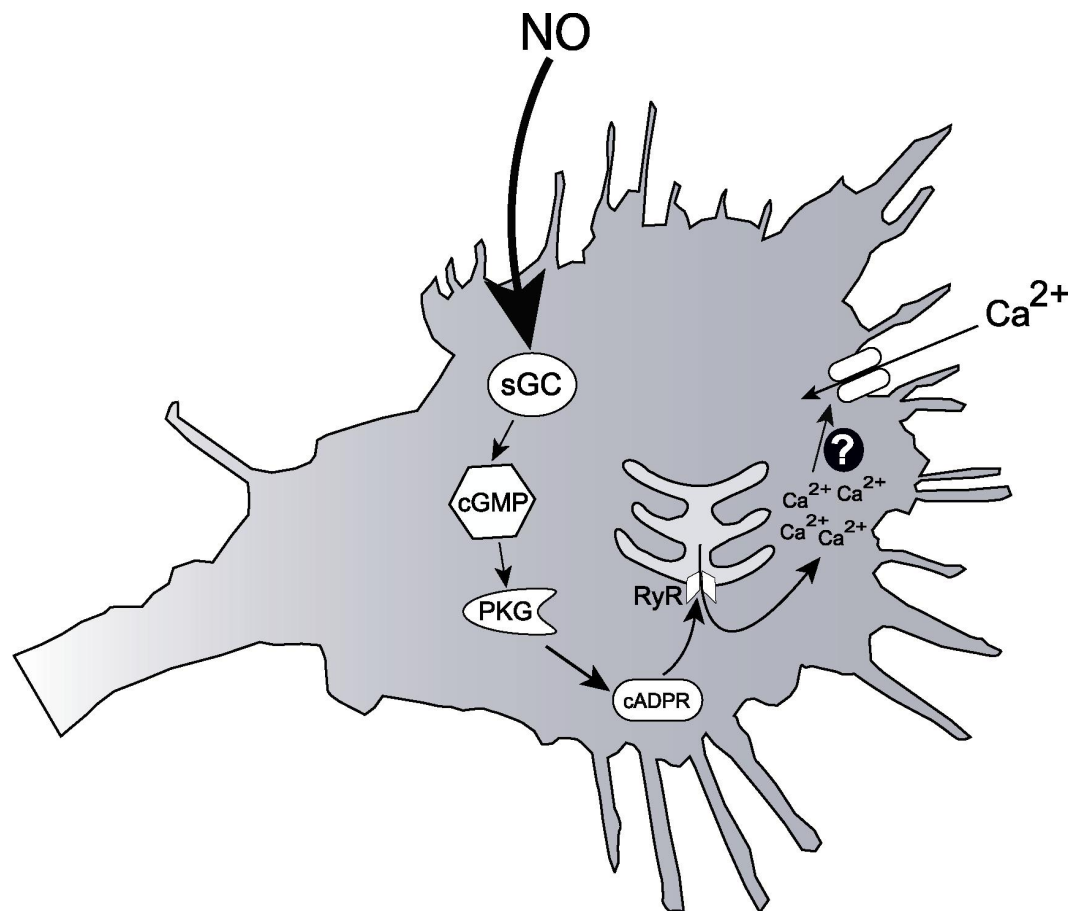
Figure 3.7: Summary of the pathway by which NO causes an increase in $[Ca^{2+}]_i$ that results in changes in growth cone morphology. NO produced in the vicinity of a migrating growth cone causes filopodial elongation and a reduction in filopodial number by stimulating the enzyme sGC that in turn increases the production of cGMP. cGMP activates protein kinase G (PKG) that in turn leads to the production of cADPR. cADPR causes the release of calcium from intracellular stores via the ryanodine receptor. The calcium release from intracellular stores is amplified by influx of calcium across the plasma membrane. The mechanism(s) by which the intracellular calcium release in B5 neurons triggers calcium influx is presently unknown.

in growth cones, and that the subsequent calcium release can directly modulate growth cone motility and thereby could affect pathfinding.

We further demonstrate immunocytochemically that PKG and the RyR, two important players in the NO-mediated pathway leading to changes in growth cone dynamics, are localized to *Helisoma* B5 growth cones. Previous studies have demonstrated immunocytochemically that both PKG and RyRs are found within growth cones of other species. A study employing the same primary antibody used in this experiment demonstrated the presence of PKG within growth cones of E7 chick dorsal root ganglion neurons (Dontchev & Letourneau, 2002). Growth cones from mouse dorsal root ganglion neurons stain for RyRs (Ooashi *et al.*, 2005). These growth cones show a staining pattern that is punctuate in nature, as would be expected for a protein located in the endoplasmic reticulum membrane, and closely resembles the pattern of staining we see within *Helisoma* B5 growth cones. Therefore, the current study demonstrates that PKG and RyRs are localized in *Helisoma* B5 growth cones, thereby further supporting the presence of this NO-induced signaling pathway as a regulator of growth cone morphology.

Nitric oxide results in a secondary influx of calcium across the plasma membrane
Our findings that any increase in $[Ca^{2+}]_i$ in response to stimulation with NO could be blocked when calcium release from ryanodine-sensitive stores was inhibited through the application of either a high concentration of ryanodine or dantrolene clearly suggested that calcium release from intracellular stores serves as a necessary step in this NO

signaling pathway. In an attempt to determine whether the increase in $[Ca^{2+}]_i$ was solely derived from intracellular stores, or whether calcium influx contributed to the overall increase in $[Ca^{2+}]_i$, we provide evidence that calcium influx across the plasma membrane contributes to the overall increase in $[Ca^{2+}]_i$ seen upon NO stimulation. This was demonstrated by the blockage of a significant amount of the calcium increase normally seen with NO stimulation upon treatment with the calcium channel blocker $LaCl_3$. We used 50 μM $LaCl_3$, because lanthanum chloride at this concentration had been shown to completely block calcium transients in a buccal neuron from *Helisoma*, but had no effect on the distribution of f-actin within the growth cone (Williams & Cohan, 1995). However, we do not know whether 50 μM $LaCl_3$ completely blocked all calcium influx in our experiments. Unfortunately, the use of higher concentrations of $LaCl_3$, such as 100 μM, has been reported to have adverse effects on growth cone shape and motility (Mattson & Kater, 1987) and could not be pursued. In their report, treatment of *Helisoma* B5 neurons with 100 μM $LaCl_3$ (double the concentration employed in our experiments) resulted in a highly significant decrease in filopodial number (Mattson & Kater, 1987). We noticed a similar effect when growth cones were treated with 50 μM $LaCl_3$, preventing us from examining the effect of blocking calcium influx on NO-induced changes in filopodial number. Although the use of $LaCl_3$ clearly indicated that calcium influx plays a significant part in the overall increase in $[Ca^{2+}]_i$ seen in B5 neurons in response to NO stimulation, the lack of specific calcium channel blockers for this preparation severely hampers immediate progress in determining the different calcium entry mechanisms that may contribute to the general calcium signal.

A number of different types of plasma membrane calcium channels have been shown to be present in growth cones, including voltage gated calcium channels and transient receptor potential (TRP) channels. L-type voltage gated calcium channels are present in growth cones from many species and are involved in the regulation of growth cone motility, including the axon outgrowth rate and growth cone turning (Ohbayashi *et al.*, 1998; Hong *et al.*, 2000; Nishiyama *et al.*, 2003; Tang *et al.*, 2003). There are two types of TRP channels that may regulate growth cone motility. TRPC channels have been demonstrated to play roles in growth cone turning and morphology (Greka *et al.*, 2003; Li *et al.*, 2005; Shim *et al.*, 2005; Wang & Poo, 2005) and a recent report demonstrated that TRPV channels may also regulate growth cone morphology (Goswami *et al.*, 2007). There is evidence, although still inconclusive and highly debated, that certain types of TRP channels may actually be the little-understood store-refilling channels, and therefore, may also be activated in the pathway described here, as a mechanism of refilling the stores that would be depleted by stimulation with NO (Ramsey *et al.*, 2006).

Despite the uncertainty regarding the contribution of calcium influx to the total increase in $[Ca^{2+}]_i$ observed upon treatment with NOC-7, it is clear that this calcium influx is secondary to the release of calcium from ryanodine-sensitive stores. It is presently unclear which mechanism might be responsible for translating the initial (and presumably short-term) release of calcium from intracellular stores into the calcium influx that ultimately results in the longer-term calcium elevation seen in response to NO. Future experiments will be directed to determine whether the initial release from intracellular stores serves as a short-term signal that results in signal amplification

mediated via calcium influx, and if this amplification is responsible for turning the brief NOC-7 stimulus, which lasts for less than one second, into a calcium signal that lasts 20-30 minutes.

Changes in $[Ca^{2+}]_i$ and their translation into cytoskeletal changes

It is apparent from our results that elevations in $[Ca^{2+}]_i$ do not need to be large to result in significant changes in filopodial parameters. Even after the increase in $[Ca^{2+}]_i$ has been reduced significantly in the presence of $LaCl_3$, compared to treatment with NOC-7 alone, filopodial elongation was still strong (Figure 3.6B). Although we do not know the absolute levels of $[Ca^{2+}]_i$ in these experiments, the general conclusion that small increases in $[Ca^{2+}]_i$ are sufficient to change filopodial length is supported by an earlier report that demonstrated that an increase as small as 50 nM in growth cones of the same neuron is sufficient to result in a significant elongation of filopodia (Rehder & Kater, 1992). Interestingly, the duration of cytoskeletal changes observed matched the time-course of elevation in $[Ca^{2+}]_i$, an observation we had also made in previous studies and that suggested that the elevation in $[Ca^{2+}]_i$ and filopodial elongation are causally related. The finding that filopodial responses were very similar between growth cones treated with NOC-7 alone versus NOC-7 and $LaCl_3$, despite a significant reduction in the $[Ca^{2+}]_i$ in the presence of $LaCl_3$, indicates that the growth cone may not be able to differentiate between the two levels of $[Ca^{2+}]_i$, or alternatively, that a ceiling has been reached beyond which further increases in $[Ca^{2+}]_i$ do not result in further increases in filopodial length. It is also possible that the calcium entering the cytosol from different sources, such as from

intracellular stores versus the extracellular space, while causing different overall calcium increases within a growth cone as measured with Oregon Green, could result in similar changes in $[Ca^{2+}]_i$ in microdomains that contain the signaling machinery responsible for regulating filopodial dynamics. In this case, the same local increase in $[Ca^{2+}]_i$ in response to different treatments (not detectable with our imaging system due to limited spatial and temporal resolution) could explain how a growth cone-wide difference in $[Ca^{2+}]_i$ could result in the same filopodial response.

Conclusions

This study identifies a NO signaling pathway in identified B5 neurons from the buccal ganglion of the fresh water snail *Helisoma trivolvis* that has been demonstrated so far mainly in non-neuronal cells. This pathway, by which NO acts via sGC to activate PKG and cADPR, which in turn causes the release of calcium from ryanodine-sensitive stores, directly affects growth cone motility, thus placing NO in a prominent position to act as an effective regulator of neuronal development.

Chapter 3.2: Additional experiments examining the role of the NO/cGMP pathway in the regulation of growth cone filopodia

Activation of neuronal nitric oxide synthase is not a major contributor to the NO-donor induced changes in filopodial dynamics

Although nitric oxide can be made by the reduction of nitrites and nitrates, it is most commonly produced through the conversion of L-arginine and oxygen to L-citrulline and NO. The enzyme responsible for this conversion is nitric oxide synthase (NOS), which is stimulated by the presence of calcium/calmodulin (Ca^{2+}/CaM). Because B5 *Helisoma* neurons are known to contain NOS (Van Wagenen & Rehder, 2001), we wanted to test the possibility that the local exogenous application of NO donor could be activating a feedback loop that would result in a changed production of NO within the B5 neuron. Theoretically, such a feedback loop could function to either amplify (positive feedback) or inhibit (negative feedback) intrinsic NO production. In the current experiment, we investigated the possibility of a positive feedback loop in which cGMP, produced by sGC in response to NO, would activate calcium, which would in turn activate Ca^{2+}/CaM, resulting in the activation of neuronal nitric oxide synthase (nNOS).

To test whether such a feedback loop might exist in B5 neurons, this hypothetical loop was broken by employing a specific intracellular inhibitor of nNOS, 7-Ni. Growth cones were preincubated with 10 µM 7-Ni for 25 minutes, and then 100 µM NOC-7 was applied using the standard paradigm. This treatment did not result in a significant difference in filopodial length or number, when comparing the 7-Ni and NOC-7

treatment to NOC-7 alone (Figure 3.8A & 3.8B; p = 0.68 as compared to 100 µM NOC-7 alone for length; p = 0.22 as compared to 100 µM NOC-7 alone for number). This result suggests that a feedback loop involving NOS does not add measurably to the concentration of NO already produced by the NO donor. It does not rule out the possibility that a feedback loop may be involved; the contribution of a feedback loop might be uncovered at lower concentrations or shorter application times of the NO donor.

An independent test of this hypothesis would be to simply activate NOS through an elevation in calcium and examine subsequent changes in growth cone morphology. In this hypothetical experiment, the intracellular calcium concentration would be elevated via depolarization of the neurons with potassium chloride. However, this experiment is not feasible because an increase in the intracellular calcium concentration (irrelevant of the source) leads to an increase in filopodial length and a decrease in filopodial number, which confounds the dependent variable. Additionally, there are no other known stimulators of NOS available, thus it is currently not possible to test this hypothesis in an independent fashion.

Inhibition of all phosphodiesterases does not result in a change in filopodial length, but does cause a decrease in filopodial number

cGMP acts on three major targets: phosphodiesterases (PDEs), cyclic nucleotide gated (CNG) ion channels, and protein kinase G (PKG). As demonstrated above, NO was shown to act through PKG, but the following experiments were performed to test whether
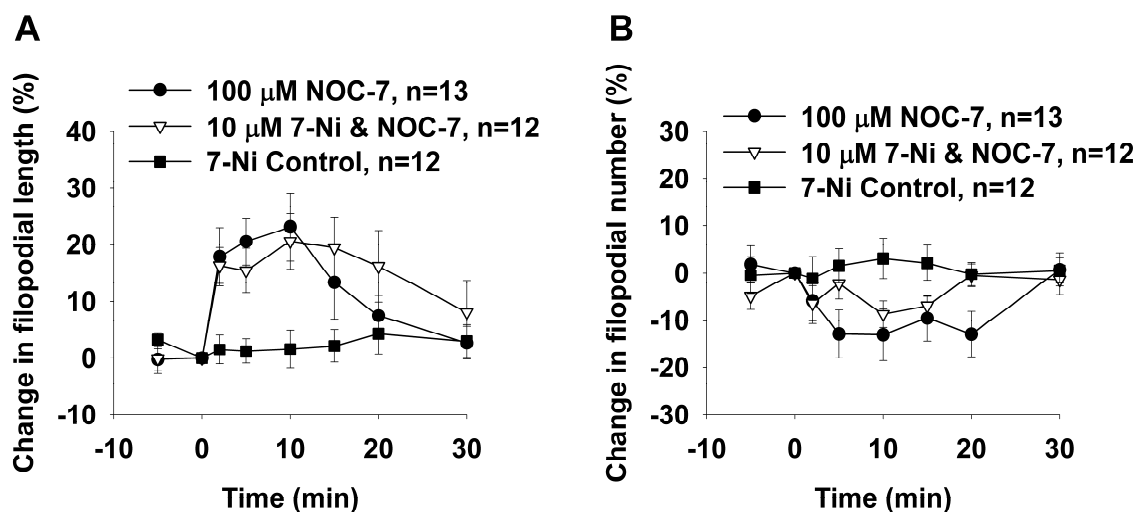
Figure 3.8: Inhibition of nNOS does not block the NO-induced changes in growth cone morphology. (A) Growth cones were pretreated with the nNOS inhibitor, 10 μM 7-Ni, for 25 minutes and then 100 μM NOC-7 was locally applied. Filopodial length transiently and significantly increased on these growth cones, as compared to control growth cones ($p \leq 0.01$). This transient increase in filopodial length was not significantly different from growth cones that were treated with NOC-7 alone ($p = 0.68$), suggesting that the NO-induced increase in filopodial length is due to the NOC-7 application and is not significantly amplified through a feedback loop involving NOS. **(B)** Pretreatment with 10 μM 7-Ni, followed by local 100 μM NOC-7 application, results in a small, non-significant decrease in filopodial number ($p = 0.16$ as compared to 10 μM 7-Ni Control). This decrease is not significant when compared to treatment with 100 μM NOC-7 alone ($p = 0.22$).

PDEs might play any role in the effects of NO described above. There are 9 different types of PDEs, which hydrolyze cAMP and/or cGMP. We were interested in investigating PDEs because of a previous study that demonstrated that the effects of NO on growth cone morphology were mediated via PDEIII (Tsukada *et al.*, 2002). In the initial experiment, a general inhibitor, IBMX, was employed to inhibit all types of PDEs. It was expected that if NO was acting via PDEIII, then its inhibition should mimic the results that are seen with local NO stimulation (i.e. increase in filopodial length and a decrease in filopodial number).

Application of the general phosphodiesterase inhibitor, 100 µM IBMX, to growth cones did not result in a significant change in filopodial length as compared to DMSO control growth cones (Figure 3.9A; $p = 0.13$ as compared to DMSO control growth cones; $p \leq 0.05$ as compared to NOC-7 alone). However, application of IBMX did result in a significant, transient decrease in filopodial number (Figure 3.9B; $p \leq 0.05$ as compared to DMSO control growth cones; $p = 0.42$ as compared to NOC-7 alone). Although phosphodiesterase inhibition did change filopodial number in a manner similar to NO application, filopodial length was not affected. As such, these results were inconclusive, especially in light of the fact that inhibiting all PDEs would have nonspecific effects on other phosphodiesterases besides the one in which we were specifically interested (PDEIII). Therefore, the next experiment employs a specific inhibitor of PDEIII to test if it specifically was involved in the NO-mediated changes in filopodial length and number.
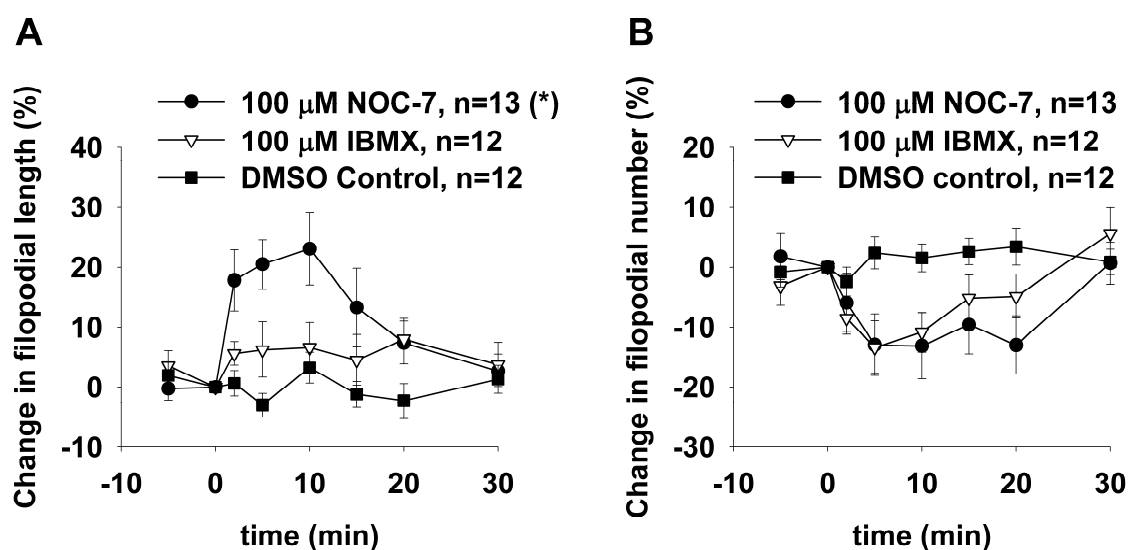
Figure 3.9: Inhibition of phosphodiesterases does not result in a change in filopodial length, but does cause a decrease in filopodial number. (A) Application of the general phosphodiesterase inhibitor, 100 µM IBMX, does not result in a significant change in filopodial length, as compared to DMSO control growth cones ($p = 0.13$ as compared to DMSO control; $p \leq 0.05$ as compared to 100 µM NOC-7). **(B)** Application of 100 µM IBMX does result in a significant decrease in filopodial number, as compared to DMSO control growth cones ($p \leq 0.05$ as compared to DMSO control growth cones; $p = 0.42$ as compared to NOC-7 alone).

Nitric oxide's effects on filopodial dynamics are not dependent on phosphodiesterase III and protein kinase A

A study in rat dorsal root ganglion neurons demonstrated that application of a NO-donor results in changes in neurite and growth cone morphology via inhibition of PDEIII and subsequent elevation of protein kinase A (PKA) (Tsukada *et al.*, 2002). Because PDEIII is inhibited by cGMP, if NO is acting via this pathway, then mimicking that inhibition pharmacologically should produce the same filopodial elongation that is seen with NO treatment. Therefore, PDEIII was inhibited with 1 μM milrinone, which resulted in a transient increase in filopodial length, reaching a maximum of $14.5 \pm 3.0\%$ five minutes following treatment and returning to pretreatment values within 15 minutes of application (Figure 3.10A; $p = 0.05$ as compared to 100 μM NOC-7, $p = 0.08$ as compared to DMSO control). However, 1 μM milrinone had no effect on filopodial number (Figure 3.10B; $p = 0.62$ as compared to DMSO control; $p \leq 0.05$ as compared to NOC-7 alone). Although inhibition of PDEIII resulted in a transient increase in filopodial length, it was not as large as that which is seen with 100 μM NOC-7 application. In addition, PDEIII inhibition did not result in a decrease in filopodial number. The effects of milrinone on filopodial dynamics may have been due to a concentration-dependent effect of this pharmacological inhibitor, and a higher concentration of milrinone may result in a larger increase in filopodial length and a decrease in filopodial number. However, a concentration-dependent effect of the drug was not investigated; instead a downstream target of PDEIII was inhibited to determine whether this pathway was involved in the NO-induced increase in filopodial length.
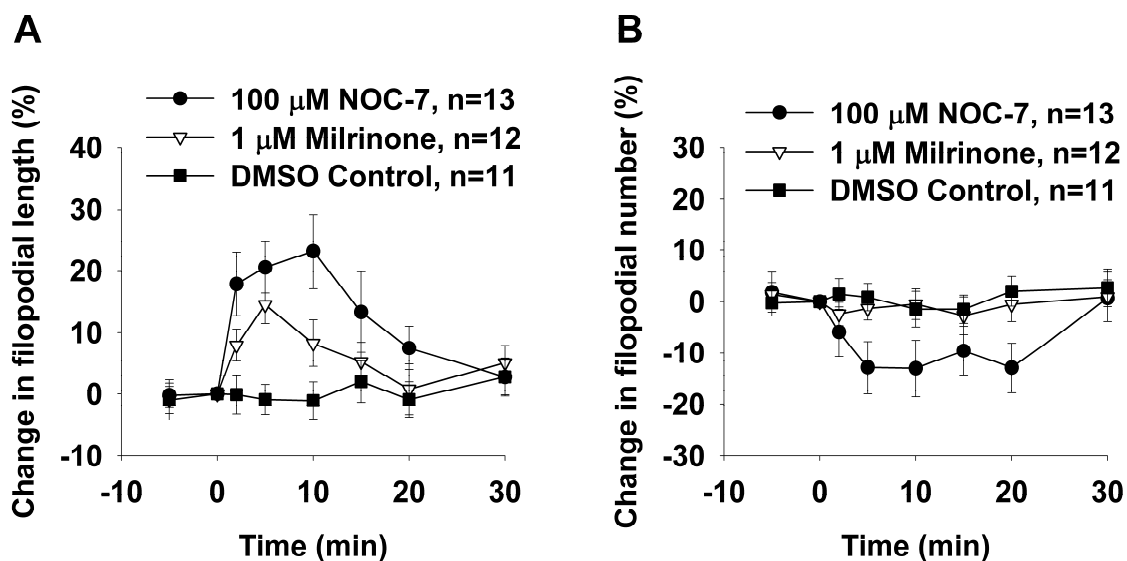
Figure 3.10: Inhibition of phosphodiesterase III (PDEIII) causes an increase in filopodial length, but does not change filopodial number. (A) Inhibition of PDEIII with 1 µM milrinone results in a transient increase in filopodial length, reaching a maximum of 14.5 ± 3.0% within 5 minutes of application, and returns to pretreatment values within 20 minutes. This increase was not significant overall as compared to DMSO control (p = 0.08), but was significant as compared to 100 µM NOC-7 alone (p = 0.05). However, analysis of individual time points did reveal significance at the 5 minute time point when comparing the 1 µM milrinone treatment to DMSO control (Student's t-test, $p \leq 0.001$). **(B)** Inhibition of PDEIII with 1 µM milrinone has no effect on filopodial number (p = 0.62 as compared to DMSO control).

PKA, which is a downstream target of PDEIII, was inhibited in order to determine if this pathway is involved in the NO-induced increase in filopodial length. In this pathway, if PDEIII is inhibited by cGMP, this would lead to an increase in cAMP, which would thereby lead to an increase in PKA. Therefore, we inhibited PKA and puffed on NOC-7 to determine if this would block the NO-induced filopodial elongation. When PKA was specifically inhibited with 1 μM Myristoylated PKA Inhibitor 14-22 (PKI) for 25 minutes and then 100 μM NOC-7 was locally applied onto growth cones, there was still a transient increase in filopodial elongation that was not significantly different from 100 μM NOC-7 treatment alone (Figure 3.11A; $p = 0.68$). Filopodial number also showed a small decrease from control values, which was not significantly different from 100 μM NOC-7 treatment alone (Figure 3.11B; $p = 0.06$). These results demonstrate that NO is not acting via PKA to result in the changes in filopodial length or number. Overall, in *Helisoma* B5 neurons, it appears that NO is not causing the changes in growth cone morphology via a pathway involving PDEIII and/or PKA. In addition, currently there are no acceptable pharmacological tools with which to study the contribution of CNG ion channels to this pathway; thus at present we conclude that local application of NO to B5 neurons is mainly leading to activation of PKG.

NO-induced changes in filopodial dynamics are mediated, at least in part, by plus-end actin addition

Although NO is acting via multiple second messengers to exert its effects on the cytoskeleton, it is unknown whether the final effects are mainly on actin. It would be
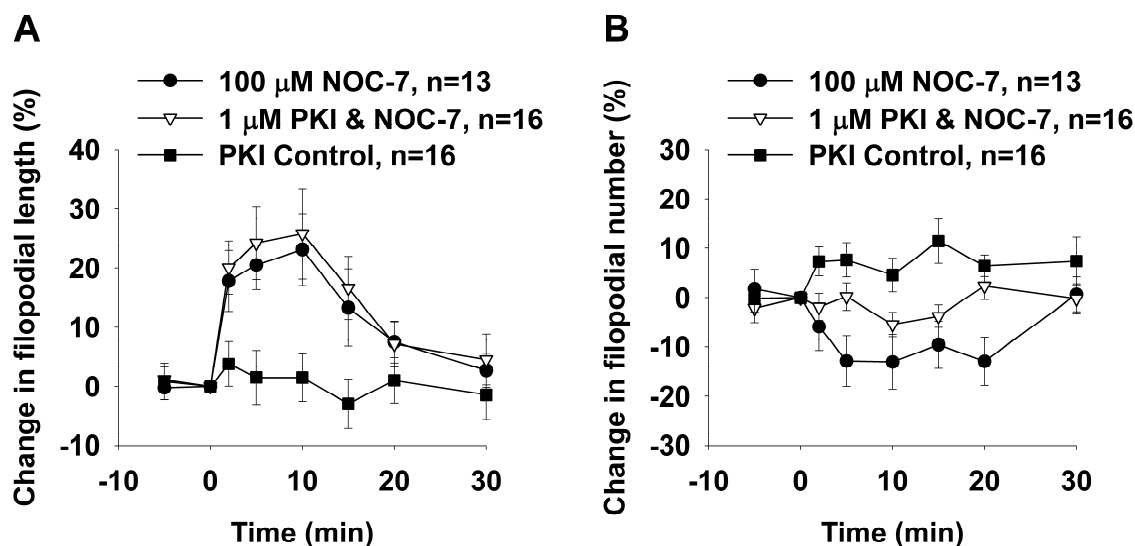
Figure 3.11: The NO-induced changes in filopodial length and number are not mediated via PKA. (A) Pretreatment with a PKA inhibitor (1 μM PKI; Myristoylated PKA Inhibitor 14-22) for 25 minutes before local application of 100 μM NOC-7 has no effect on the transient NO-induced filopodial elongation. This transient increase in filopodial length was not significantly different from growth cones that were treated with 100 μM NOC-7 alone (p = 0.68), indicating that the NO-induced increase in filopodial length does not involve PKA. Neither control growth cones (1μM PKI Control) nor 1 μM PKI by itself result in a change in filopodial length over the experimental period. **(B)** Pretreatment with 1 μM PKI followed by local NOC-7 application results in a small decrease in filopodial number (p ≤ 0.05 as compared to 1 μM PKI Control). This decrease in filopodial number is not significantly different from 100 μM NOC-7 application alone (p = 0.06).

expected that NO would ultimately be acting on actin because it is the major cytoskeletal component within filopodia. Therefore, we employed cytochalasin B, which is an inhibitor of actin plus-end addition. At high concentrations, cytochalasin B is known to cause f-actin depolymerization, however we applied this drug at a concentration that is known to decrease the amount of plus-end actin addition to the point at which there is no net change in filopodial length (Geddis *et al.*, 2004; Tornieri *et al.*, 2006). This concentration also has been shown not to affect the total amount of f-actin present in the growth cone (Tornieri *et al.*, 2006). When growth cones were pretreated with 30 nM cytochalasin B (CytoB) and then NOC-7 was locally applied, the NO-induced increase in filopodial length was significantly decreased (Figure 3.12A; $p = 0.05$ as compared to NOC-7 alone). Additionally, the NO-induced decrease in filopodial number was abolished by pretreatment with 30 nM cytochalasin B (Figure 3.12B; $p \leq 0.01$ as compared to NOC-7 alone). This result demonstrates that the NO-induced increase in filopodial length is mediated, at least in part, via actin plus-end addition.
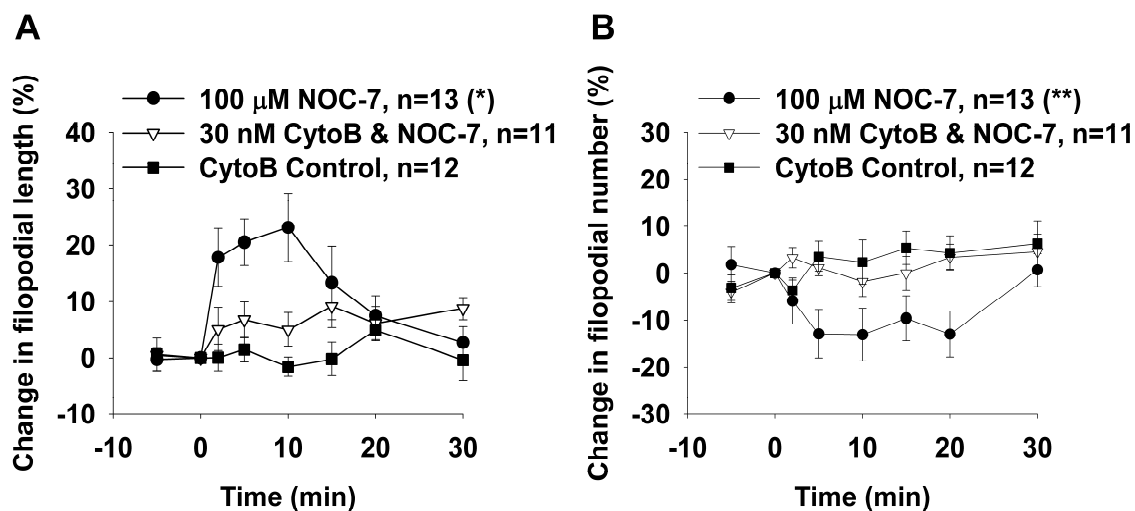
Figure 3.12: The NO-induced change in filopodial length is mediated, at least in part, via plus-end actin addition. (A) Pretreatment with an inhibitor of actin plus-end addition, 30 nM cytochalasin B (CytoB), before local application of 100 μM NOC-7 significantly reduces the NO-induced increase in filopodial length ($p = 0.05$ as compared to NOC-7 alone). **(B)** Pretreatment with 30 nM CytoB prior to local application of 100 μM NOC-7 eliminates the NO-induced decrease in filopodial number ($p \leq 0.01$ as compared to NOC-7 alone).

Chapter 4: Additional experiments published in collaboration

This chapter has been published as:

Tornieri K, Welshhans K, Geddis MS, and Rehder V. (2006) Control of neurite outgrowth and growth cone motility by phosphatidylinositol-3-kinase. Cell Motility and the Cytoskeleton 63:173-192.

K. Welshhans provided the original research for Figures 5 and 10 in the original publication. Moreover, K. Welshhans contributed significantly to the writing of the entire manuscript. However, only the contributions to which K. Welshhans provided the original research are presented here.

Introduction

During development growth cones play an important role in guiding neuronal processes to their targets. Growth cones function by integrating intracellular signals that are elicited by the binding of extracellular cues to membrane-bound or intracellularly located receptors, and by translating these signals into a coordinated motor output that results in directed neurite advance. The filopodia on growth cones undergo continuous cycles of extension and retraction, thereby placing their receptors at varying distances from the growth cone proper and resulting in changes in the 'sensory radius' of the growth cone. Filopodial length and neurite outgrowth are under the control of extracellular cues, and several treatments, mainly acting through an increase in the intracellular calcium concentration, have been demonstrated to cause a transient increase in filopodial length (Davenport & Kater, 1992; Rehder & Kater, 1992; Cheng *et al.*, 2002) and a decrease in neurite extension (Cohan *et al.*, 1987; Mattson & Kater, 1987; Lankford & Letourneau, 1989; Kater & Mills, 1991; Neely, 1993).

Phosphatidylinositol-3-kinase (PI-3K) has been implicated in a variety of cellular activities, including cell survival, mitogenesis, and differentiation (Krasilnikov, 2000; Rodgers & Theibert, 2002). PI-3K is activated by binding to receptor- and non-receptor tyrosine kinases, as well as by G-protein coupled receptors, and its activation is known to affect multiple targets (Raffioni & Bradshaw, 1992; Soltoff *et al.*, 1992a; Soltoff *et al.*, 1992b; Duronio *et al.*, 1998; Wymann & Pirola, 1998; Virdee *et al.*, 1999; Krasilnikov, 2000; Cantrell, 2001). In addition to its involvement in mediating cell survival, PI-3K has been reported to stimulate neurite outgrowth in PC12 cells (Kita *et al.*, 1998), to mediate

ephrin A5 and slit-2 induced growth cone collapse in chick retinal ganglion cells (Wong *et al.*, 2004), and to be required for the NCAM-mediated neurite outgrowth of primary neurons (Ditlevsen *et al.*, 2003). In addition, PI-3K has been shown to play a role in lamellipodial formation of PC12 cells (Posern *et al.*, 2000) and in the regulation of neuronal polarity (Shi *et al.*, 2003; Menager *et al.*, 2004). These effects are likely mediated by changes at the level of the neuronal cytoskeleton. The mechanism by which PI-3K affects neurite outgrowth is presently unclear, but prominent targets downstream of PI-3K include Akt (PKB), regulators of Rho-GTPase family members, and the RAS/RAF/ERK pathway (Corvera & Czech, 1998; Duronio *et al.*, 1998; Vanhaesebroeck & Waterfield, 1999; Bishop & Hall, 2000; Krasilnikov, 2000; Cantrell, 2001). To determine whether the effect of PI-3K activity on neurite outgrowth might be explained by PI-3K affecting growth cone motility through its effects on the neuronal cytoskeleton, we here studied several key targets within the larger PI-3K signaling cascade to investigate the signaling pathway by which PI-3K affects the actin cytoskeleton of neuronal growth cones.

PI-3K has a double-enzymatic activity, that of a lipid kinase and a protein kinase (Dhand *et al.*, 1994; Krasilnikov, 2000). The protein kinase activity regulates the PKC, Ras/ERK, and Rac/JNKK/JNK signaling pathways, whereas the lipid kinase activity controls the Akt anti-apoptotic signaling pathway and the activity of Rho kinase (ROCK) (Krasilnikov, 2000; Cantley, 2002). By using two inhibitors of PI-3K, wortmannin and LY 294002, we show that PI-3K activity is involved in regulating both neurite outgrowth and filopodial dynamics. We further show that this regulation involved members of the

lipid kinase (ROCK or Akt) and the protein kinase (MEK) pathways of PI-3K signaling. Fast time course studies of filopodial dynamics showed that the rapid filopodial elongation seen after different treatments was achieved mainly by changes in two parameters of filopodial motility: increases in the extension rate and in the time that individual filopodia spend extending. By employing drugs that interfere with actin polymerization and myosin II activity, we further provide evidence that filopodial elongation seen after inhibition of PI-3K is mainly due to an increase in actin polymerization at the barbed end, and not through inhibition of retrograde actin flow. Because filopodial elongation and a decrease in the rate of neurite outgrowth seen after inhibition of PI-3K in this study are similar to growth cone behavior observed at "decision points" during pathfinding *in vivo* (Taghert *et al.*, 1982; Tosney & Landmesser, 1985; Holt, 1989), these data suggest that signaling through PI-3K could be of critical importance for growth cone motility, and that a lack of stimulation or inhibition of the PI-3K pathway could result in slow-down and search behavior in advancing neurites.

Materials & Methods

Neuronal culture and image acquisition

Identified B5 neurons were dissected from *Helisoma trivolvis* buccal ganglia and plated for neuronal culture. Neurons used for filopodial experiments were plated on poly-L-lysine (hydrobromide, MW 70,000-150,000, 0.25mg/ml; Sigma, St. Louis, MO) coated glass cover slips that were glued to the bottom of 35 mm cell culture dishes (Falcon 1008). Neurons used for outgrowth experiments were plated onto either the same glass dishes described above, or onto poly-L-lysine coated plastic cell culture dishes as described in Trimm and Rehder (2004). Cells were kept at room temperature and used 24-48 hours after plating. Neurons were grown in conditioned medium (CM) prepared by incubating two snail brains per milliliter in defined medium (DM) for 3-4 days. DM was produced by dilution of Leibovitz L-15 medium (Gibco #41300, Grand Island, NY) with distilled water to obtain the appropriate ionic composition and contained final concentrations of: 46 mM NaCl, 1.8 mM KCl, 1.5 mM $MgCl_2$, 4.1 mM $CaCl_2$, 10 mM HEPES, 50 μg gentamycin/ml, 0.15 mg glutamate/ml in distilled water (pH=7.3). Growth cones were viewed through 100x oil immersion objectives on either an Axiovert (Carl Zeiss, Thornwood, NY) or a Sedival (aus Jena, Germany) microscope. Neurite outgrowth was imaged through a 40x objective on a Sedival microscope. Images were captured with a cooled CCD camera (CH250, Photometrics, Tucson AZ) or a regular CCD camera (Model: C-72, MIT Dage, Michigan City, IN). Images were digitized on a frame grabber (Scion LG-3, Scanalytics, Fairfax, VA) and analyzed with "Scion Image" software (Scion

Corporation; Frederick, Maryland) on a Power Macintosh (Apple Computer, Cupertino, CA) or a Compaq Presario (Hewlett-Packard Company, Palo Alto, CA).

Pharmacological agents

Akt inhibitor and cytochalasin B (actin polymerization inhibitor) were dissolved in DMSO to obtain stock concentrations of 45 mM and 60 μM respectively. The Rho-kinase inhibitor Y27632 was dissolved in water to a stock concentration of 10 mM. All agents were purchased from Calbiochem (San Diego, CA).

Design and analysis of neurite outgrowth experiments

Images of neurons were taken at 20 minute intervals for a total of 3 hours per experiment as previously described (Trimm & Rehder, 2004). Neurite outgrowth was determined by measuring neurite length starting from a fixed point in the dish (e.g. soma) and measuring the distance to the growth cone's central domain using the software package "Scion Image." Neurites that advanced less than 6 μm during the control period (one hour before treatment) or that fasciculated with other neurites during the experiment were excluded from analysis. Outgrowth during the first hour of treatment following drug addition was measured by subtracting neurite length at $t = 0$ from $t = 60$. Outgrowth during the second hour of treatment following drug addition was measured by subtracting neurite length at $t = 60$ from $t = 120$. In order to introduce the experimental condition, 0.2 mL of conditioned medium was removed from the dish, a drug was premixed in this volume, and the 0.2 mL was subsequently added back to the dish to obtain the final concentration.

Solvents used in the reconstitution of pharmacological agents were tested by themselves in control experiments and had no significant effect on neurite outgrowth.

Actin labeling and analysis of actin fluorescence

Growth cones were fixed and stained according to Cohan *et al*. (2001) with the variation that rhodamine phalloidin was used (Molecular Probes) at a concentration of 0.165 µM. Growth cones were viewed through a 100x oil immersion objective on a Zeiss Axiovert inverted microscope equipped with a rhodamine filter set (Omega Optical, Brattleboro, VT). Images were acquired using a cooled Photometrics CCD camera, and stored on a Macintosh computer. A camera exposure time of 200 ms was used for all images. Image intensity was analyzed with Scion Image software (Scion Corporation) and two measurements were taken to quantify f-actin content in growth cones. To calculate the mean fluorescent intensity of f-actin in the growth cone's p-region, a line was drawn outlining the lamellipodial region and the measured fluorescence averaged. The fluorescent intensity of actin bundles forming the core of filopodia was analyzed according to Cohan *et al.* (2001). Briefly, a line was drawn across individual actin bundles within the middle of the lamellipodium. The peak intensities for each bundle (the average of 3 pixels for each bundle) were determined and this procedure repeated for at least 5 filopodia per growth cone, except when that was impossible due to loss of filopodia (condition with 500 nM Cytochalasin B). These values were then expressed as an average peak intensity for each growth cone. Staining was done in parallel for

different experimental conditions (Control, 30 nM Cytochalasin B, and 500 nM Cytochalasin B) to minimize differences in staining intensity between dishes.

Statistical analysis

For filopodial experiments, statistical comparisons between conditions was determined by performing an analysis of variance (1-way ANOVA or ANOVA with time as repeated measures), and with a *t*-test for dependent and independent samples, with SuperANOVA (Abacus Concepts, Berkeley, CA). Fisher's protected least significant difference (PLSD) test was used for post-hoc tests of statistical significance. For neurite outgrowth, fast time-course and actin labeling experiments, significance between conditions was determined by performing a Student's t-test (for unpaired or paired samples) with Excel (Microsoft; Redmond, WA). Significant differences are indicated as: $*p \leq 0.05$, $**p \leq 0.01$, $***p \leq 0.001$.

Results

Inhibition of Akt or ROCK slows neuronal outgrowth

To investigate the pathway by which PI-3K might regulate growth cone motility, we pharmacologically inhibited major targets downstream of PI-3K with the assumption that their inhibition should mimic the effect of PI-3K inhibition and result in filopodial elongation and/or a slow down in neurite outgrowth. PI-3K has a double enzymatic activity, acting as a protein kinase and a lipid kinase (Krasilnikov, 2000; Cantley, 2002) (Fig. 4.1). Therefore, we wanted to investigate which of the two activities might be involved in controlling neurite outgrowth.

In these experiments, the effect of inhibition of Akt and ROCK on neurite outgrowth was studied. When Akt was inhibited, neurite outgrowth was not affected in the first hour following drug addition (16.2 ± 2.8 µm in the hour prior to drug addition and 13.6 ± 3.2 µm in first hour following drug addition; Fig. 4.2A). However, in the second hour following drug addition, neurite outgrowth was significantly slowed to 6.7 ± 3.0 µm (p ≤ 0.001 as compared to the hour prior to drug addition). When ROCK was inhibited with Y27362 - neurite outgrowth also was not affected in the first hour following drug addition (20.5 ± 2.1 µm in the hour prior to drug addition and 18.8 ± 2.6 µm in first hour following drug addition; Fig. 4.2B). However, in the second hour following drug addition, neurite outgrowth was significantly decreased to 12.0 ± 2.6 µm (p ≤ 0.01 as compared to the hour prior to drug addition). Taken together, these results are consistent with the idea that the lipid kinase activity of PI-3K is involved in controlling neurite outgrowth through Akt and ROCK.
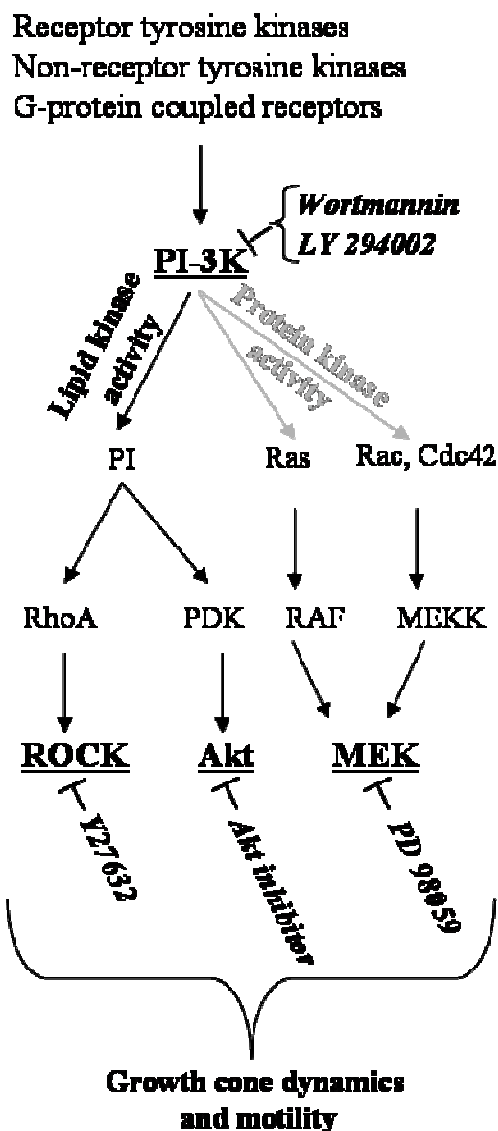
Figure 4.1: PI-3K may regulate growth cone dynamics through multiple signaling pathways. PI-3K is activated by multiple effectors. The PI-3K signaling pathway is bifurcated and has two branches, resulting from its lipid- and protein kinase activities. Through its lipid kinase activity, PI-3K phosphorylates phosphatidylinositol (PI) and its phosphorylated derivatives. Then phosphoinositides activate the RhoA/ROCK pathway, and the phosphoinositide-dependent kinase (PDK), which in turn activates Akt. Through its protein kinase activity (in gray), PI-3K binds directly to Ras and Rac-Cdc42, leading to the activation of MEK. Kinases investigated in this study are in bold typeface and underlined. Inhibitors are indicated in *italics*.
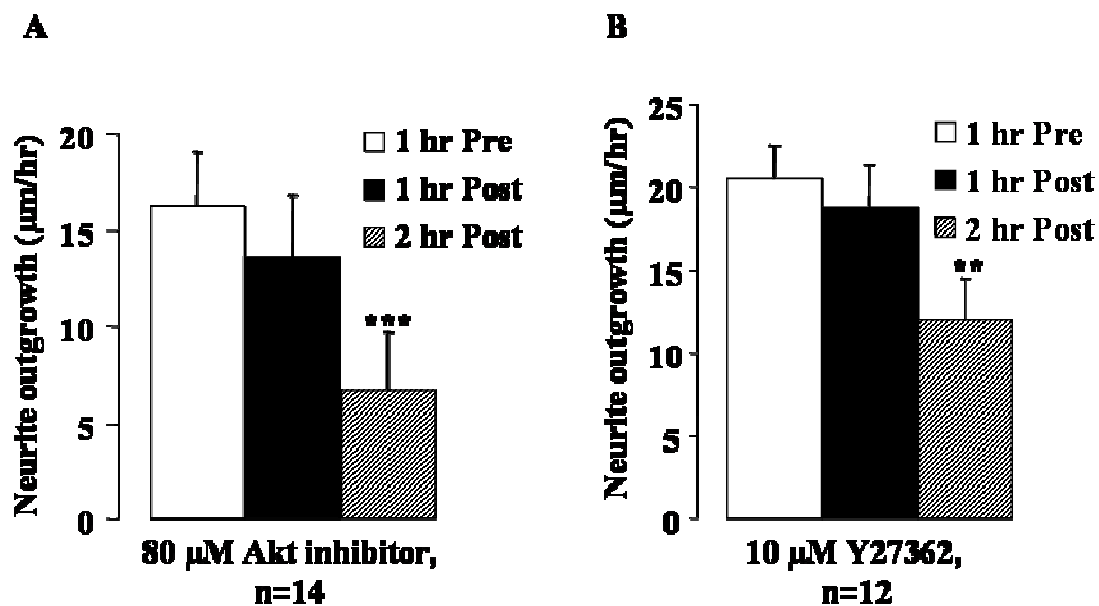
Figure 4.2: Regulation of neurite outgrowth by Akt and ROCK. (A) Inhibition of Akt with Akt inhibitor (80 μM) did not significantly affect neurite outgrowth in the first hour following drug addition. However, neurite outgrowth was slowed significantly in the second hour following drug addition ($p \leq 0.001$). **(B)** Inhibition of ROCK with 10 μM Y27362 did not significantly affect neurite outgrowth in the first hour after drug addition. However, neurite outgrowth was slowed significantly in the second hour following drug addition (Student's t-test, **$p \leq 0.01$).

30 nM Cytochalasin B does not change total actin content within the growth cone

Filopodia are composed of bundles of filamentous (f-) actin (Gordon-Weeks, 1987) and the barbed ends, where net addition of monomeric actin occurs, are located towards the filopodial tip. Theoretically, filopodial elongation could result from: (i) an increase in actin polymerization at the barbed end, (ii) a decrease in retrograde flow of f-actin without affecting the normal net addition of monomeric actin at the barbed end, or (iii) a combination of both (Figure 4.3). In initial experiments we wanted to obtain a qualitative assessment of the contribution of these mechanisms to filopodial length changes in untreated growth cones. In these experiments, the pharmacological agent, cytochalasin B (CytoB), was employed to interfere with the addition of monomeric actin to the barbed end of f-actin. Although CytoB has been shown to result in the depolymerization of f-actin (Forscher & Smith, 1988), we used CytoB at a concentration (30 nM) that had no net effect on overall filopodial length (Geddis *et al.*, 2004). However, because CytoB has been shown to depolymerize f-actin at higher concentrations, it was important to confirm that overall f-actin content within the growth cone was not affected by the concentration at which we were employing it.

To confirm that the total f-actin content was not affected by the treatment with 30 nM CytoB, we employed a fluorescently labeled mushroom toxin, rhodamine phalloidin, which binds to f-actin. Overall, growth cones treated with 30 nM CytoB for 30 minutes appeared no different from control growth cones (Fig. 4.4A). However, treatment with a higher concentration of CytoB (500 nM) resulted in an obvious decrease in f-actin
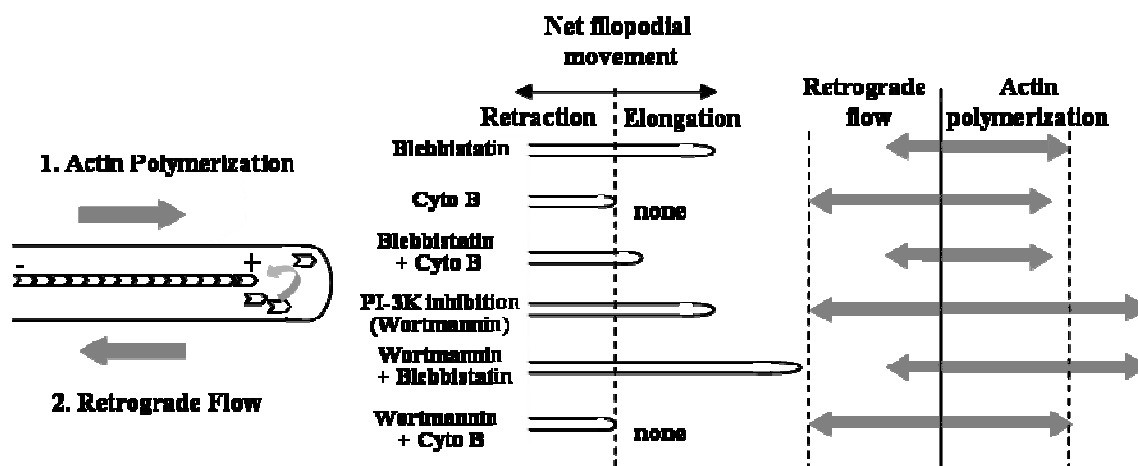
Figure 4.3: Filopodial elongation resulting from PI-3K inhibition requires actin polymerization. Model of filopodial length changes. Filopodial length is mainly regulated by actin polymerization/depolymerization events at the barbed end and the retrograde flow by which f-actin is transported centrally (left). The curved arrow indicates actin polymerization onto the barbed (+) end of f- actin, which would result in filopodial elongation. Arrows pointing to the right symbolize actin polymerization and arrows pointing to the left symbolize retrograde flow. The middle panel shows the net effect of various experimental treatments on overall filopodial length. The right panel shows the hypothesized relative contributions (indicated by the length of the arrows) of actin polymerization and retrograde flow on filopodial length under these experimental conditions.
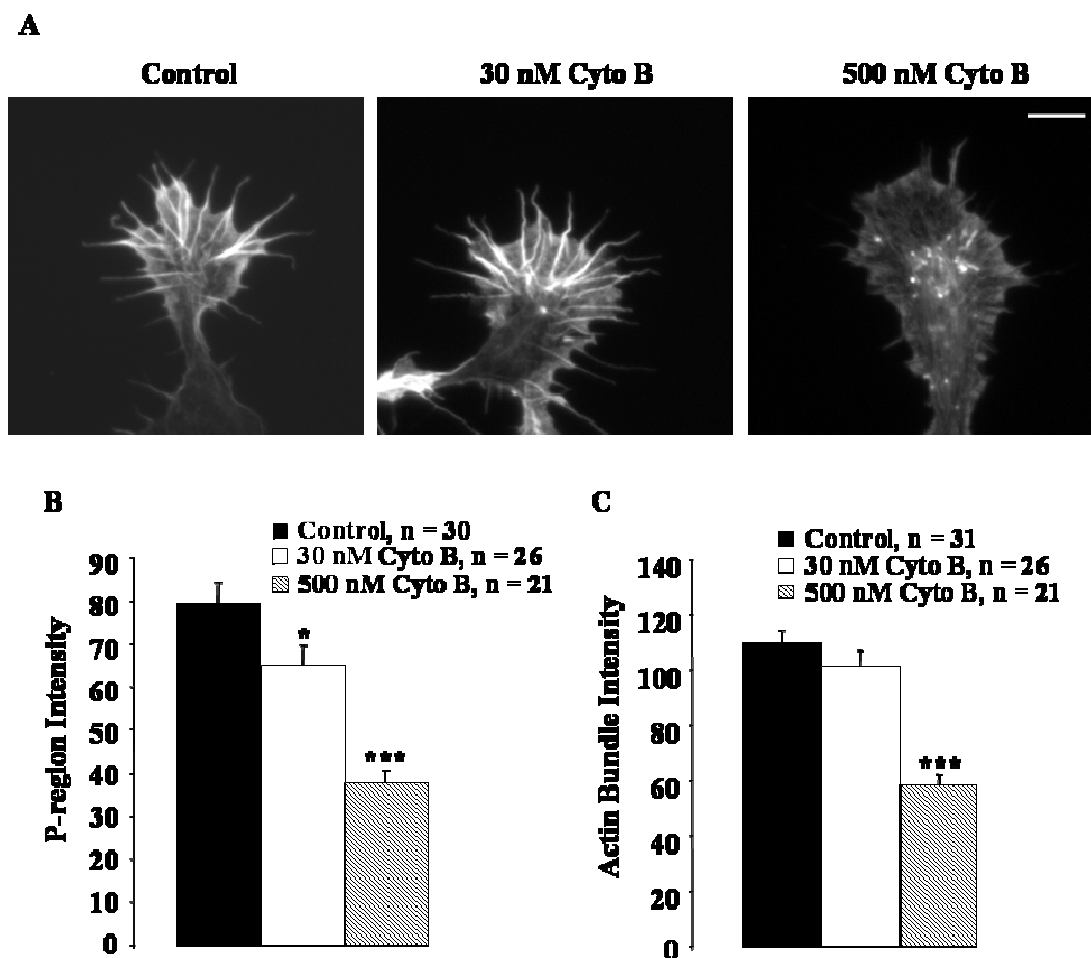
Figure 4.4: A low concentration of cytochalasin B (30 nM) does not affect filopodial actin bundles, but slightly reduces overall f-actin staining intensity within the p-region. Growth cones received one of three treatments (L-15 medium exchange (Control), 30 nM Cyto B in L-15, or 500 nM Cyto B in L-15) for 30 minutes and were subsequently fixed in parformaldehyde/glutaraldehyde and reacted with rhodamine phalloidin. **(A)** Growth cones that received the 30 nM Cyto B treatment look indistinguishable from control growth cones regarding overall morphology, as well as number and intensity of fluorescent F-actin bundles visible in the growth cone. Note the noticeable loss of f-actin staining and filopodia in growth cones treated with 500 nM Cyto B. Scale: 10 μm. **(B)** Intensity of f-actin staining in the p-region was significantly reduced (from 79.4 ± 4.8 to 65.1 ± 4.4) by treatment with 30 nM Cyto B ($p \leq 0.05$ as compared to Control). Treatment with 500 nM Cyto B reduced the intensity of f-actin staining within the p-region to an even greater extent (to 37.7 ± 3.0; $p \leq 0.001$ as compared to Control). **(C)** Actin bundle intensity was not affected by treatment with 30 nM Cyto B ($p = 0.23$ as compared to Control). However, treatment with 500 nM Cyto B significantly reduced actin bundle intensity from 110.0 ± 4.4 to 58.2 ± 3.9 ($p \leq 0.001$ as compared to Control).

staining and a loss of filopodia (Fig. 4.4A). Quantification of the intensity of f-actin staining within the lamellipodial P-region of growth cones (see methods for details), however, revealed a small decrease in the intensity of staining in growth cones treated with 30 nM CytoB when compared to control growth cones (from 79.4 ± 4.8 to 65.1 ± 4.4 fluorescence units; Fig. 4.4B; $p \leq 0.05$, t-test). Treatment with 500 nM CytoB showed a large reduction in f-actin staining in the P-region (to 37.7 ± 3.0) (Fig. 4.4A and B; $p \leq 0.001$, t-test). When f-actin content of individual f-actin bundles (forming the core of filopodia) was measured (see Methods for details), no difference between control growth cones and those treated with 30 nM CytoB was found (Fig. 4.4C; $p = 0.23$, t-test). Growth cones treated with 500 nM CytoB, however, showed a significant loss in actin bundle intensity (from 110.0 ± 4.4 to 58.2 ± 3.9; Fig. 4.4C; $p \leq 0.001$, t-test). These results suggested that although 30 nM Cyto B slightly reduced the amount of f-actin within the P-region of the growth cone, the f-actin content within filopodia was not measurably affected.

Discussion

Phosphatidylinositol-3-kinase (PI-3K) is central to many signaling pathways and has been shown to function in cellular events such as cell survival, mitogenesis, differentiation and motility (Duronio *et al.*, 1998; Krasilnikov, 2000; Cantrell, 2001; Rodgers & Theibert, 2002). PI-3K can be activated by receptor tyrosine kinases, non-receptor tyrosine kinases, and G-protein coupled receptors (Stephens *et al.*, 1994; Stoyanov *et al.*, 1995; Lopez-Ilasaca *et al.*, 1997; Duronio *et al.*, 1998; Vanhaesebroeck & Waterfield, 1999; Cantrell, 2001) but the mechanism by which PI-3K affects neurite outgrowth is not well understood. Here we set out to investigate whether the effect of PI-3K on neurite outgrowth might be explained by its action on the actin cytoskeleton in neuronal growth cones.

ROCK, Akt, and MEK regulate filopodial dynamics and neurite outgrowth

PI-3K can be activated by receptor- and non-receptor tyrosine kinases, as well as by G-protein coupled receptors (Stephens *et al.*, 1994; Stoyanov *et al.*, 1995; Lopez-Ilasaca *et al.*, 1997; Duronio *et al.*, 1998; Vanhaesebroeck & Waterfield, 1999; Cantrell, 2001). PI-3K, in turn, has two modes of action. It functions as a lipid kinase by phosphorylating the 3'-OH position on the inositol ring of several phosphoinositides, thereby producing inositol lipid products, which are important mediators of intracellular signaling (Duronio *et al.*, 1998; Vanhaesebroeck & Waterfield, 1999; Cantrell, 2001). This signaling pathway leads to the stimulation of guanine nucleotide exchange factors for Rho-GTPases, as well as to the activation of the PH-domain containing kinase, PDK-1, which

in turn activates Akt (Alessi *et al.*, 1997; Downward, 1998; Meier & Hemmings, 1999; Vanhaesebroeck & Alessi, 2000) (Fig. 4.1). Secondly, PI-3K functions as a protein kinase resulting in the activation of the Ras/Raf/Erk pathway (Bondeva *et al.*, 1998; Vanhaesebroeck & Waterfield, 1999; Krasilnikov, 2000).

We found that inhibition of two of the downstream targets of the lipid kinase pathway, Akt or ROCK, resulted in a decrease in neurite outgrowth in the second hour following drug addition (Fig. 4.2A and B). This late onset of an effect on neurite outgrowth, compared to an effect on filopodial elongation observed within minutes, suggested that filopodial elongation could occur without a concomitant decrease in neurite outgrowth. As such, the slow-down and search behavior seen in this study can be divided into two behaviors: "slow-down" and "search" (Fig. 4.5). As observed with both ROCK and Akt inhibition, it is possible for a growth cone to elongate its filopodia over a short time course (the "search" behavior) while maintaining a constant outgrowth speed. Yet, at other times these behaviors can be coupled into the "slow-down and search" behavior that is seen with PI-3K inhibition in the first hour of drug addition. Given that the treatments in this study were long-term and may not reflect shorter and probably more physiologically relevant episodes of kinase activation/inhibition, one could envision scenarios in which changes in filopodial length and neurite outgrowth rates could either be regulated independently or in conjunction, depending on the signaling cues received by the pathfinding growth cone.
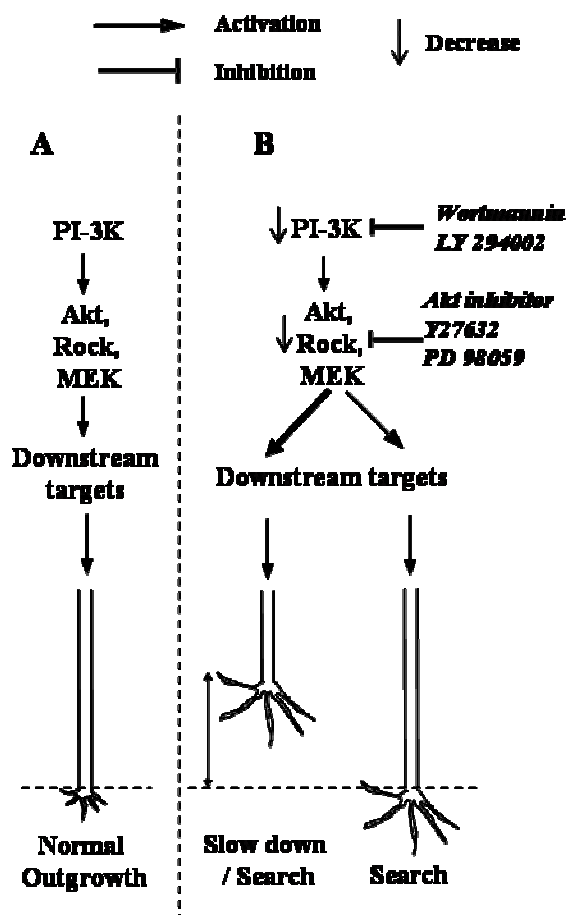
Figure 4.5: Model of regulation of neurite outgrowth and filopodial motility by PI-3K. **(A)** Baseline PI-3K activity leads to downstream signaling events that result in growth cones advancing with 'baseline' speed and having filopodia of certain lengths. **(B)** When PI-3K or key kinases in the proposed pathway downstream of PI-3K are inhibited or otherwise reduced in their activity, growth cones can undergo either a "slow-down and search" behavior, characterized by filopodial elongation and a concomitant decrease in the rate of neurite advance, or a "search" behavior, characterized by filopodial elongation alone.

RhoA, an activator of ROCK, has been shown to have opposite effects on neurite outgrowth depending on the cell type and the stage of outgrowth studied (Kranenburg *et al.*, 1997; Threadgill *et al.*, 1997; Kuhn *et al.*, 1999; Sebok *et al.*, 1999). In agreement with ROCK promoting neurite outgrowth, inactivation of RhoA has been shown to slow the rate of neurite outgrowth in NGF-primed differentiating PC12 cells (Sebok *et al.*, 1999).

Although we found that inhibition of Akt resulted in a slowing of neurite outgrowth, other recent studies reported the opposite effect, namely that expression of a dominant inhibitory form of Akt increased NGF induced neurite outgrowth in PC12 cells (Bang *et al.*, 2001; Piiper *et al.*, 2002). This difference in results may be explained by the fact that while we investigated neurite outgrowth on already extended neurites, the other studies focused on neurite initiation. It is, thus, possible that Akt may affect neurite initiation and neurite maintenance differently, as has been reported for RhoA (Sebok *et al.*, 1999). The results from the Sebok *et al.* study suggest that RhoA holds different roles in the regulation of neurite growth, depending on the developmental stage. RhoA may affect neurite growth differently during various developmental stages due to activation of different signaling cascades. This mechanism that allows for RhoA to affect neurite outgrowth in multiple ways during development may also hold true for Akt, but has yet to be discovered.

Conclusions

Taken together, our results demonstrate that signaling events leading to the inhibition of PI-3K resulted in an increase in filopodial length and a decrease in neurite outgrowth, and as such could act as a signal for a slow-down and search behavior (Fig. 4.5). Inhibition of key kinases located downstream of PI-3K activity also resulted in filopodial elongation (ROCK, Akt, and MEK) and in a decrease in neurite advance (ROCK and Akt), consistent with the notion that PI-3K might act through these kinases to affect growth cone motility. In extension, other signaling pathways converging on these kinases are expected to have predictable effects on neurite outgrowth and filopodial behavior. Filopodial elongation in response to PI-3K inhibition was shown to result largely from an increase in actin polymerization, and not from an inhibition of the retrograde flow. Future studies will investigate the growth factors that bind to receptors (e.g. receptor tyrosine kinases) and activate PI-3K, leading to the currently described signaling pathway. The detailed pathways that link the activity of these kinases to changes in the growth cone cytoskeleton will also have to be investigated in future studies.

Chapter 5: Additional experiments using *Helisoma trivolvis* as a model system

5.1 Regeneration of the *Helisoma* B5 neuron *in vivo*

Introduction

Spinal cord injury affects around 250,000 to 400,000 people in the United States alone. Because the central nervous system (CNS) of humans does not regenerate, this is a devastating type of injury for which we do not have an effective treatment. Interestingly, when the nerves from a mollusc, *Helisoma trivolvis*, are crushed, the axons of neurons contained in these nerves will regenerate and make connections with their original appropriate targets. Therefore, this provides us with an excellent model system in which to study the process of permissive regeneration.

This project examined the *in vivo* regeneration of the B5 neuron from *Helisoma trivolvis*. Normally, the axon of the B5 neuron exits the esophageal nerve trunk (ET) and then divides into two projections (Figure 5.1) (Berdan *et al.*, 1989). The major projection exits through the gastric nerve to innervate the gut. It is known that this axon of the B5 neuron extends into the muscle of the esophagus, however the specific type and location of its innervation is unknown. The minor projection exits through the dorsobuccal nerve to innervate the buccal mass (Murphy & Kater, 1980a; Berdan *et al.*, 1990). If the ET is crushed, the B5 neuron will regenerate its axons and almost always follow the "correct" paths to reinnervate its appropriate targets (Murphy & Kater, 1980a). Previous studies have begun to examine this neuron *in vivo*, under nerve crush conditions. However, these studies crushed the ET nerve, allowed a specific amount of regeneration time and then injected the B5 neuron with Lucifer yellow and fixed the tissue. Therefore, this project
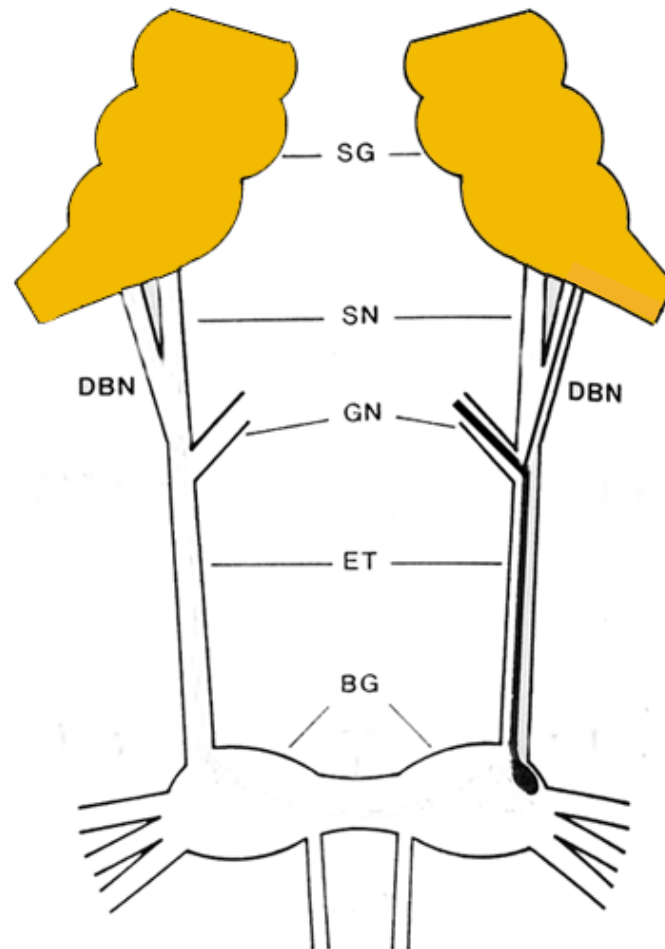
Figure 5.1: The *Helisoma* buccal ganglion and B5 projection. The projection of the B5 neuron exits the buccal ganglion (BG) through the esophageal nerve trunk (ET) and splits into two projections. The major projection exits the gastric nerve (GN) to innervate the esophagus and the minor projection exits the dorsobuccal nerve (DBN) to innervate the buccal mass. Modified from Kruk and Bulloch 1992. SG: salivary gland; SN: salivary nerve

had 2 main foci: one, to watch this regeneration as it occurred *in vivo*, and two, to monitor calcium levels throughout the regeneration process.

Materials and Methods

Dissection and Organ Culture

Adult freshwater snails (*Helisoma trivolvis*) are removed from their shell and placed into HEPES-buffered Helisoma saline (51.3 mM NaCl, 1.7 mM KCl, 4.1 mM CaCl$_2$, 1.5 mM MgCl$_2$; buffered to pH 7.55 with HEPES). They are then placed into a 25% solution of Listerine™ in Helisoma saline for 10 minutes, followed by 10 minutes in antibiotic (AB) Helisoma saline (gentamycin, 150 µg/ml). The snail was placed with the dorsal side up and a small incision was made in the dorsal body wall. The esophagus was cut, pulled through the brain and pinned above the head. The esophageal nerve trunk (ET) was then crushed using fine forceps and firm pressure for 5 seconds. These nerves were crushed a little more than halfway between their insertion into the buccal ganglion and the split into the gastric nerve and the salivary nerve (toward the split).

Following nerve crush, the entire CNS, including the buccal ganglion, was removed and placed either in AB Helisoma saline or in conditioned medium with extra antibiotics (gentamycin 150 µg/ml). In order to remove the CNS, the nerves were cut as close as possible to their insertion points into various targets. In addition, the salivary gland, the buccal mass, and a portion of the esophagus were retained. The CNS with attached structures was placed into AB saline or conditioned medium and kept in a darkened box until it was ready to be used.

In Vivo Regeneration

As an alternative to organ culture, a protocol was designed (based on Kruk & Bulloch, 1992) that allowed for a true *in vivo* situation. Snails were anesthetized with a solution of increasing concentrations of menthol in pond water over 90 minutes. The snails were then clamped into position under a dissecting microscope by their shells and the head was gently pulled out of its shell by forceps. A small incision was made between the tentacles and the esophagus and salivary gland were pulled out through the incision until the ET could be seen. The ET was then crushed and the esophagus and salivary gland were placed back into the cavity. The incision was flushed with AB saline and the snails were placed back into normal pond water to recover. After a defined amount of time to allow for regeneration to occur, the buccal ganglion was removed as described above.

Injection of Indicator Dyes and Imaging

Prior to pressure injection of calcium green, the ganglia were placed into protease (0.1%; Sigma) for 5 minutes and then pinned down in a Sylgard coated dish containing Helisoma AB saline. Calcium green (10 mM, in HEPES buffer; Molecular Probes), fluo-4 (Molecular Probes) or FITC dextran (10 mM, in HEPES buffer; Molecular Probes) was pressure injected, using a Picospritzer (General Valve Corp., Fairfield, NJ), into the B5 neurons 1 to 7 days following nerve crush. Before confocal imaging, the dye was given 15-30 minutes diffusion time. In order to keep the ganglion in place for confocal imaging, a drop of agar mixture was placed over the ganglion (Hadley *et al.*, 1982). Bacto agar (0.6%) and gelatin (0.6%) was combined in Helisoma AB saline. This mixture was

heated with a stir bar until clear. Then, it was removed from the hot plate and allowed to cool to 37°C. Meanwhile, the ganglion was positioned with its dorsal side up on a glass coverslip glued to the bottom of a drilled Falcon dish. Once the temperature of the agar reached 37°C, one to two drops were placed over the ganglion. The mixture was given 30-45 seconds to solidify and then AB saline was added to the dish. All ganglia were imaged using either a LSM 510 laser confocal microscope (Carl Zeiss, Thornwood, NY) or a Zeiss Axiovert 135 microscope in combination with a cooled CCD camera (CH250, Photometrics; Tuscon, AZ) and stored on a Macintosh Quadra 800 (Apple Computer Inc.; Cubertino, CA).

Results

In order to examine the regeneration process, injury is induced by crushing the right esophageal trunk nerve of the buccal ganglion with forceps. Following nerve crush, the entire ganglion is placed in organ culture. This procedure allows for an internal control because a buccal ganglion contains two B5 neurons, each exiting out of its own esophageal trunk nerve. Therefore, one nerve was crushed and the other remained intact and served as an internal control. Following 1-7 days of regeneration time, the B5 neuron was injected with calcium green and the regenerating projection visualized. Although many iterations of this experiment were completed, with various protocols, ultimately, regeneration halted upon injection of the imaging dye. Some of the various techniques employed and difficulties encountered during this project will be outlined here.

Originally, calcium green was employed as the injection dye of choice. One of the immediate aims of this project was not only to image changes in calcium throughout the regeneration process, but also to alter the levels via uncaging calcium within regenerating growth cones and examine how that may alter regeneration rates. The success rate of injecting the B5 neuron and being able to visualize its projections became acceptable over time (about 50% success rate); however, one of the major limitations of this project was that after injection, there was usually not just one growth cone evident, rather there were multiple projections extending out from the regenerating axon. Therefore, it was difficult to determine which may be the major projection to follow. The second major limitation was that regeneration halted following injection of any calcium indicator dye. Although injecting the B5 neuron at various time points following crush (e.g. 2, 3, 4, 5 days) demonstrated that the B5 neuron was regenerating, when a growth cone was chosen to follow after injection, it did not advance at all during the imaging session (a time period of 3 to 7 hours). However, it was possible to uncage calcium within growth cones of regenerating axons, evident from the increase in fluorescence of the calcium indicator dye, calcium green (Figure 5.2 A&B), which indicates an increase in the intracellular calcium concentration. Yet, it was impossible to determine if this had an effect on regeneration because these axons were not regenerating following injection of the calcium indicator dye.

As mentioned previously, the axons were not regenerating following injection with the calcium indicator dye, calcium green. We thought that this might be due to the large amount of calcium green that needed to be injected in order to visualize the axon
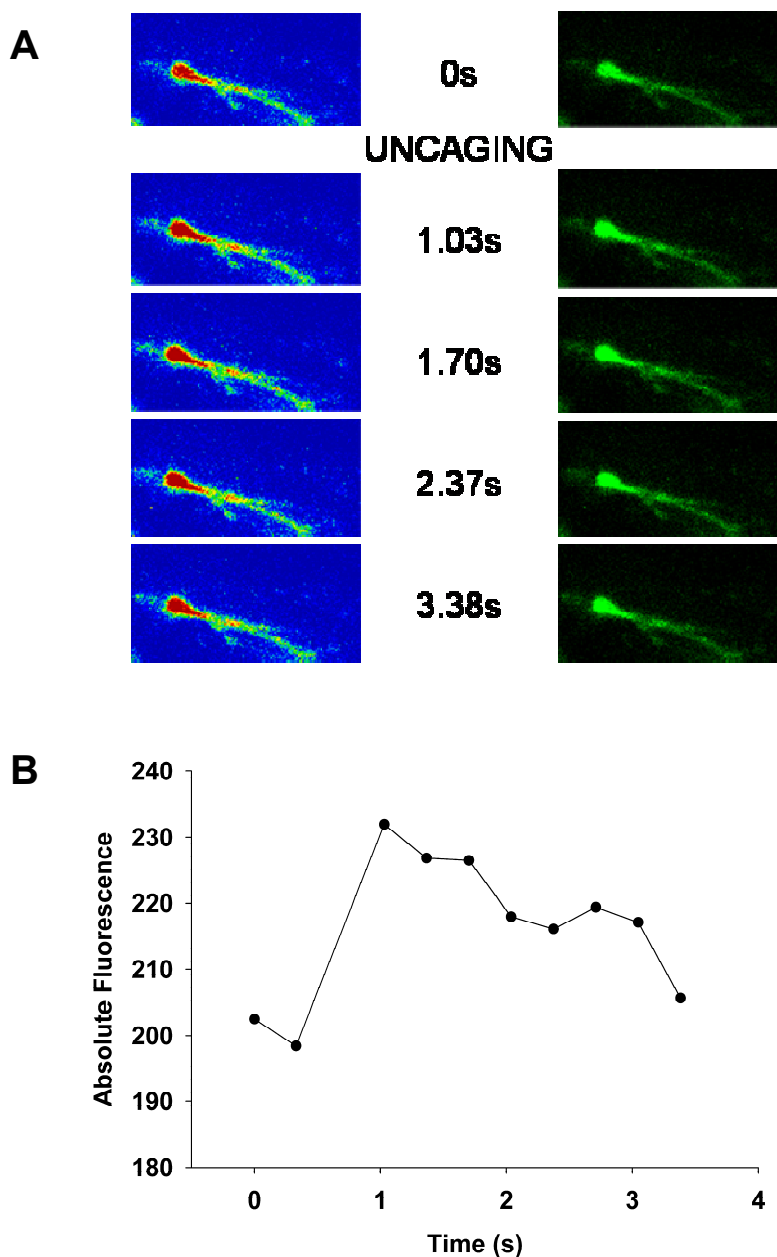
Figure 5.2: Calcium can be uncaged within a regenerating B5 growth cone. (A) *In vivo* calcium uncaging in the growth cone. Caged calcium was injected into the growth cone, in combination with the calcium indicator dye calcium green, and then uncaged with a flash of UV light for 0.7s. The left column is a set of false color images created for improved visualization of the calcium intensity present in the confocal images (right column). **(B)** Intensity of calcium fluorescence in the growth cone prior to and following uncaging. Following uncaging (which takes places immediately following the image acquired at $t = 0.33$ seconds), calcium increases within the growth cone.

and growth cones. Because calcium indicator dyes bind calcium, they can act as calcium buffers within the cytosol and interfere with the maintenance of a normal intracellular calcium concentration. Subsequently, this could lead to an inhibition of regeneration. Therefore, we employed a different calcium indicator dye, fluo-4, that has a stronger fluorescence signal. This property allows us to inject less dye, thereby reducing the possibility of calcium buffering. Unfortunately, although the axons were regenerating following crush, once again, the regeneration halted following dye injection of fluo-4 (Figure 5.3).

The next stage of this project used DiI in various protocols in order to label the neurite and growth cone *in vivo*. Since DiI is a lipophilic dye that inserts itself into the outer membrane, it should accurately label the neuron along with its projection, including the growth cone and its filopodia. The first method for labeling involved simply putting DiI crystals on top of the B5 neuron. Although this did work on individual cells in cell culture, it was difficult to accurately place the crystals only on the B5 neuron when the whole ganglion was in organ culture. Therefore, crystals were sprinkled on that entire side of the ganglion, which might result in labeling of the B5 neuron, but most likely in combination with other neurons. Although projections were seen with this labeling technique (Figure 5.4), especially across the ganglia (Figure 5.4 A-C), and some projections exiting other nerves (Figure 5.4 D-F), no projections were seen exiting the ET. Additionally, many cells were labeled in the vicinity of the B5, which made it difficult to determine exactly which projections belonged to the B5 neuron.
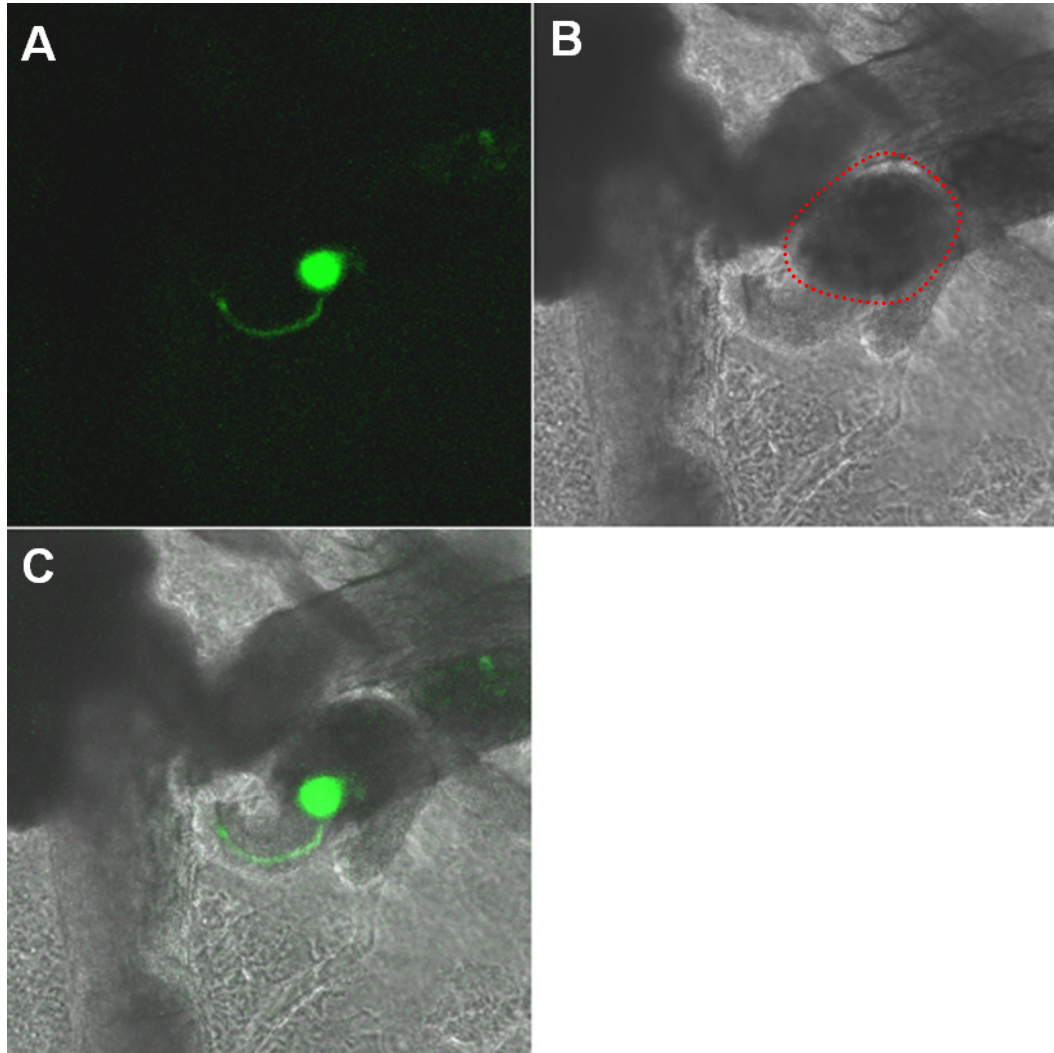
Figure 5.3: Fluo-4 labeling of the regenerating B5 neuron in organ culture. (A) 10x fluorescent image of a B5 neuron that has been injected with the calcium indicator dye fluo-4. **(B)** 10x phase contrast image of the buccal ganglia. The hemiganglion containing the injected neuron is outlined in red for easier visualization. (C) 10x combined (fluorescent and phase contrast) image of the injected B5 neuron and its projection. Note the projection emanating out of the buccal ganglion from the B5 neuron and into the esophageal trunk nerve.
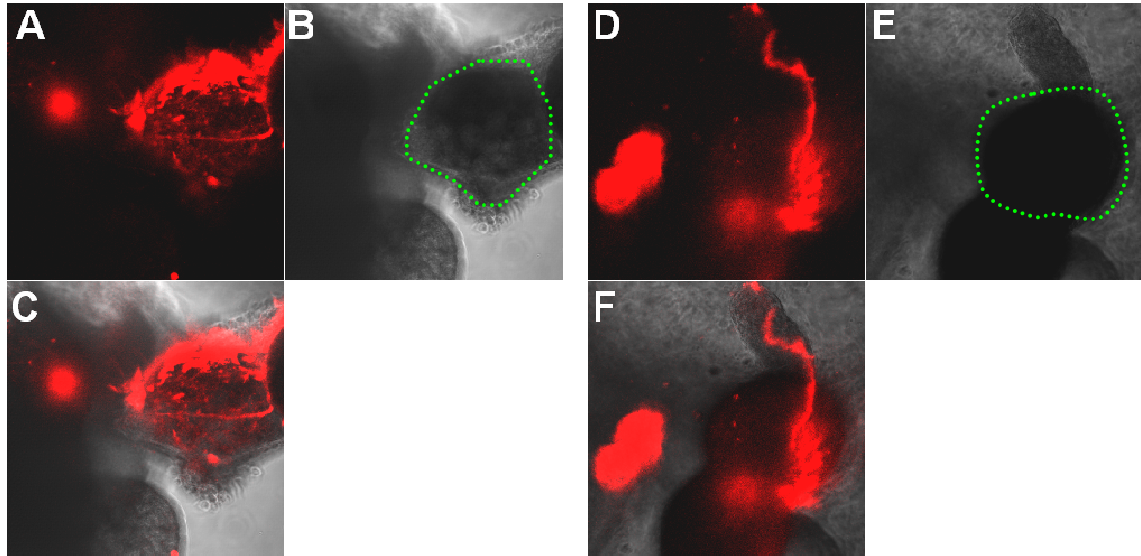
Figure 5.4: DiI labeling of the regenerating B5 neuron in organ culture. (A) 20x fluorescent image of DiI labeled neurons in the buccal ganglion. Note the projection traveling across the hemisphere of the ganglion. This is possibly a B5-B5 connection that occurs transiently following ET crush. **(B)** 20x phase contrast image of the buccal ganglion. The hemiganglion containing the DiI labeled neurons is outlined in green for easier visualization. **(C)** 20x combined (fluorescent and phase contrast) image of the labeled neurons. **(D)** 20x fluorescent image of a DiI labeled neuron and its projection. Although this neuron is not a B5, this demonstrates that it is possible to label neurons and their projections in the buccal ganglion. **(E)** 20x phase contrast image of the buccal ganglion. The hemiganglion containing the DiI labeled neurons is outlined in green for easier visualization. **(F)** 20x combined (fluorescent and phase contrast) image of the labeled neuron.

Another protocol, based on a model in *Drosphila* (Bossing & Technau, 1994), dissolved DiI in oil and placed a drop of that oil onto the neuron of interest. Using this method, no labeling of any neurons or projections was seen. An additional method attempted involved labeling the B5 neuron by touching the neuron overnight with a micropipette coated with DiI (Gelperin & Flores, 1997). There was no labeling visualized with this method either.

Because we thought that perhaps injection of the calcium indicator dyes was buffering calcium within our cells and halting regeneration, two fluorescent dyes that are not calcium indicators were investigated, FITC-dextran and Lucifer Yellow. Injection of these dyes would allow regeneration to be followed; however, changes in the intracellular calcium concentration could not be recorded. FITC-dextran did allow visualization of the axon, but once again, regeneration was not evident after cells were injected with this dye. Lucifer Yellow injections were also investigated. However, this method was abandoned once it was determined that cells injected with Lucifer yellow died following an extremely brief exposure to light (Figure 5.5).

One final issue in imaging growth cones was that often it was impossible to image the regenerating growth cones because they would be above the focal plane. Agar was used to hold the ganglia in place against the coverslip; however, if the nerve did not lie completely flat against the cover glass when the agar was added, imaging was impossible.
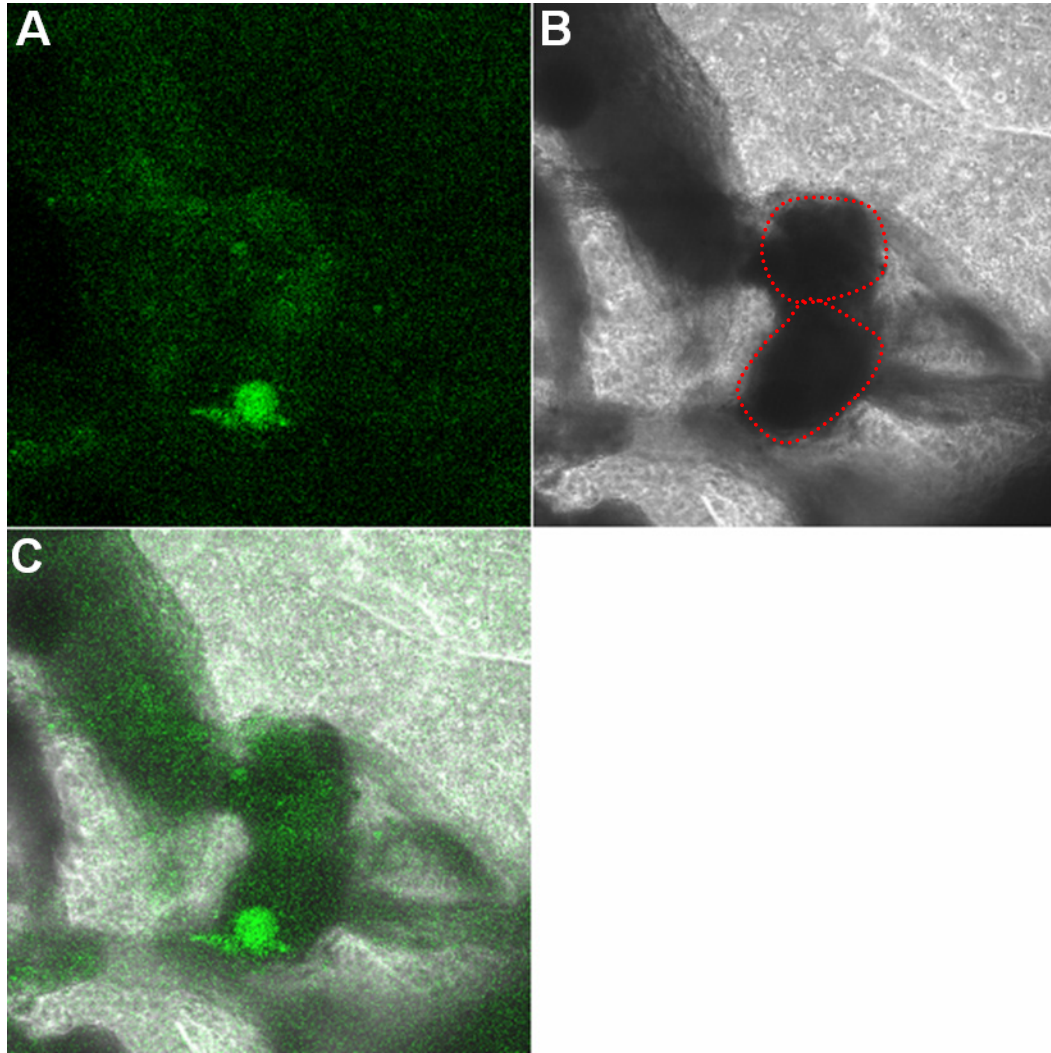
Figure 5.5: Lucifer yellow labeling of the regenerating B5 neuron in organ culture.
(A) 10x fluorescent image of a B5 neuron that has been injected with Lucifer yellow. **(B)** 10x phase contrast image of the buccal ganglia. The entire buccal ganglion has been outlined in red for easier visualization. **(C)** 10x combined (fluorescent and phase contrast) image of the injected B5 neuron and its small projection.

Discussion

The major difficulty with this project was that when neurons were injected with a calcium indicator dye, and imaged over hours, no regeneration was apparent. This could be due either to damage to the cell upon injection or to the calcium indicator dyes' property as a calcium buffer. However, it appears that the buffering property was not the issue because regeneration also did not occur in the presence of a non-calcium indicator dye, FITC-dextran. Therefore, it appears that the injury resulting simply from injection of the dye into the cell caused the neuron to stop regenerating. It is important to note that a large amount of dye was required to completely fill the neuron and its projection and the injury caused by injecting this amount of dye may have halted regeneration. It is also possible that although regeneration was halted during the imaging period following regeneration (around 7 hours), if the neuron was allowed to sit and recover, it might begin its regeneration process again. However, the dye usually had faded (or been removed from the cell) within 12-15 hours, making it impossible to know if regeneration had begun again. It is not possible to inject these cells a second time because following injection they are encased in agar, from which it is impossible to remove them without severe damage to the ganglion. Therefore, the set of DiI experiments were attempted to allow visualization of regeneration over a much longer time course, but this also had many difficulties.

Although the protocol with DiI coated electrodes has worked in the snail, *Limax*, there are a number of reasons why it may not be working in the current preparation (Gelperin & Flores, 1997). First of all, in the *Limax* study, the procerebral lobe of the

cerebral ganglion was labeled through a tear in the connective tissue sheath. Cutting the sheath on the buccal ganglia in *Helisoma* does not work, because the cells die from being exposed to saline for the length of time it takes to label the cells. To account for the sheath, however, the *Helisoma* ganglia were exposed to 0.1% protease for 5 minutes before DiI application. Additionally, DiI C_{12} was used in the *Limax* study, and the current study employed DiI C_{18}. The authors of the *Limax* study stated that using DiI C_{12} resulted in much improved staining compared to DiI C_{18}. In the future, the DiI experiment could be attempted again, perhaps using DiI C_{12} and/or using a higher concentration of protease, but for a shorter period of time.

An additional important issue that is critical to the effectiveness of regeneration involved the site of the crush. Previous studies have shown that the site of axotomy plays a vital role in whether the B4 neuron will regenerate and also in the extent of its regeneration (Kruk & Bulloch, 1992). Therefore, the ET nerves were crushed more than midway between the insertion into the buccal ganglia and the split into the salivary nerve and the gastric nerve (closer to the nerves' Y-split point). Not only does regeneration not always occur if the crush is too close to the insertion of the ET nerve into the buccal ganglion, but sprouting is also usually more pronounced in this situation.

The other major issue with the regeneration project was the extensive sprouting that was evident following dye injection into the B5 neuron. Because the neuron had so many projections emanating out of the regenerating stump, it was often difficult to determine which branch to image. Interestingly, the tips of these branches or growth cones had no filopodia, only a growth cone "stump." This could be due to a number of

factors. One possibility is that perhaps there are few to no filopodia on this growth cone when it is growing *in vivo*. If this is true, it may be due to the growth cone being fasciculated or following a "known" track. However, another possibility is simply that the filopodia are not loaded well enough or are too small to resolve in the ganglia using these dyes and confocal imaging. Alternatively, it could be that there are normally filopodia on the regenerating growth cone, but they retract following dye injection. Therefore, although this study confirms earlier findings that B5 neurons do regenerate *in vivo*, and that calcium uncaging within regenerating growth cones is possible, the simple fact that the regeneration process halted following dye injection did not allow this project to succeed.

5.2 Transfection of *Helisoma* neurons

Introduction

The current set of experiments explored the feasibility of transfecting either whole buccal ganglia or mass dissociated neuronal cultures from *Helisoma* with plasmids that have relatively standard promoters. If *Helisoma* neurons could be transfected with a plasmid containing a standard promoter, this would be advantageous because we could use this protocol to transfect *Helisoma* neurons with plasmids encoding calcium sensor proteins or other proteins related to the nitric oxide pathway. The major promoters that were employed were cytomegalovirus (CMV) and baculovirus. The plasmid was potentially introduced into the neurons with one of two methods, a lipid-based reagent, lipofectamine, which forms a complex with the DNA and delivers it to the interior of the cell, or direct microinjection of the plasmid into the soma of the neuron. In order to determine whether the cells were expressing these plasmids, two methods of detection were employed: either fluorescence or β-galactosidase (β-gal) staining.

There were a number of plasmids investigated in this project, including EGFP (enhanced green fluorescent protein), a potential calcium sensor (ER2), a cloned serotonin receptor from a crustacean, the spiny lobster (5-HT$_{2\beta Pan}$; Clark *et al*., 2004), CREB-EGFP, or pcDNA3.1/His/*lacz* (Invitrogen).

Materials & Methods

Lipofection of Mass Dissociated Neurons

Mass dissociated cultures of neurons from the buccal ganglion were plated and allowed 3 hours to adhere before transfection. Mass dissociated cultures were prepared by dissociating entire buccal ganglia with a micropipette and placing all cells into a culture dish. If whole ganglia were used, they were placed into a 24 well plate (3 ganglia per well) and transfected immediately following removal. Following removal, these cultures were transfected using lipofectamine (Invitrogen; Carlsbad, CA) in combination with either Opti-MEM I Reduced Serum Medium or L-15 (Invitrogen).

To transfect mass dissociated cultures or whole ganglia, first the DNA was diluted in Opti-MEM I Reduced Serum Medium or L-15 medium (DNA concentrations range from 0.8 µg to 5 µg per well/dish). Next, lipofectamine was diluted in Opti-MEM or L-15 in appropriate amounts to allow for ratios of 1:1 to 1:5 of DNA to lipofectamine. This mixture was allowed to sit at room temperature for 5 minutes. Then, the lipofectamine and DNA mixtures were combined and allowed to sit for 20 minutes. The cells or ganglia were rinsed twice with Opti-MEM or L-15 and then the cells/ganglia were incubated in the lipofectamine/DNA mixture for 4 to 48 hours. The cells and ganglia were incubated for various time periods to determine if it may have an effect on transfection efficacy. Following this time period, the cells or ganglia were rinsed with L-15 and then incubated in conditioned medium.

Microinjection of Plasmids

Micropipettes were pulled from glass capillaries (A-M System, Everett, WA) on a microelectrode puller (Fredrick Haer and Co., Bowdinham, ME) and filled with a combination of plasmid (from 0.1-1 µg/µl) and fast green (from 0.1-2%). Neurons were injected, allowed three days for expression and then fixed and stained using a β-Gal staining kit (Invitrogen) to check for expression.

Plasmids and Visualization

The following plasmids were used: EGFP (enhanced green fluorescent protein; Clontech; Palo Alto, CA), GFP (green fluorescent protein; Invitrogen; Carlsbad, CA), a potential calcium sensor (gift from laboratory of Jenny Yang), a cloned serotonin receptor from a spiny lobster (5-HT$_{2\beta Pan}$; Clark *et al*., 2004), CREB-EGFP (Clontech), or pcDNA3.1/His/*lacZ* (Invitrogen, Carlsbad, CA). Expression of plasmids was determined either by visualization of fluorescence within the soma or growth cones (EGFP plasmids) or a β-galactosidase (β-Gal) staining kit (*lacZ* plasmid; Invitrogen).

Results

In the first set of experiments, either mass dissociated primary neuronal cultures or whole ganglia were lipid transfected with a number of different plasmids. Neuronal cultures were transfected with EGFP (employing a CMV promoter) or GFP (employing a baculovirus promoter). With both of these plasmids, however, it was apparent that autofluorescence is prominent in *Helisoma* neurons because fluorescence was apparent in

the soma of untransfected cells when imaged with the appropriate filter sets for either of these proteins. This autofluorescence is quite prominent in the soma of *Helisoma* neurons, but is not present in the growth cones, and thus is not a factor for fluorescent imaging experiments employing growth cones.

Because some autofluorescence was evident in all wavelengths examined (although it was greatest in the FITC range), we employed a plasmid that would produce a protein that would increase its fluorescence upon stimulation, under the idea that this stimulated fluorescence would be brighter than the autofluorescence seen under normal conditions. Therefore, *Helisoma* neurons were transfected with CREB-EGFP that increases in fluorescence when CREB is phosphorylated. To these cultures, 10 μM forskolin was added (forskolin activates PKA that phosphorylates CREB), and an increase in fluorescence was seen. This initially seemed promising, but control (non-transfected) cultures also showed an increase in fluorescence in response to forskolin (Figure 5.6). This means that the autofluorescence in the soma of untransfected *Helisoma* neurons increases with standard FITC excitation. Although autofluorescence is known to be prominent in the soma of these neurons, we hoped to avoid this issue by examining fluorescence in growth cones. Growth cones did not exhibit autofluorescence, however no fluorescence was ever present in growth cones following transfection.

An additional set of experiments involved lipid transfection of mass dissociated neuronal cultures with the 5-HT$_{2\beta Pan}$ receptor from spiny lobster (Clark *et al.*, 2004), followed by loading the cells with fura-2 (a calcium indicator dye) and then applying 50 μM serotonin. Because it has been shown that around 50% percent of cells in the buccal
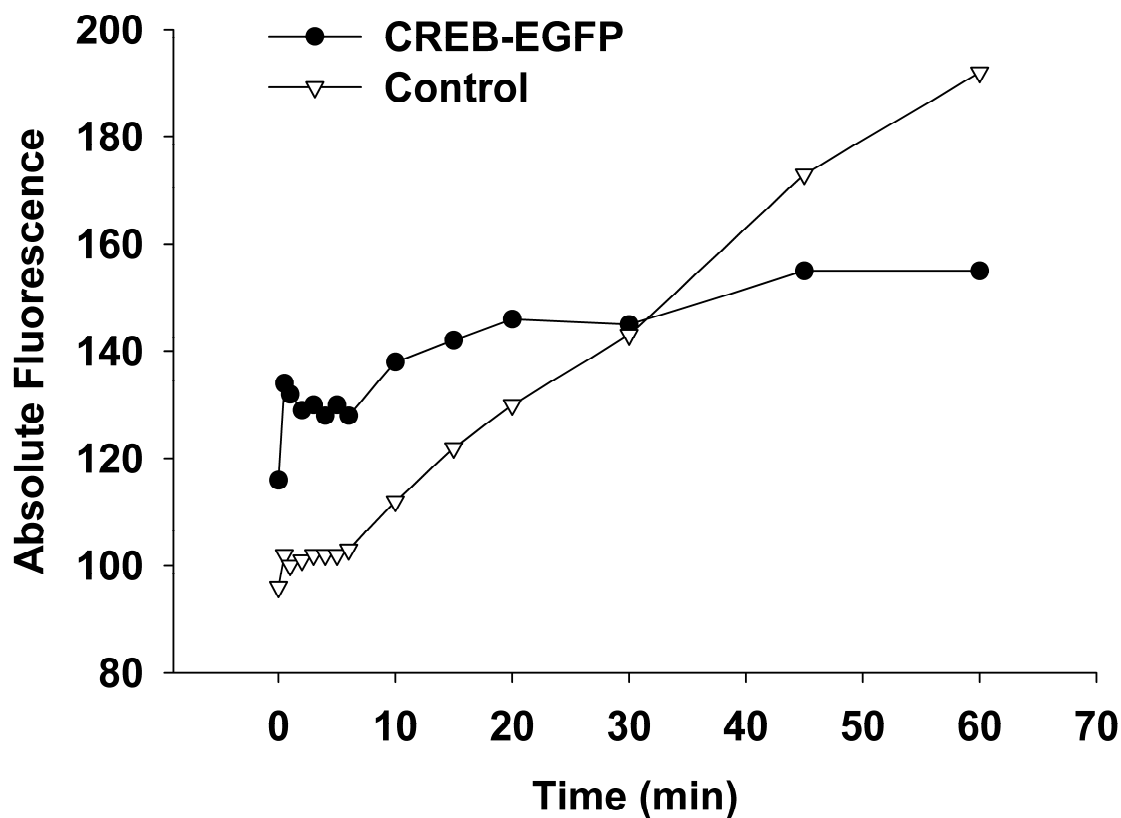
Figure 5.6: **Absolute fluorescence in the soma increases following addition of 10 µM forskolin to CREB-EGFP transfected neurons and control neurons.** Following addition of 10 µM forskolin to CREB-EGFP transfected neurons and control neurons, absolute fluorescence increases within the soma of both types of neurons. This suggests that autofluorescence increases in the soma of control neurons following repeated light exposure with a standard FITC filter set. 0 minutes represents the time point immediately prior to forskolin addition. Forskolin was then added between time 0 and 1 minute (n = 1).

ganglion usually respond to serotonin with an increase in calcium (Goldberg *et al.*, 1992), it was thought that if this receptor was active in these neurons, then we should see an increase in that percentage. However, an increase from reported values was not seen; in fact, even fewer neurons responded to serotonin with an increase in calcium.

In the next set of experiments mass dissociated neurons were lipid transfected with a 5-HT$_{2\beta Pan}$ receptor from spiny lobster (Clark *et al.*, 2004) and then subsequently stained with an antibody to this receptor. The goal of this experiment was to determine if the neurons were able to express the plasmid encoding the 5-HT$_{2\beta PAN}$ receptor. Following transfection, the neurons sat for 3 days to allow time for plasmid expression, and then were fixed and stained with a fluorescent antibody to this receptor. Because autofluorescence is a problem in *Helisoma* neurons, control dishes were made at the same time by transfecting neurons with an empty vector (PIRES$_{neo}$). These dishes were fixed and stained at the same time and then the fluorescence level between the control and 5-HT$_{2\beta PAN}$ receptor dishes were compared. In this experiment, a higher level of fluorescence was seen in the dishes that were transfected with the 5-HT$_{2\beta PAN}$ receptor as compared to the control empty vector transfected dishes (Figure 5.7, p$\leq$0.001). This result suggested that *Helisoma* neurons were expressing the 5-HT$_{2\beta PAN}$ receptor.

Because autofluorescence is quite prominent and variant in our neuronal cultures, in order to conclusively determine if our neurons were actually expressing the plasmid, the cultures were lipid transfected with a pcDNA3.1/His/*lacZ* plasmid. Through the use of a β-Gal staining kit, it would be easy to determine visually if the neurons were expressing the plasmid, and eliminate the confounding factor of autofluorescence.
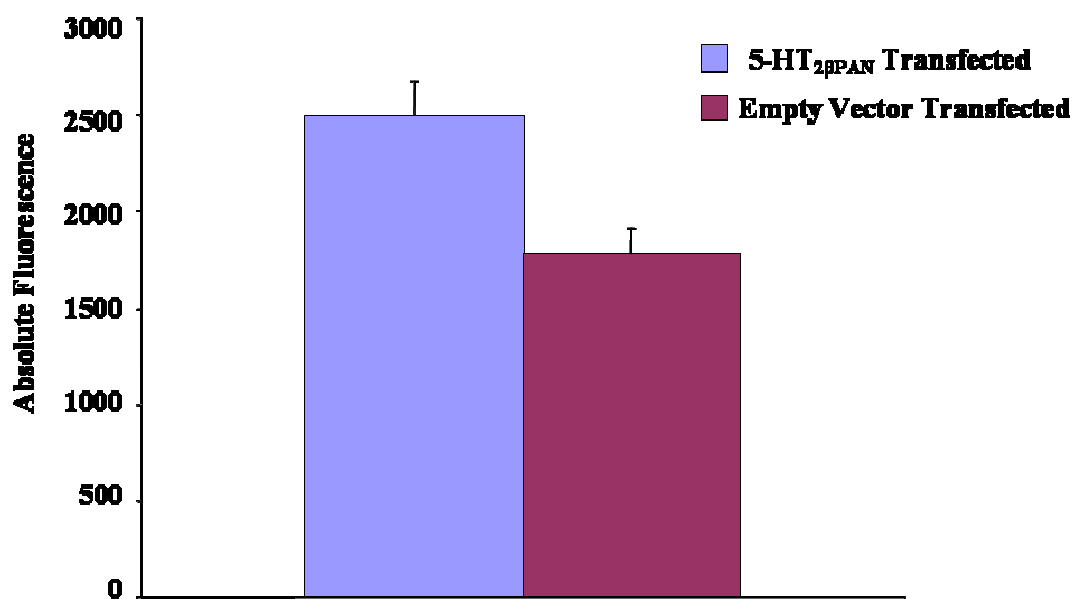
Figure 5.7: 5-HT$_{2\beta PAN}$ transfected neurons are more fluorescent than empty vector transfected neurons. Neurons that are transfected with a plasmid containing the 5-HT$_{2\beta PAN}$ receptor are more fluorescent than neurons that are transfected with an empty vector (n = 30 cells, 1 dish per condition). Three days following transfection, cells were fixed and stained with an antibody to the 5-HT$_{2\beta PAN}$ receptor. Neurons that are transfected with the serotonin receptor are significantly more fluorescent than those that are transfected with an empty vector (p $\leq$ 0.001).

Therefore, neuronal cultures were transfected with the pcDNA3.1/His/*lacZ* plasmid and then stained with the β-Gal staining kit. However, staining was not apparent (n = 6 dishes).

In the final set of experiments, *Helisoma* neurons were plated and allowed 1-2 days to adhere to the substrate. They were then directly microinjected with a combination of pcDNA3.1/His/*lacZ* plasmid (from 0.1-1μg/μl) and fast green (from 0.1-2%). After the neurons were injected, three days were allowed for expression. Then, the neurons werefixed and stained using a β-Gal staining kit to check for expression. Unfortunately, expression was not evident in any cell (n = 4 dishes).

Discussion

In this set of experiments, both whole ganglia and mass dissociated neuronal cultures were transfected with a number of different plasmids. The first step in this set of experiments was to determine if the plasmids were actually being expressed. Initially, it appeared that *Helisoma* neurons were expressing these proteins, but upon closer examination it was observed that the soma of *Helisoma* neurons have a great deal of autofluorescence. Therefore, it is impossible to separate out the autofluorescence from the possible EGFP expression. This autofluorescence may be due to a number of factors. First of all, it has been reported that transfecting cells with lipofectamine does cause vacuole type autofluorescence, which also has been observed in *Helisoma* neurons (personal observations). Secondly, many of the neurons from the buccal ganglion are pigmented, which also causes autofluorescence. In another snail, this problem was

addressed by raising snails from birth on a diet entirely of lettuce. This study reported that doing such reduced the pigmentation in the soma of these neurons (Elliott & Kleindienst, 1990). However, preliminary studies conducted in *Helisoma* did not seem to give the same result (personal observations).

Mass dissociated neurons were also lipid transfected with either EGFP, GFP, 5-HT$_{2\beta Pan}$, or CREB-EGFP. Although results with a number of these probes initially appeared promising, it has also been determined that the autofluorescence in *Helisoma* buccal neurons increases with repeated imaging (excitation with the FITC filter set). It is also important to note that it has been reported that autofluorescence can emit even more green light than what is emitted by EGFP (Doyle *et al.*, 2003). Therefore, distinguishing transfected cells by looking for an increase in fluorescence could be misleading because it may just mean that there an increased amount of autofluorescence in that cell. Autofluorescence in the central nervous system is usually due to the presence of lipofuscin, which increases in amount with age (Doyle *et al.*, 2003). However, it is unknown if this is the cause of the autofluorescence seen in *Helisoma* neurons.

Because autofluorescence is very prominent and variant in *Helisoma* neurons, in order to confirm that our neurons were expressing these plasmids, they were lipid transfected or injected with the pcDNA3.1/His/*lacZ* plasmid and then stained with a β-Gal staining kit. However, staining was not evident in these experiments. In order to determine whether perhaps the lipid based transfection reagent was not in fact delivering the plasmid to the interior of the cell, direct microinjection of the plasmids was

performed. However, expression of this plasmid was not evident following direct microinjection either.

The major downfall to this project may have been the type of promoter chosen. Most of the plasmids used thus far employ either a CMV or a baculovirus promoter. Although there are two previous papers that demonstrate the successful use of a CMV promoter in mollusks, these studies were not using neuronal cultures. One study used liposomes to successfully express a plasmid with a CMV promoter in oyster heart primary cell cultures (Boulo *et al.*, 1996). Another study employed a lipofectamine-type reagent (DOTAP) to express a plasmid with a CMV promoter in a snail (*Biomphalaria glabrata*) embryonic cell line (Lardans *et al.*, 1996). However, these cell types may be quite unlike neurons, and as such, a different promoter type may be required for *Helisoma* neuronal expression.

Previous studies in *Aplysia* have observed plasmid expression in primary neurons via microinjection of plasmids with particular promoters (Kaang, 1996b; a). In these studies, when a plasmid that had a CMV promoter was injected, expression was not seen. Because a CMV promoter was employed in the current set of experiments, this may be the major issue. Promoters that have been shown to work in *Aplysia* include RSV, AP-1 RSV, VIP, and *c-fos* (Kaang, 1996a). Although many of these promoters are not commercially available in a plasmid, a future study would most likely benefit greatly from obtaining the most successful of these plasmids, the pNEX vector, which employs the AP-1 RSV promoter.

5.3 Turning of *Helisoma* neuronal growth cones

Introduction

When growth cones are migrating to their point of synaptic connection, the migration usually does not occur in a straight line. Therefore, turning of growth cones during development is an important process, which has recently begun to be studied in depth. There are multiple studies that have demonstrated that growth cones *in vitro* will turn in response to an extracellular gradient of a variety of chemotropic molecules, including netrin-1, retinoic acid and glutamate (Zheng *et al.*, 1996; Ming *et al.*, 1997; Dmetrichuk *et al.*, 2006). Interestingly, work employing *Xenopus* spinal neuron growth cones has shown that netrin-1 can serve as either an attractive or repellant cue, depending on the concentration of specific second messengers within those growth cones (Nishiyama *et al.*, 2003). Turning has also been exhibited by growth cones from invertebrate neurons. In the pond snail, *Lymnaea*, a gradient of retinoic acid results in attractive turning of growth cones (Dmetrichuk *et al.*, 2006). Additionally, *Helisoma* growth cones exhibit repulsive turning in response to a gradient of a myosin light chain kinase inhibitor, ML-7, that disrupts actin bundles within growth cones (Zhou *et al.*, 2002). Because previous studies had demonstrated that nitric oxide causes a slow down in neurite outgrowth at lower concentrations and growth cone collapse at high concentrations, we thought that it might serve as a chemorepellant factor in growth cone migration (Trimm & Rehder, 2004). In *Helisoma*, the migration route of the B5 neuron contains multiple branch points and nitric oxide could act as a repellant factor at those branch points to mediate growth cone

migration away from the inappropriate nerve branch. Therefore, in the current study, we sought to determine if growth cone turning could be initiated by an extracellularly applied gradient of nitric oxide.

Materials & Methods

Individual B5 neurons from *Helisoma trivolvis* were plated onto poly-L-lysine coated glass coverslips and allowed 1-2 days to extend projections tipped with growth cones. NOC-7 or NOC-5 (Calbiochem) were employed at various concentrations as the nitric oxide donor. NOC-7 or NOC-5 were locally applied to one side of a growth cone via micropipette, in combination with a Picospritzer (General Valve Corporation, Fairfield NJ) and stimulator. The concentration of NOC-7 within the pipette, as well as the duration and frequency of application were varied to determine the parameters that would result in growth cone turning.

Results

Although this experiment was performed numerous times, with variations in the concentration of the nitric oxide donor, the micropipette distance from the growth cone, frequency of application and burst duration, turning was never definitively observed (see Table 5.1 for representative parameters tested). In all experiments conducted, growth cones either collapsed or continued growing in their initial direction, and turning was never observed.

Table 5.1: Growth cone turning parameters tested.

Date	Drug & Concentration	Angle to Growth Cone	Distance from Growth Cone	Duration of Puff	Frequency of Application	Result
7.13.05	100 μM NOC-5	45°	50 μm	40 ms	5 puffs/20 seconds	No turning
7.13.05	500 nM CytoB	45°	50 μm	35 ms	5 puffs/20 seconds	No turning
7.14.05	100 μM ML-7	45°	75-100 μm	10 ms	5 puffs/20 seconds	No turning
8.17.05	100 μM NOC-5	45°	75-100 μm	10 ms	1 puff/second	No turning
8.18.05	100 μM NOC-5	45°	75-100 μm	10 ms	1 puff/second	No turning
9.14.05	200 μM NOC-5	45°	100 μm	5 ms	2 puffs/second	No turning
9.16.05	200 μM NOC-5	45°	100 μm	20 ms	2 puffs/second	No turning
9.21.05	200 μM NOC-5	45°	50 μm	20 ms	2 puffs/second	No turning

Discussion

In vitro studies suggest that nitric oxide can act as a "stop and search" signal for migrating *Helisoma* B5 growth cones (Trimm & Rehder, 2004). *In vivo*, it may be that nitric oxide released from cells along a growth cone's migration route mediates appropriate motility. In order to investigate the possibility of NO acting as a guidance cue, the current set of experiments addressed *in vitro* turning of B5 growth cones as a result of repeated local NO application. The concentration of the nitric oxide donor, micropipette distance from the growth cone, frequency of application, and burst duration were varied in these experiments to find parameters that would cause growth cone turning. However, in all experiments attempted, growth cones either collapsed or continued growing in their initial direction, and turning was never observed.

A previous study employing *Helisoma* B5 neurons demonstrated that an extracellular applied gradient of a myosin light chain kinase inhibitor, ML-7, to growth cones results in repulsive turning away from the gradient (Zhou *et al.*, 2002). It is thought that this application of ML-7 resulted in local actin bundle loss on one side of the growth cone, resulting in turning away from the gradient. Therefore, that study demonstrated the ability of *Helisoma* growth cones to exhibit turning *in vitro*, suggesting that there may be a narrow range of parameters that result in turning. However, it is also possible that nitric oxide is not a cue that initiates turning of *Helisoma* B5 growth cones.

5.4 Vesicle movement within *Helisoma* growth cones

Introduction

Vesicle trafficking is important for neurite extension and growth cone steering during development, because vesicles serve as membrane donors and transport needed proteins to the growth cone (Craig *et al.*, 1995; Henley & Poo, 2004). Until recently, it was thought that vesicles were found in the central domain of the growth cone, but were not present in filopodia (Rees *et al.*, 1976; Cheng & Reese, 1985; Diefenbach *et al.*, 1999). However, a recent study suggests the presence of vesicles in filopodia of rat visual cortical neurons (Sabo & McAllister, 2003). Additionally, an earlier study using chick ciliary ganglion neurons demonstrated that there are two types of endocytotic vesicles (endosomes) within growth cones: evoked endosomes and constitutive endosomes (Diefenbach *et al.*, 1999). Evoked endosomes are dependent on depolarization for their formation and release, whereas constitutive endosomes are not. Therefore, vesicles are a prominent structure within the growth cone.

Because the two aforementioned studies found opposing results on the localization of vesicles within filopodia (Diefenbach *et al.*, 1999; Sabo & McAllister, 2003), we sought to determine if vesicles were localized within filopodia of *Helisoma* growth cones. *Helisoma* growth cones lend themselves to this type of study because in comparison to chick and rat growth cones, *Helisoma* growth cones are quite large and the filopodia are numerous and well-defined. Therefore, the current experiment examined vesicle placement and movement within *Helisoma* neuronal growth cones, by employing

a fluorescence dye that stains vesicles, termed FM 1-43. *Helisoma* B5 neurons were loaded with the vesicular marker, FM 1-43. The vesicles in the neurons were then "unloaded" through the use of a depolarizing stimulus, potassium chloride (KCl). In this experiment, vesicle placement within specific regions of the growth cone prior to and following unloading were examined.

Materials and Methods

FM 1-43 Loading and Unloading

B5 neurons were removed from the buccal ganglion and plated on poly-L-lysine coated glass coverslips. They were used for experimentation once they had extended neurites tipped with growth cones (1-2 days following plating). Once growth cones were apparent, B5 neurons were loaded with 4 μM FM 1-43 and 34 mM KCl in L-15 (2ml total) for 1 minute. Following loading, the cells were rinsed 3 times with L-15. The neurons were unloaded using 34 mM KCl in L-15. Growth cones were imaged using a Zeiss Axiovert 135 microscope in combination with a cooled CCD camera (CH250, Photometrics; Tuscon, AZ) and stored on a Macintosh Quadra 800 (Apple Computer Inc.; Cubertino, CA).

Results

Vesicular placement and movement was examined using FM 1-43, a fluorescent dye that specifically labels vesicular membranes. In order to load B5 neurons with this dye, they were exposed to 4 μM FM 1-43 and 34 mM KCl in L-15 for 1 minute. Following

loading, the cells were rinsed 3 times with L-15. The neurons were then unloaded using 34 mM KCl in L-15. Vesicle placement and movement within the growth cone was examined after loading and unloading. Immediately following loading, vesicle counts were highest in the central domain of the growth cone (34.5 ± 6.1 vesicles per growth cone) and much lower in the lamellipodia (8 ± 2.6 vesicles per growth cone; Figure 5.8). Few to no vesicles were seen in the filopodia (0.2 ± 0.1). One minute following unloading with 34 mM KCl, the average number of vesicles in the central domain dropped to 24.9 ± 5.5. By five minutes, this was reduced further to 11.5 ± 2.7 vesicles in the central domain.

Discussion

With the use of FM 1-43, it was possible to determine that most vesicles in the *Helisoma* B5 growth cone lie in its central domain. There are a few vesicles present in the lamellipodia, but almost none are found in filopodia. Although a previous study using FM 1-43 in chick ciliary neuronal growth cones demonstrated that vesicles are found throughout the growth cone, they were rarely seen in filopodia (Diefenbach *et al.*, 1999). However, this is in contrast to a recently published paper that suggests that vesicles are commonly found in filopodia of rat cortical neurons (Sabo & McAllister, 2003). This difference that is seen could be due to the type of neurons used in each study (*Helisoma* buccal neurons and chick ciliary neurons versus rat cortical neurons). However, it is also possible that the technique used with the rat cortical neurons (Sabo & McAllister, 2003)
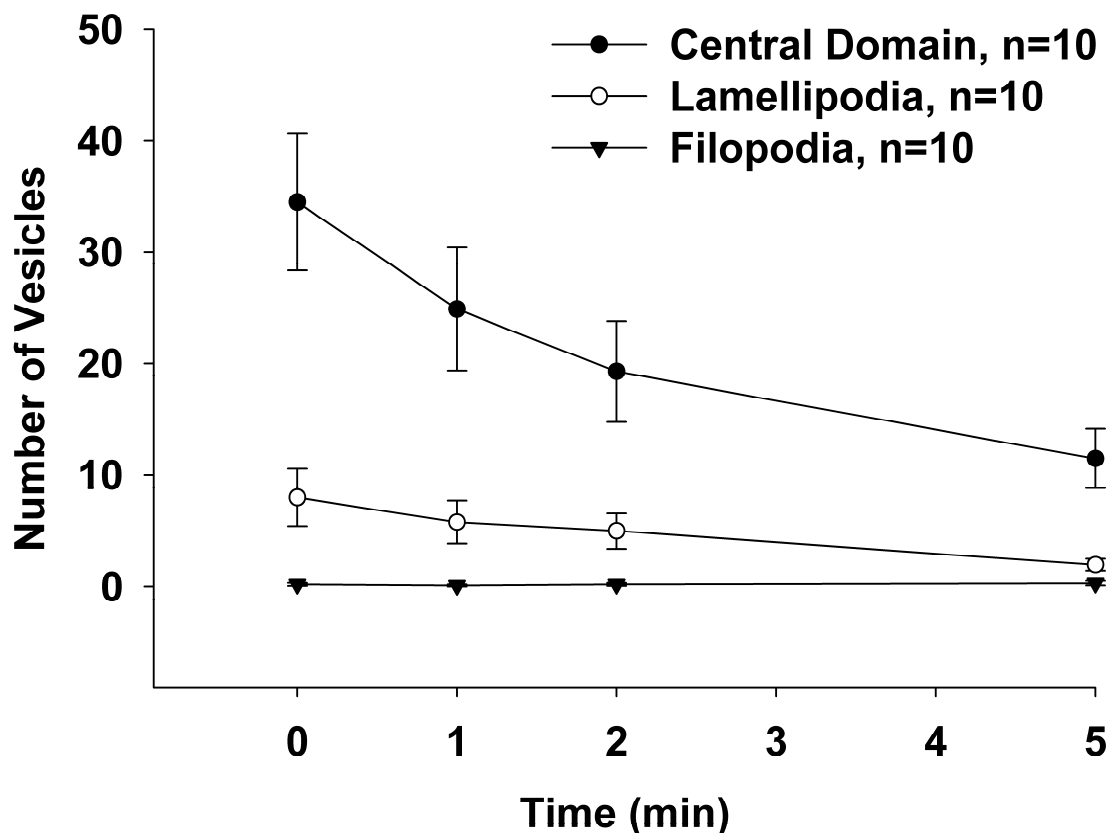
Figure 5.8: Vesicles are most prominent in the central domain of growth cones, lower in the lamellipodial region, and few to no vesicles are seen within filopodia. *Helisoma* B5 growth cones were loaded with the vesicular marker dye, FM 1-43 (t = 0 minutes) and then unloaded with 34 mM KCl (immediately following t = 0 minutes). Immediately following loading, vesicle counts were highest in the central domain of the growth cone, much lower in the lamellipodial region, and few to no vesicles were seen in filopodia. Five minutes following unloading with 34 mM KCl, the average number of vesicles within the central domain was reduced by more than 50%, in comparison to pretreatment values.

allowed for the visualization of vesicles in filopodia because they used a different vesicular dye (FM 4-64) than in the present study and the one employing chick ciliary neurons (Diefenbach *et al.*, 1999). Therefore, the results of this study are inconclusive and further studies should be conducted to further investigate the localization of vesicles within the filopodia of *Helisoma* growth cones.

5.5 Protein kinase inhibition slows neurite outgrowth

Introduction

Growth factors are molecules that promote neuritogenesis and neurite outgrowth. Neurite outgrowth from *Helisoma* neurons will not occur unless they are cultured in conditioned medium, which is made by incubating *Helisoma* ganglia in Leibovitz's L-15 medium (L-15) for 3-4 days (Wong *et al.*, 1981). During this period, the ganglia will release growth factors, mostly unidentified, that are required for neurite extension. Previous experiments in the Rehder lab demonstrated that removal of growth factors from the medium (by replacing conditioned medium with standard L-15 once neurite outgrowth has been initiated) results in filopodial elongation and a decrease in neurite outgrowth (K. Tornieri, personal communication). Because many growth factors act via protein tyrosine kinases, we sought to examine whether inhibition of protein tyrosine kinases would result in similar effects on growth cone morphology and outgrowth. If the inhibition of these protein tyrosine kinases resulted in similar effects on growth cone morphology and outgrowth, it is likely that they may mediate effects of growth factors on the cytoskeleton. Furthermore, knowledge about the particular protein tyrosine kinases that are involved in growth cone motility may provide us with clues about the particular growth factors that mediate outgrowth in *Helisoma*.

Materials & Methods

Genistein and Lavendustin A, two tyrosine kinase inhibitors, were made up in dimethylsulfoxide (DMSO, Sigma) to obtain stock concentrations of 100 mM and 20 mM, respectively. Genistein was added to conditioned medium to result in final concentrations of 50 µM, 100 µM, and 200 µM. Lavendustin A was added to conditioned medium to result in final concentrations of 10 µM and 20 µM. Control experiments were also performed in which growth cones were exposed only to the vehicle (DMSO) in appropriate concentrations. Growth cones exposed to vehicle only showed no change in neurite outgrowth over the 2 hour time period (data not shown).

In this set of experiments, B5 neurons were removed from the buccal ganglion, plated into conditioned medium and allowed to grow for 1-2 days. For outgrowth experiments, growth cones were imaged through the 40X objective of an ausJENA Sedival microscope. The images were captured with a CCD C72 camera (MIT Dage, Michigan City, IN), digitized on a frame grabber (Scion LG-3; Scanalytics, Fairfax, VA) and stored on an Apple Macintosh G3 (Apple Computer Inc.; Cupertino, CA). Images were obtained every 20 minutes, for 1 hour prior to drug addition (t = -60, -40, -20, and 0min) and two hours after drug addition (t = +20, +40, +60, +80, +100, +120min). Drugs were added immediately following image acquisition at t = 0min. To add the drug to the medium, 0.2 ml of conditioned medium was removed from the dish and the drug was added into this medium and then replaced in the dish. Outgrowth length was determined by measuring from a fixed point in the dish to the central domain of the growth cone at

each time point through the use of "Scion Image" software (Scion Corporation; Frederick, Maryland).

Results

Inhibition of protein tyrosine kinases results in a slowing/stoppage of neurite outgrowth

In the current set of experiments, *Helisoma* B5 neurons were exposed to genistein, a general protein tyrosine kinase inhibitor, to examine its effects on neurite outgrowth. At the 50 and 100 µM concentrations of genistein, neurite outgrowth was significantly slowed in the first hour and further decreased in the second hour (Figure 5.9, both effects $p \leq 0.001$). At the 200 µM concentration, neurite outgrowth was stopped in the first hour (from 17.0 ± 1.3 µm/h to 0.43 ± 1.9 µm/h; Figure 5.9) and did not recover in the second hour (-2.2 ± 0.96 µm/h; both effects $p \leq 0.001$). In addition, the stoppage of outgrowth occurred within the first 20 minutes after addition of 200 µM genistein (data not shown).

Inhibition of EGF RTK results in a slowing/stoppage of neurite outgrowth

Genistein is a general protein tyrosine kinase inhibitor. Therefore, we employed a more specific receptor tyrosine kinase inhibitor, Lavendustin A, to determine its effects on filopodial length and neurite outgrowth. Lavendustin A specifically inhibits epidermal growth factor receptor tyrosine kinases (EGF RTK). Addition of Lavendustin A had a dose-dependent effect on neurite outgrowth (Figure 5.10). At the 10 µM concentration, neurite outgrowth slowed significantly in the second hour of drug addition (from $20.4 \pm$
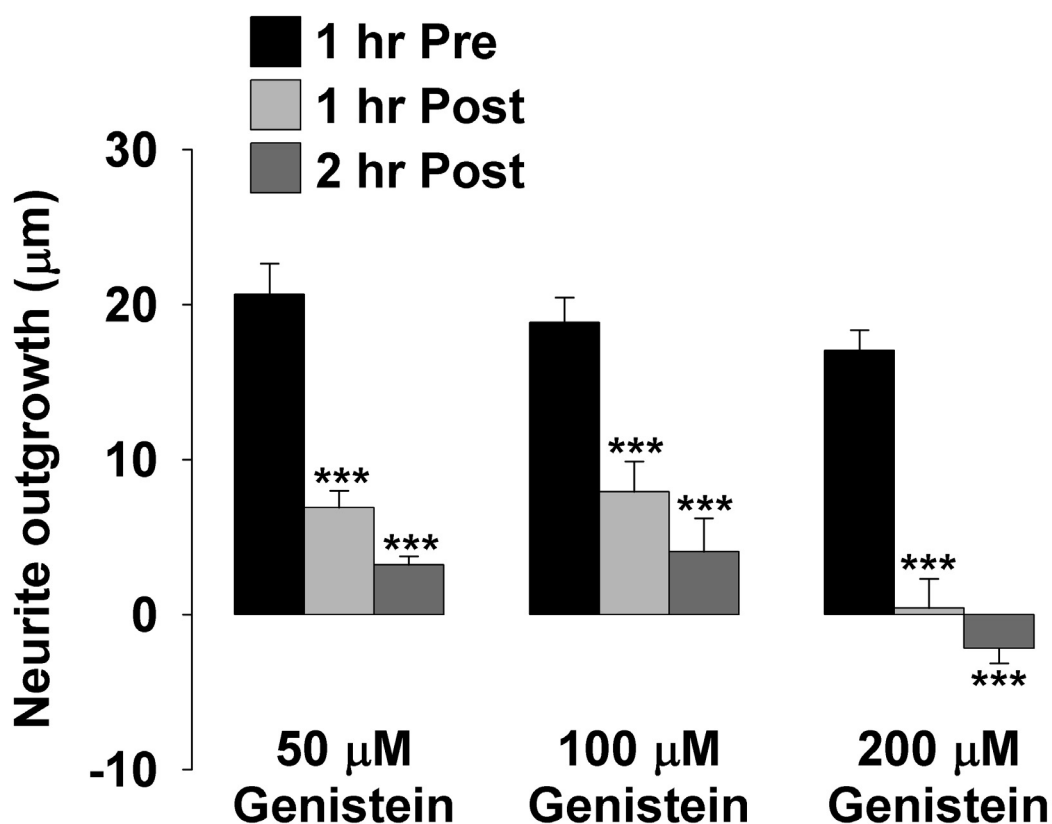
Figure 5.9: Inhibition of protein tyrosine kinases results in a dose-dependent decrease in neurite outgrowth. Inhibition of protein tyrosine kinases with 50 µM (n = 18) and 100 µM (n = 13) genistein causes a slow-down in the rate of neurite outgrowth in the first and second hour following drug addition. Two hundred µM Genistein (n = 14) results in a complete stoppage of outgrowth in the first hour following drug addition and a slight retraction in the second hour. All of these effects were highly significant (student's t-test, $p \leq 0.001$) when comparing the growth rates in the hour before treatment to the growth rates in the first and second hour following drug addition.
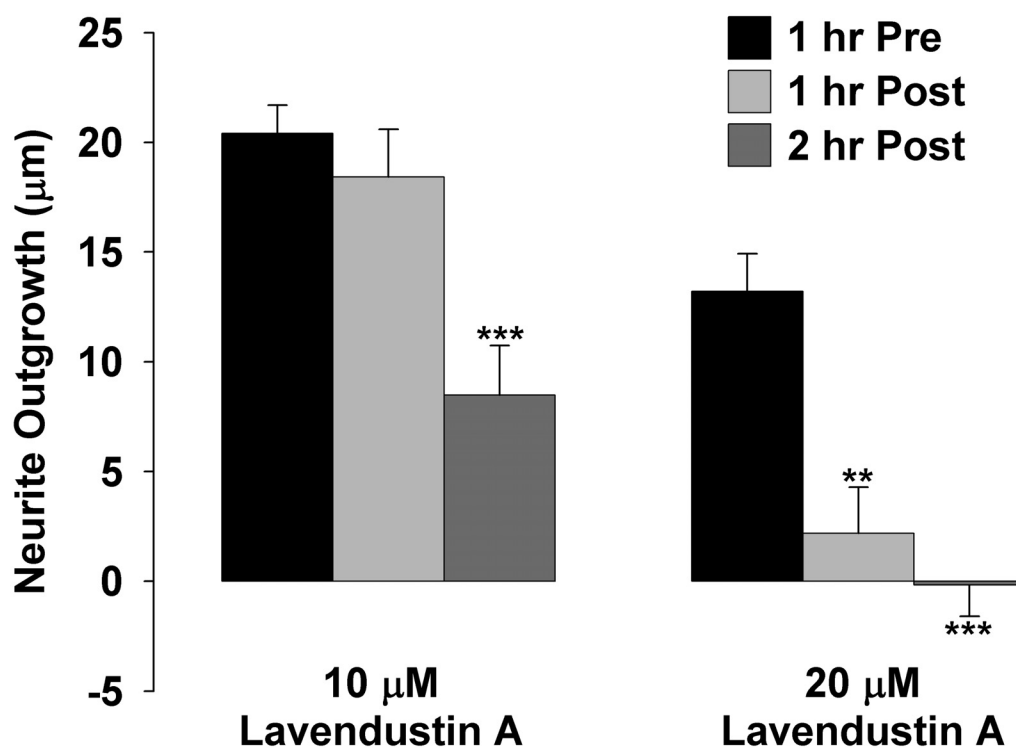
Figure 5.10: Inhibition of EGF RTK results in a slowing of neurite outgrowth. Inhibition of EGF RTK with 10 μM Lavendustin A (n = 14) has no effect on neurite outgrowth in the first hour following drug addition, but causes a significant slow-down in outgrowth in the second hour following drug addition (as compared to the hour before treatment, $p \leq 0.001$). Twenty μM Lavendustin A (n = 11) results in a significant slow-down in neurite outgrowth in the first and second hours following drug addition (as compared to the hour before treatment, $p \leq 0.01$ for 1 hr Post and $p \leq 0.001$ for 2 hr Post).

1.3 μm in the hour prior to drug addition to 8.5 ± 2.3 μm; p ≤ 0.001). Twenty μM

Lavendustin A caused neurite outgrowth to be slowed more rapidly and strongly, and

completely halted outgrowth in the second hour following drug addition (from 13.2 ± 1.7

μm in the hour prior to drug addition to -0.2 ± 1.4 μm in the second hour following drug

addition). However, it is also important to note that neurite outgrowth rates in the hour

prior to Lavendustin A addition are different between the 10 μM and the 20 μM

conditions. This is common when measuring *Helisoma* neurite outgrowth rates, which

usually range from 10-20 μm per hour, but can vary from dish to dish. In the current

study, both 1 hour pretreatment groups fall into this common range of outgrowth rates,

but do appear to be different from one another.

Discussion

The current experiments demonstrate that inhibition of protein tyrosine kinases, and

specifically, EGF RTK, results in a slow-down of neurite outgrowth. These findings

complement a previous study from this lab that demonstrated that 200 μM genistein

results in significant filopodial elongation, but has no effect on filopodial number (Cheng

et al., 2000). Therefore, inhibiting protein tyrosine kinases in *Helisoma* B5 neurons

results in a slow down and search behavior that is characterized by a reduction in neurite

outgrowth along with filopodial elongation. Additionally, these changes in growth cone

dynamics mimic the effect of removing growth factors.

Another study from this lab demonstrated that inhibition of members of the PI-3K

pathway results in a slow down and search behavior, which is characterized by an

increase in filopodial length and a decrease in the rate of neurite outgrowth (Tornieri *et al.*, 2006). This behavior also mimics that which is seen when growth factors are depleted from the medium. Specifically, growth factors are thought to act via RTKs, and if RTKs are inhibited with genistein or Lavendustin A, the result is similar to that which is seen when growth factors are depleted. This suggests that when a growth cone is pathfinding where concentrations of growth factors may be low, a growth cone would slow its outgrowth rate and increase its filopodial length, in order to sample a larger portion of the environment, thereby allowing for appropriate pathfinding.

Examination of targets of the lipid kinase activity of PI-3K (ROCK and Akt) demonstrated that filopodial dynamics can be regulated independently of neurite outgrowth (Tornieri *et al.*, 2006). In these experiments, filopodial dynamics were affected in the first 30 minutes following drug addition, but an effect on neurite outgrowth was not seen until the second hour following drug addition. This means that the "slow-down and search" behavior that is seen can actually be divided into two parts: "slow-down" and "search." This would be useful for a growth cone that may need to maintain a constant speed, while increasing its action radius. This is what is seen with inhibition of Akt or ROCK. However, if a growth cone needs to sample its environment more closely, the behaviors can be coupled into the entire "slow-down and search" behavior that is seen with inhibition of RTKs.

5.6 NGF or BDNF alone are not sufficient to result in sprouting of *Helisoma* neurons

Introduction

Helisoma buccal neurons are cultured in conditioned medium, which is made by incubating the central ring ganglia from *Helisoma* in Leibovitz's medium for 3 to 4 days. During this process, these ganglia release growth factors into the medium that are necessary for neurite outgrowth (Wong *et al.*, 1981). Although attempts have been made to characterize the factors present in this conditioned medium, only one factor has been identified, which is a laminin-like ~300 kD extracellular matrix protein (Miller & Hadley, 1991). Therefore, a study was conducted to determine if two of the well-described growth factors would be sufficient to allow for neurite outgrowth of *Helisoma* neurons. In these experiments, neurons were mass dissociated in Leibovitz's medium containing nerve growth factor (NGF) or brain derived neurotrophic factor (BDNF). Following plating, neurite sprouting was counted in each culture for three days. However, in *Helisoma* mass dissociated cultures neither NGF nor BDNF had any effect on sprouting.

Materials and Methods

Mass dissociated cultures were prepared by incubating the entire central ring ganglia (includes cerebral, pleural, pedal, parietal, and visceral ganglia) in 0.3% collagenase (type XI, Sigma) for 90 minutes at 37°, followed by an incubation in trypsin (0.15%) for 60 minutes, and then trypsin inhibitor (0.2%) for 30 minutes. Ganglia were then placed in cell extraction medium (2μl of 1M $CaCl_2$ in 1 ml L-15) for 15 minutes. Neurons were

then dissociated and plated in defined medium (L-15) with the addition of either NGF (concentrations of 100, 200, 300, or 400 ng/ml) or BDNF (at concentrations of 50 or 100 ng/ml). Outgrowth was scored 1, 2, and 3 days following plating.

Results

In these experiments, mass dissociated central ring ganglia were plated into dishes containing L-15 with various concentrations of NGF (100, 200, 300, or 400 ng/ml) or BDNF (50 or 100 ng/ml). These dishes were monitored for evidence of neurite sprouting for each of 3 days following plating. Sprouting was not evident on any cell in any dish.

Discussion

A previous study in *Lymnaea stagnalis* demonstrated that plated motorneurons and interneurons show a sprouting response when they are plated in defined medium with added NGF (Ridgway *et al.*, 1991). However, in our related species (*Helisoma trivolvis*), when mass dissociated central ring ganglia were plated in defined medium with added NGF (100, 200, 300, 400 ng/ml), no sprouting was seen. Interestingly, the *Lymnaea* paper had tested one concentration (400ng/ml) of NGF on *Helisoma* pedal A cluster motorneurons and also observed no sprouting. Thus, our results are in line with previous data and with a report in *Aplysia* that demonstrates that NGF causes a reduction in neurite outgrowth in bag cell neurons (Gruenbaum & Carew, 1999). In reference to BDNF, this study in *Aplysia* also demonstrated that neurite outgrowth was increased when bag cells were plated on laminin and fibronectin, but was reduced when cells were plated on poly-

L-lysine. In our system, mass dissociated central ring ganglia from *Helisoma* plated in defined medium with added BDNF (50 or 100 ng/ml) showed no sprouting. Therefore, a NGF or BDNF-like factor does not appear to modulate sprouting in *Helisoma*. This project could be continued further by investigating other growth factors that may possibly be involved, such as EGF. An additional study could examine the possible effect of substrate-dependence on sprouting with various growth factors. It is also likely that all *Helisoma* neurons would not respond in the same manner to an individual growth factor. An individual growth factor may affect one population of neurons, but not others. It is also possible that there is a specific combination of growth factors that would be required to initiate neurite outgrowth in *Helisoma* neurons.

Chapter 6: General Discussion and Conclusions

During development, neurons must find their way to, and make connections with their appropriate targets. This process of neuronal pathfinding is one that is multi-faceted involving extracellular cues, intracellular signaling pathways, and cytoskeletal changes. Although many guidance cues and a few key intracellular signaling pathways have been well-defined, there is still much unknown about the regulation of growth cone behavior during the pathfinding process. This dissertation focuses in large part on the effect that a gaseous molecule, nitric oxide, can have on growth cone behavior, and defines the intracellular pathway though which its effects are mediated.

The current studies demonstrate that exogenous, local application of nitric oxide to an individual *Helisoma* B5 growth cone results in an increase in filopodial length, a decrease in filopodial number and an increase in the $[Ca^{2+}]_i$. Furthermore, the effects of nitric oxide on growth cone dynamics and calcium are transient and limited only to the stimulated growth cone. Nitric oxide mediates its effects via an intracellular signaling cascade that involves sGC, PKG, cADPR, and RyR-mediated intracellular calcium release. Calcium influx across the plasma membrane is also a contributor to the nitric oxide-induced increase in the $[Ca^{2+}]_i$. Taken together, these studies suggest that nitric oxide can regulate growth cone morphology via a signaling cascade that involves an important second messenger, calcium.

Nitric oxide is a gaseous messenger that can regulate growth cone dynamics.

Although not commonly viewed as a conventional guidance cue, nitric oxide (NO) has recently been regarded as an important regulator of growth cone morphology and

migration during development (Hess *et al.*, 1993; Renteria & Constantine-Paton, 1996; Gibbs & Truman, 1998; Van Wagenen & Rehder, 1999; Ernst *et al.*, 2000; Haase & Bicker, 2003; Trimm & Rehder, 2004; Zhang *et al.*, 2005). In the nervous system, NO is formed by the conversion of L-arginine and oxygen to L-citrulline and NO. This reaction is catalyzed by the enzyme neuronal nitric oxide synthase (nNOS), which requires the presence of calcium/calmodulin (Ca^{2+}/CaM) (for review see Alderton *et al.*, 2001). Staining for NOS or NADPH (a cofactor required for the production of NOS) has demonstrated that NOS is localized at the correct place and time in parts of the developing nervous system to act as a regulator of neuronal migration, neurite outgrowth and synaptogenesis (Williams *et al.*, 1994; Gibbs & Truman, 1998; Santacana *et al.*, 1998; Haase & Bicker, 2003).

Nitric oxide as a gaseous messenger

Perhaps one of the most striking aspects of NO is that it is a gas, which allows it to diffuse across cell membranes and affect intracellular targets. Yet, because NO is a gas, this also limits the scope of its action radius. The half-life of NO was originally thought to be approximately 5 seconds (Wood & Garthwaite, 1994), because in aqueous solutions nitric oxide reacts with oxygen to be converted to nitrites and nitrates (Moncada & Higgs, 1993; Kelm, 1999). However, a recent study, employing more physiologically-relevant concentrations of NO, instead suggests that the half-life of NO is approximately 10 ms (Hall & Garthwaite, 2006). The area of influence that NO could affect has been modeled in a number of studies. One study suggests that a point source of NO, released for 1-10

seconds, has a sphere of influence of about 200 μm (Wood & Garthwaite, 1994). A more recent study that has modeled the diffusion of NO from a variety of cell sizes suggests that a cell with a radius of 100 μm (similar to the size of the B5 neuron) would affect an area 2.8 times the size of its radius (Philippides *et al.*, 2000). Therefore, NO's limited diffusion restricts its action radius, but highlights its role as a detailed regulator of developmental processes.

Because NO is a gas, it is possible that NO could act as both an intra- and inter-cellular messenger during development. It is easier to imagine the role of NO as an intercellular messenger, because NO could be released by cells along a growth cone's migratory path or by cells within the target region of a neuron. However, NO could also act as an intracellular messenger. For instance, B5 neurons from *Helisoma trivolvis* not only respond to NO, they also demonstrate staining for its synthetic enzyme, NOS (Van Wagenen & Rehder, 2001). In addition, NO released from a B5 neuron can affect a migrating growth cone on another B5 neuron *in vitro* (K. Tornieri and V. Rehder, personal communication). Moreover, inhibition of endogenous NOS in B5 neurons results in a decrease in their own neurite outgrowth rate (Trimm & Rehder, 2004). This study suggests that B5 neurons require an intrinsic production of NO in order to maintain an optimal outgrowth speed and departures from this optimal level result in a slowing of neurite outgrowth. The production of NO within a neuron can be modified by a number of factors. For example, stimulation of *Helisoma* neurons with electrical activity leads to an increase in the intracellular calcium concentration (Cohan *et al.*, 1987). Increased intracellular calcium concentrations could then lead to activation of NOS, via Ca^{2+}/CaM.

It is important to note that any signaling event that results in an increase in the intracellular calcium concentration could lead to an increase in NO production because the activity of NOS is stimulated by Ca^{2+}/CaM.

It is possible that NO is an intracellular messenger and can act upon itself via a positive feedback loop. In the current set of experiments, we investigated whether exogenous application of an NO donor could result in the activation of an intracellular feedback loop (through cGMP, Ca^{2+}/CaM, and NOS) that would ultimately lead to an increased production of NO. In the current study, exogenous application of NO resulted in an increase in filopodial length and a decrease in filopodial number. Inhibiting NOS (to break this hypothesized feedback loop) before applying exogenous NO resulted in the same changes in filopodial length and number that are seen with NO application alone. Therefore, exogenous NO application does not appear to be activating a feedback loop that affects filopodial dynamics in the current study. However, it could be that *in vivo* the B5 neuron produces NO that activates this feedback loop, resulting in a continued production of NO. This scenario describes a role for NO as an intracellular messenger in B5 neurons, allowing NO to regulate its own growth cone morphology and neurite outgrowth rate. This has been demonstrated previously in *Helisoma*, because inhibition of endogenous NOS in B5 growth cones results in a reduction in its neurite outgrowth rate (Trimm & Rehder, 2004). Therefore, NO's action as an intracellular messenger could be essential to the pathfinding process *in vivo*.

Nitric oxide acts locally at the growth cone

Previous studies have demonstrated that global application of NO results in changes in growth cone morphology and the neurite outgrowth rate (Van Wagenen & Rehder, 1999; Trimm & Rehder, 2004). However, these studies did not provide information about the site of action of NO. In the current study, by locally applying NO to growth cones using a micropipette, and employing a millisecond burst duration, the results suggest that NO acts directly at the growth cone proper. A previous study from the Rehder lab has also demonstrated immunocytochemically that the immediate target of NO, sGC, is present within B5 growth cones (Van Wagenen & Rehder, 2001). The current study extends these findings to demonstrate that two downstream targets of NO signaling, protein kinase G (PKG) and ryanodine receptors (RyR), are also localized to *Helisoma* B5 growth cones. Therefore, because the radius of NO's action is limited by the application method and the half-life of NO, and because the machinery necessary to transduce NO's signal into cytoskeletal changes is localized within the growth cone, it is probable that the complete signaling action of NO takes place within the growth cone proper. These data suggest that if NO is released either by cells lining the migratory path of the growth cone or by the target tissue *in vivo*, it could initiate the second messenger signaling cascade described here within the growth cone proper and lead to the formation of appropriate connectivity within the nervous system of *Helisoma*.

The radius of action of nitric oxide is limited both spatially and temporally. This property of nitric oxide can be considered advantageous and disadvantageous. On the beneficial side, NO has a very limited half-life, thereby allowing for specific regulation

of a single growth cone or synapse. It may be that NO would need to act on the motility of only an individual growth cone or a subset of neurites. Therefore, the spatial and temporal limitations of NO would allow for specific regulation of the motility of certain processes, but not others. An example of this has been demonstrated in cortical pyramidal neurons, because the dendrites of these neurons grow toward the pial surface and the axons grow toward the white matter (Polleux *et al.*, 2000). This process of directed outgrowth is mediated by differing reactions of dendrites and axons to semaphorin 3A (Polleux *et al.*, 2000). Interestingly, the dendrites of these neurons contain high levels of sGC, whereas the axons do not, and this allows for a mechanism via which nitric oxide could have precise control over a region of a cell (e.g. dendrites versus axons). However, it is also known that NO can diffuse far enough to act on multiple cells, thus making the sGC receptor an integral part of the signaling system. sGC is found only in certain cells or certain compartments of an individual cell, thereby allowing only the cells that should be affected by NO to have the ability to sense and respond to its presence. Therefore, sGC allows a larger diffusion radius of NO to still result in target specificity. On the negative side, nitric oxide is removed quickly from the system and thus requires tissues or cells to continuously produce NO, which may be energetically costly. Furthermore, depending on the "sinks" for NO in the surrounding environment, nitric oxide may not always reach its intended target or may reach too many targets, resulting in inappropriate effects on the nervous system. Although there are some detriments to the NO-sGC signaling system, the specificity of NO for sGC allows for precise regulation of

individual cells, neuritic processes and growth cones, resulting in the appropriate development of the nervous system.

Very low concentrations of nitric oxide can have large effects on growth cone morphology

In the current study, NO is applied in a very temporally-restricted fashion. To apply NO locally, a picospritzer was employed to allow for a millisecond burst of NO that would cover the growth cone in a cloud, but then dissipate within 2 to 3 seconds. Although the exact concentration of NO released by this puff is not known, it is reasonable to assume that the concentration is much lower than that occurring during global application. Importantly, very spatially- and temporally-restricted applications of NO had effects on growth cone morphology that lasted on a timescale of minutes. In addition, low concentrations of NO appear to be amplified through the signaling cascade, resulting in a 25% increase in filopodial length and approximately a 65 nM increase in the intracellular calcium concentration ($[Ca^{2+}]_i$). It may be that such a small concentration of NO could have such large effects, because the half-maximal effective concentration of NO that activates sGC in cells has been estimated to be 45 nM (Bellamy & Garthwaite, 2001; 2002). Additionally, studies have demonstrated that NO's binding to the heme group of sGC results in up to a 200-fold activation of the enzyme (for review see Koesling *et al.*, 2004). Overall, this suggests that a very short-lived application of NO activates a signaling cascade that results in much longer and larger changes in growth cone morphology.

Physiological concentrations of NO in the brain from a variety of species are thought to be in the low nanomolar range (for review see Hall & Garthwaite, 2005). There are a few studies that have estimated the NO concentration specifically within molluscan nervous systems. A study in *Lymnaea* demonstrated that the buccal ganglion endogenously produces NO at concentrations ranging from 30-100 nM (Moroz *et al.*, 1995). Another study in *Lymnaea* found a peak NO concentration of 21 nM released from the buccal ganglion following sucrose stimulation (Kobayashi *et al.*, 2000). The discrepancies between these studies may result from a few factors. First, the meters and microelectrodes employed in these studies are known to be inaccurate, especially when measuring low concentrations of NO. Additionally, it has been demonstrated that the concentration range of NO can vary a great amount, depending on the location of the microelectrode over the tissue (i.e. different regions may have more or less NO-producing cells); this explains why the first study mentioned above found a large range of NO concentrations produced by the buccal ganglion (Moroz *et al.*, 1995). It is important to note that these studies are limited because they measure NO release from an entire ganglion, which typically contains only a few NO-producing neurons. Moreover, as mentioned previously, NO has a very short half-life and its diffusion is severely limited by the surrounding environment. Therefore, the concentrations measured may only be a fraction of what is actually released. Current studies have begun to address these issues using a special microelectrode and state that it is possible to measure NO release from a single neuron (Patel *et al.*, 2006). Presently, measuring NO release accurately is difficult, however future improvements in equipment should allow for quantification of NO release

from a single neuron, thereby allowing for more accurate measurements of physiological concentrations of NO.

The role of nitric oxide during the developmental period of neuronal outgrowth

NOS, the enzyme that produces NO, is present at the proper developmental time and location to regulate processes such as migration, outgrowth and synaptogenesis in a variety of species (Williams *et al.*, 1994; Gibbs & Truman, 1998; Santacana *et al.*, 1998; Haase & Bicker, 2003). For example, in the chick visual system, NADPH staining correlates temporally to the point at which retinal axons innervate the tectum (NADPH is a cofactor required for the production of NO) (Williams *et al.*, 1994). In grasshoppers, the migration of a population of midgut neurons is dependent on the presence of NOS that is produced by the cells lining the gut (Haase & Bicker, 2003).

In *Helisoma trivolvis*, preliminary data on staining for NADPH demonstrates heavy staining for NADPH in the salivary gland and lighter bands of staining within the esophagus (K.Welshhans, personal observations). The B5 neuron has two projections emanating out from the esophageal nerve trunk. The major projection makes a connection in the esophagus whereas the minor projection terminates within the buccal mass (Murphy & Kater, 1980a; Berdan *et al.*, 1989; Berdan *et al.*, 1990). Because the esophagus demonstrates staining for a cofactor of NO production, NO may be produced within the esophageal region. Therefore, NO could act as a regulator of B5 growth cone motility during the point when it is approaching and/or forming a synapse on the esophageal muscle. Because there are many branching nerves radiating out from the

buccal ganglion, and because NO acts as a "stop and search" signal (Trimm & Rehder, 2004), it is also possible that NO is acting as a regulator of growth cone motility at these branching points *in vivo*; however, we do not see any staining for NADPH in these branch points *in vivo*.

It has been hypothesized that NO acts as a "stop and search" signal within the developing nervous system (Trimm & Rehder, 2004). An increase in filopodial length coupled with a decrease in filopodial number and a decrease in the neurite outgrowth rate defines this "stop and search" behavior. *In vivo*, growth cones may "stop and search" in response to release of NO at either a choice point or within a target region, thereby increasing their action radius and allowing them to search for the cue that will direct them either down the proper nerve or to the correct portion of their target. However, one can also visualize a situation in which graded release of NO could have very different effects on growth cone behavior. In the current study, we demonstrated that a millisecond release of NO affects growth cone dynamics for a time span of approximately 20 minutes. Previous studies have found that a prolonged release of NO results in changes in growth cone morphology and outgrowth lasting for a longer time span (Van Wagenen & Rehder, 1999; Trimm & Rehder, 2004). Therefore, NO may hold multiple roles. For instance, NO's release on a migrating growth cone could range from a shorter "search" signal that would affect filopodial dynamics on a short time scale, as demonstrated in the current study, to a much longer "stop and search" signal that affects filopodia and outgrowth for an extended period of time, as demonstrated previously (Trimm & Rehder, 2004). However, we need to investigate the effect of a spatially- and temporally-restricted

application of NO on the neurite outgrowth rate before this determination can be made. In any case, growth cones can display a variety of behaviors that are involved in achieving appropriate pathfinding and synaptogenesis. In *Helisoma*, the variety of behaviors that the B5 growth cone displays may hold an integral role in allowing appropriate pathfinding to and synapse formation on the esophageal muscle wall.

The wiring of the nervous system is a process that is essential during the overall developmental period. There are a number of human diseases that can result when growth cones do not pathfind correctly or make appropriate connections with their targets. For example, L1 is a cell adhesion molecule that is involved in neuritogenesis, fasciculation, and neurite outgrowth (as reviewed in Kenwrick *et al.*, 2000; Kiryushko *et al.*, 2004; Maness & Schachner, 2007). Mutations in the L1 gene result in disease characterized by mental retardation and hydrocephalus. Another disease that results in mental retardation is Fragile X syndrome. Fragile X syndrome is characterized by the loss of an mRNA binding protein that is localized to growth cones. The loss of this protein results in reduced growth cone motility, contributing to the pathology of this disease (Antar *et al.*, 2006). One additional disease resulting from a lack of and/or inappropriate connectivity is spinal muscular atrophy, a neuromuscular disorder that results from deficiencies in neurite outgrowth and improper development of the neuromuscular junction (Fan & Simard, 2002). Spinal muscular atrophy results from the loss of the Survival of Motor Neuron (SMN) protein, which is localized to growth cones. Overall, these studies suggest that the correct wiring and patterning of the nervous system is a delicate process that can be easily disrupted through the mutation or loss of a single molecule or protein.

The current finding that nitric oxide can regulate growth cone motility via a multi-tiered second messenger cascade also has implications for human health and disease. Because nitric oxide regulates the motility of B5 growth cones *in vitro* and because NOS is produced within *Helisoma in vivo*, particularly within the target area of this neuron, these data suggest that nitric oxide may act as a guidance cue or target recognition factor *in vivo*. Nitric oxide is expressed during the development of the nervous system in many animals. Furthermore, nitric oxide acts to regulate a number of processes during this period when the connectivity of the nervous system is established (for review see Hall & Garthwaite, 2005). If this connectivity is not established properly, a diseased state can result. Therefore, understanding how nitric oxide acts on growth cone motility *in vitro* in a simple system will help us understand how it functions to regulate the development of a more complicated system, such as the mammalian nervous system. The development of the nervous system is easily affected by the loss of certain molecules and proteins, resulting in a diseased state. Thus, these data allow for further understanding of how one of these cues, NO, may regulate the proper wiring of the nervous system.

Nitric oxide activates a signaling cascade that results in calcium release.

Nitric oxide acts via sGC, PKG, and cADPR

Nitric oxide has been demonstrated to affect filopodial motility via the s-nitrosylation pathway (Cheung *et al.*, 2000), as well as through sGC (current report and Van Wagenen & Rehder, 1999; 2001; Trimm & Rehder, 2004). Although NO has been demonstrated to affect filopodial motility via s-nitrosylation in rat retinal ganglion cells (Cheung *et al.*,

2000), NO does not appear to act via this pathway to regulate filopodial dynamics in the current report. Because the effects of NO on filopodial motility and $[Ca^{2+}]_i$ can be completely blocked via inhibition of sGC, PKG, or the ryanodine receptor, it is unlikely that nitric oxide also acts via s-nitrosylation to affect these parameters. However, it is possible that s-nitrosylation mediates additional effects of NO that were not studied in the current report, such as a NO-induced depolarization. Overall, it appears that NO acts via sGC, and not s-nitrosylation, to initiate a change in filopodial dynamics and $[Ca^{2+}]_i$ within *Helisoma* B5 growth cones.

There are numerous developmental processes that have been shown to signal through the NO - sGC pathway (Gibbs *et al.*, 2001; Leamey *et al.*, 2001; Haase & Bicker, 2003; Zhang *et al.*, 2005; Mejia-Garcia & Paes-de-Carvalho, 2007). sGC converts GTP to cGMP and subsequently, cGMP acts on three major targets: cyclic nucleotide gated (CNG) ion channels, phosphodiesterases (PDEs), and PKG. The experiments in this dissertation demonstrate that exogenous local application of NO to B5 neurons activates a second-messenger pathway involving sGC, PKG, cADPR and RyR-induced calcium release. This is supported by immunocytochemical evidence that demonstrates the presence of sGC, PKG and RyRs within *Helisoma* B5 growth cones (current report and Van Wagenen & Rehder, 2001).

Application of NO acts via the sGC pathway to result in an increase in filopodial length and the intracellular calcium concentration in B5 neurons, but when NO is applied to the B19 neuron, there is no change in filopodial motility or calcium. In addition, a previous report demonstrated that B19 neurons show little to no staining for sGC and

addition of a sGC activator has no effect on these neurons (Van Wagenen & Rehder, 2001). However, application of a cGMP analog or direct injection of cGMP into B19 neurons does result in an increase in filopodial length. This suggests that the level of convergence for different signaling pathways on filopodial motility, at least for B5 and B19 neurons, is at the level of cGMP. It is currently unknown whether the filopodial effects of cGMP on B19 neurons are mediated via activation of PKG and cADPR-modulated release of calcium through the RyR. However, because cADPR and RyRs are known to be relatively well-conserved molecules (Tunwell *et al.*, 1996; Quinn *et al.*, 1998; Bultynck *et al.*, 2001; Vazquez-Martinez *et al.*, 2003; Guse, 2004), it is expected that B19 neurons would respond to injection of cADPR in the same manner as B5 neurons.

As mentioned previously, there are three major targets of cGMP: CNG ion channels, PDEs and PKG. In the current set of experiments, we were unable to examine the possible contribution of CNG ion channels, due to limitations in the available pharmacological tools. However, it is unlikely that the local application of NO employed in the current study led to activation of CNG ion channels because the effects of NO could be completely eliminated via pharmacological inhibition of PKG. In addition, the possibility of the phosphodiesterase pathway leading to regulation of growth cone morphology was eliminated by the results obtained from pharmacological experiments. A previous study demonstrated that NO can signal via the phosphodiesterase pathway in rat dorsal root ganglion neurons to regulate neurite and growth cone morphology (Tsukada *et al.*, 2002). However, taken in combination with the current findings, these results

highlight the diversity of signaling that can be activated by NO. It is currently unknown why NO activates different signaling pathways to regulate growth cone morphology. One possibility, although currently unsupported, is divergent evolution in a variety of species. Alternatively, it is possible that during different development periods, there may be differential activation of signaling pathways by the same signaling molecule. This occurs in neural stem cells, where application of bone morphogenic protein to stem cells taken from periods early in development leads to a neuronal fate, whereas later in development, the same molecule leads to an astrocytic fate (as reviewed in Temple, 2001; Chen & Panchision, 2007). Another possibility is that the same signaling molecule may need to activate different pathways in different neurons. For example, in the cortex, ephrinA5 is a repulsive cue for layer 2/3 axons, yet promotes branching of layer 6 pyramidal cell axons (for review see Bolz *et al.*, 2004). Different NO donors, concentrations of donors and application methods may also lead to activation of different signaling pathways. Evidence for this also comes from neural stem cells; application of a low concentration of epidermal growth factor leads to their continued proliferation into multipotential cells, whereas higher concentrations lead to differentiation into astrocytes (Burrows *et al.*, 1997; Temple, 2001). It is important to note that in *Xenopus* growth cones, the concentration ratio of cAMP to cGMP determines whether netrin-1 acts as an attractive or repellant cue, and this differential behavior occurs via activation of different second messengers (Nishiyama *et al.*, 2003). These data suggest that there is a diversity of signaling that can be achieved by a single signaling molecule.

In the current study, we have demonstrated the NO is mediating its effects on filopodial dynamics via PKG. One target of PKG is ADP-ribosyl cyclase, which is the enzyme necessary for the formation of cyclic adenosine diphosphate ribose (cADPR) (Galione et al., 1993; Willmott et al., 1996b; Lee, 2001). cADPR is a second messenger that modulates calcium release from RyR-gated intracellular stores (as reviewed in Lee, 2001; Guse, 2005). cADPR was originally discovered in sea urchin eggs (Lee et al., 1989), however, its importance and universality as a second messenger has only recently been discovered (Higashida et al., 2001; Lee, 2001; Guse, 2005). cADPR modulates RyR-induced calcium release, however, whether this modulation is direct or through an intermediate binding protein is still unknown (as reviewed in Higashida et al., 2001; Guse, 2005). In addition, cADPR's function is varied, depending on the species. In *Aplysia* and *Helisoma*, injection of cADPR results directly in an increase in the $[Ca^{2+}]_i$ (Mothet et al., 1998 and Chapter 3 of current study). cADPR also causes calcium release in permeabilized rat pituitary cells and mouse pancreatic acinar cells directly (Koshiyama et al., 1991; Thorn et al., 1994). However, in other types of neurons, such as rat cerebellar granule cells and NG108-15 neuroblastoma cells, cADPR does not directly cause an increase in the $[Ca^{2+}]_i$, but instead potentiates calcium release initiated by other factors (De Flora et al., 1996; Hashii et al., 2000).

cADPR was originally discovered as a downstream signaling molecule of NO in sea urchin eggs (Willmott et al., 1996a). However, more recent reports have demonstrated that the NO-cADPR pathway also functions in the regulation of other cellular functions. NO signaling via cADPR is necessary for the induction of long-term

depression within the hippocampus, but not in the cerebellum (Linden *et al.*, 1995; Reyes-Harde *et al.*, 1999a; Reyes-Harde *et al.*, 1999b). Additionally, in PC12-16A cells, exogenous application of NO results in an increase in the $[Ca^{2+}]_i$ that is mediated through cADPR (Clementi *et al.*, 1996). Finally, a recent study demonstrated that NO potentiates inhibitory GABA release via cADPR in the rat nucleus tractus solitarii (Wang *et al.*, 2006). Thus, NO has a variety of cellular functions, however, this dissertation is the first report of NO acting via cADPR in a regenerative function, as a modulator of growth cone motility.

Exogenous application of nitric oxide results in calcium release from intracellular stores
It is well-known that calcium signaling is essential to everyday cellular processes (Berridge *et al.*, 2003). In the current studies, we demonstrate that intracellular calcium release, mediated through RyRs, is necessary for the NO-induced changes in growth cone morphology. RyRs are usually viewed as mediators of calcium-induced calcium release; but their modulation by cADPR has been suggested in a variety of cell types (Empson & Galione, 1997; Noguchi *et al.*, 1997; Lee, 2001; Thomas *et al.*, 2001; Franco *et al.*, 2006; Morita *et al.*, 2006). Here, we demonstrated that calcium release through the RyR, most likely from endoplasmic reticulum calcium stores, is necessary for the NO-induced changes in growth cone morphology and $[Ca^{2+}]_i$, because inhibition of the RyR before NO application completely eliminates these effects. However, it is important to note that in these experiments a burst of NO lasting milliseconds results in an increase in the $[Ca^{2+}]_i$ that lasts for approximately 20 minutes, and this prolonged increase in calcium

may possibly have excitotoxic effects on the cell. We do not currently know the mechanism through which this calcium increase remains elevated for such a lengthy period of time. However, it is likely that influx of calcium across the plasma membrane contributes to this prolonged increase in calcium.

In the current studies, we provide evidence that extracellular calcium influx across the plasma membrane is a component of the NO-induced increase in $[Ca^{2+}]_i$. However, we currently do not know how the release of calcium from intracellular stores activates the extracellular calcium influx. It is possible that the depletion of calcium from intracellular stores activates store-operated channels that serve to refill the intracellular calcium stores (Verkhratsky, 2005). Unfortunately, very little is known about the existence of store-operated channels in neurons, and currently there are no acceptable pharmacological tools available to study their contribution to the NO-induced signaling pathway. There is some evidence, although highly debated, that store-operated channels may actually be a type of transient receptor potential (TRP) channel (as reviewed in Minke, 2006; Ramsey *et al.*, 2006). Release of calcium from intracellular stores in growth cones, albeit through inositol triphosphate receptors, has been shown to lead to the activation of TRPC channels and calcium influx, thereby allowing for a mechanism by which intracellular calcium release could lead to calcium influx across the plasma membrane (Li *et al.*, 2005). Although there are some pharmacological tools available to study the contribution of TRP channels to the NO-induced calcium increase, their specificity, both for TRP channels and within our system, is questionable.

We are still unaware of the mechanism by which calcium remains elevated for the extended period following a millisecond application of NO. One possible mechanism is through inhibition of the machinery that reduces the intracellular calcium concentration, such as Na^+/Ca^{2+} exchangers, plasma membrane $Ca^{2+}/ATPase$ pumps, and/or sarcoendoplasmic reticulum Ca^{2+}-ATPase pumps (for review see Berridge *et al.*, 2003). Future experiments could employ pharmacological tools to test the contribution of these various pumps and exchangers to the prolonged calcium increase. There is preliminary evidence suggesting that exogenous application of NO results in a depolarization of B5 neurons (L. Artinian, personal communication). It is possible that this depolarization results in calcium influx and a prolonged calcium increase. Electrophysiological studies are currently underway to investigate the particular ion channels that contribute to the NO-induced calcium increase and depolarization. However, another possibility is that the signaling cascade remains activated for an extended period of time. There is some evidence, although disputed, that are two binding sites on sGC for NO; one of these sites allows for a reduced (10-20% of maximal stimulation) but prolonged activation of this enzyme (Cary *et al.*, 2005; Roy & Garthwaite, 2006). If this is the case, it is a mechanism that could allow for a low-level prolonged activation of the NO-induced signaling cascade, perhaps leading to a long-lasting increase in the $[Ca^{2+}]_i$. Two final mechanisms through which NO may cause a prolonged increase in calcium are via continuous release of calcium from intracellular stores or maintenance of a continuous influx of calcium. These mechanisms may involve some of the same channels that are involved in the initial calcium increase, such as ryanodine receptor mediated channels. In order to test the

contribution of these channels to the prolonged calcium increase, and dissociate their contribution to the initial calcium increase from the prolonged increase, specific pharmacological inhibitors of intracellular calcium release or calcium influx would need to be added following NO application. These experiments would still allow the initial calcium increase to occur, but block the contribution of the channels, if any, to the prolonged calcium increase. Overall, these experiments would shed light on the possible contributions of various channels, pumps, and exchangers to the prolonged calcium increase induced by NO.

Changes in the intracellular calcium concentration within growth cones lead to changes in the cytoskeleton.

Correlation between the intracellular calcium concentration and growth cone dynamics

There are numerous studies that have demonstrated that growth cone morphology and the neurite outgrowth rate are dependent on the $[Ca^{2+}]_i$ (Mattson & Kater, 1987; Davenport & Kater, 1992; Rehder & Kater, 1992; Bandtlow *et al.*, 1993; Gomez *et al.*, 1995; Kuhn *et al.*, 1998; Bird & Owen, 2000; Cheng *et al.*, 2002; Tang *et al.*, 2003). In the current study, NO-induced changes in the $[Ca^{2+}]_i$ are correlated with changes in growth cone morphology. Specifically, an increase in the $[Ca^{2+}]_i$ results in an increase in the length of filopodia, as well as a decrease in filopodial number. The coupling of these two parameters (changes in length and number) has also been demonstrated in previous studies (Bonsall & Rehder, 1999; Geddis *et al.*, 2004; Lebrand *et al.*, 2004; Chen *et al.*, 2006). However, it has also been demonstrated that growth cones may change filopodial

length, without an accompanying change in filopodial number (Cheng *et al.*, 2002; Tornieri *et al.*, 2006). Taken together, these studies suggest that the regulation of filopodial length and number can take place in a coupled or independent fashion, and might be dependent on the demands for appropriate pathfinding behavior. In the context of *Helisoma*, it is likely that a pathfinding growth cone may need to display a variety of morphologies during its journey to the appropriate target. Calcium may directly regulate many of these behaviors, to ensure proper pathfinding, target identification and innervation.

Calcium dependent regulation of growth cone dynamics, and specifically filopodial dynamics, appears to be a wide-spread phenomenon. Examination of filopodia on growth cones has demonstrated that calcium regulates even the smallest part of the growth cone. For example, in *Helisoma* neurons, there is a direct correlation between the $[Ca^{2+}]_i$ within growth cones and the amount of filopodial elongation (Rehder & Kater, 1992). Studies in *Helisoma* have also demonstrated that local increases in calcium within a single filopodium result in elongation of only that filopodium (Cheng *et al.*, 2002). In rat hippocampal neurons, calcium influx through TRPC5 channels are essential for regulating filopodial length; as such, a dominant-negative inhibition of TRPC5 channels results in a significant increase in filopodial length (Greka *et al.*, 2003). In addition, spontaneous calcium transients have been shown to occur within *Xenopus* spinal neurons (Gomez *et al.*, 2001). Interestingly, when these calcium transients are artificially imposed within a filopodium, they lead to filopodial stabilization (Robles *et al.*, 2003). It is important to note that in the current study, the change in the $[Ca^{2+}]_i$ closely parallels the

changes in filopodial dynamics, that is, when the calcium concentration returns to pre-treatment values, the filopodial dynamics return as well. These data suggest that there is tight coupling between the $[Ca^{2+}]_i$ and growth cone morphology in the NO-induced signaling pathway. Furthermore, data from the present study and previous studies highlights the essential role of calcium in regulating the motility of growth cones and subsequently, the connectivity of the nervous system.

Calcium and its effectors can mediate growth cone cytoskeletal changes

A change in the intracellular calcium concentration can affect the cytoskeleton through a number of calcium-mediated effectors such as Ca^{2+}/CaM, Ca^{2+}/CaM-dependent protein kinase II (CAMKII), and calcineurin (for review see Henley & Poo, 2004). In *Helisoma*, we do not know which effectors of calcium act on the cytoskeleton; however, there is good evidence that the changes in the cytoskeleton are due mainly to changes in actin. Filopodia are composed of bundled f-actin and inhibition of actin polymerization with cytochalasin B significantly reduced the NO-induced increase in filopodial length. Thus, we are relatively confident that the calcium increase resulting from exogenous NO application further activates calcium effectors that subsequently act on the actin cytoskeleton. There are three mechanisms by which an increase in filopodial length can result: one, a decrease in the retrograde flow of actin; two, an increase in the addition of actin monomers to the barbed end of the actin filament; or three, a combination of these two factors. A study in *Helisoma* has demonstrated that a prolonged increase in calcium can lead to a decrease in the retrograde flow of actin (Welnhofer *et al.*, 1999). In the

current study, we do not know whether the rate of retrograde flow is affected by the NO-induced calcium increase, although this possibility is suggested by the findings of Welnhofer *et al*. However, we do know that global application of a NO donor to *Helisoma* B5 neurons results in an increase in filopodial length by increasing the rate of filopodial extension, as well as increasing the time the filopodia spend extending (Van Wagenen *et al.*, 1999). Yet, NO did not affect the retraction of filopodia in this study (retraction rate is thought to be driven by retrograde flow), arguing against the possibility that NO alters retrograde flow, as suggested by the Welnhofer *et al.* study. Additionally, the Van Wagenen *et al.* study demonstrated that the decrease in filopodial number was due to a decrease in the insertion frequency of new filopodia and again, not due to a retraction of existing filopodia.

There are a few known actin-binding proteins that are calcium-dependent, including gelsolin, myosin II and ADF/cofilin (for review see Henley & Poo, 2004). Gelsolin is activated in a calcium-dependent fashion and is involved in the severance of f-actin filaments and the initiation of the filopodial retraction (for review see Henley & Poo, 2004). Additionally, gelsolin has been localized to growth cones and gelsolin null mice exhibit delayed retraction of filopodia in their growth cones, which leads to an increase in filopodial number (Lu *et al.*, 1997). Myosin II, which is activated by Ca^{2+}/CaM-dependent myosin light chain kinase (MLCK), is involved in the regulation of many aspects of growth cone morphology and motility (for review see Henley & Poo, 2004). In *Helisoma* growth cones, indirectly inhibiting myosin II (by inhibiting MLCK) leads to growth cone collapse and f-actin bundle loss at high concentrations (Zhou &

Cohan, 2001) and a decrease in filopodial number at lower concentrations (Cheng *et al.*, 2000). Additionally, a recent study has shown the importance of myosin II for actin dynamics. When myosin II is directly inhibited, retrograde flow and actin bundle severing is significantly decreased in growth cones from *Aplysia* neurons (Medeiros *et al.*, 2006). ADF/cofilin is involved in the severance of f-actin filaments and increasing the dissociation rate of actin monomers from the pointed end (for review see Sarmiere & Bamburg, 2004). In addition, ADF/cofilin is dephosphorylated and activated by Ca^{2+}/CaM-dependent protein phosphatase 2B (calcineurin) (for review see Flynn *et al.*, 2007). Interestingly, calcineurin is necessary for the calcium-mediated increases in filopodial length in *Helisoma* B5 neurons (Cheng *et al.*, 2002). Therefore, it is possible that the NO-induced calcium release leads to dephosphorylation and activation of ADF/cofilin by calcineurin. This might then lead to filopodial elongation. Support for this hypothesis is provided by another study in chick retinal neurons, where exogenous application of BDNF resulted in an increase in filopodial length that was mediated via activation of ADF/cofilin (Gehler *et al.*, 2004a; Gehler *et al.*, 2004b). Although much is still unknown about many calcium-binding proteins within growth cones, and the current studies were unable to address which actin-binding proteins may be directly involved in the changes in growth cone morphology, potential candidates have been identified due to their calcium-sensitivity.

Conclusions

Overall, this dissertation addresses three major specific aims that answer questions about the regulation of growth cone motility by the gaseous messenger, nitric oxide.

Specific Aim 1: How does a spatially- and temporally-restricted application of nitric oxide affect growth cone morphology and calcium?

Local application of NO in a spatially- and temporally-restricted fashion results in an increase in filopodial length, a decrease in filopodial number and an increase in the $[Ca^{2+}]_i$. These effects are transient, lasting for approximately 20 minutes, and are limited to the stimulated growth cone. In addition, these experiments place the location of action of NO at the growth cone proper. Therefore, these experiments demonstrate that a very spatially- and temporally-restricted application of nitric oxide can have long-lasting effects on growth cone morphology and the intracellular calcium concentration.

Specific Aim 2: What is the downstream pathway through which nitric oxide exerts its effects on growth cone morphology?

NO exerts its effects on growth cone morphology through a pathway involving sGC, cGMP, PKG, and cADPR. This has been demonstrated using pharmacological tools and is further supported by immunocytochemical evidence that sGC and PKG are localized within *Helisoma* B5 neuronal growth cones. Therefore, these experiments demonstrate that NO exerts its effects on growth cone morphology through activation of a multi-tiered intracellular signaling cascade that results in the production of cADPR.

Specific Aim 3: How do intracellular and extracellular calcium cascades contribute to the nitric oxide-induced calcium dynamics?

Exogenous NO application initiates a pathway that results in calcium release from intracellular stores, via the ryanodine receptor. However, calcium influx across the plasma membrane is also a necessary secondary component of the NO-induced increase in the intracellular calcium concentration. Therefore, these experiments demonstrate that exogenous application of nitric oxide results in an increase in the intracellular calcium concentration via initial release from ryanodine receptor-mediated intracellular stores and secondary calcium influx across the plasma membrane.

Overall, these studies demonstrate that NO can activate an intracellular signaling cascade that affects growth cone morphology. Additionally, these studies have implications for processes that take place during growth cone pathfinding *in vivo*. Nitric oxide may have a larger role than previously suspected in guiding neuronal growth cones to their appropriate targets. At the most minimal, nitric oxide is an intercellular messenger that regulates growth cone morphology and neurite outgrowth. However, it is likely, based on the localization of nitric oxide production within the nervous system, that it is a regulator of growth cone pathfinding *in vivo*. In the current studies, we have identified a nitric oxide-induced second messenger pathway that leads to an increase in the intracellular calcium concentration and subsequently results in changes in the cytoskeleton of a migrating growth cone. These studies provide a mechanism through which nitric oxide can directly and locally affect growth cone morphology and implicate nitric oxide as a

regulator of neuronal pathfinding during the regeneration of the nervous system. Understanding the intricacies of neuronal growth cone pathfinding and the cues that allow for proper wiring will further allow us to understand clinical disorders that result from misguidance or inappropriate connectivity.

Literature Cited

Ahern, G.P., Klyachko, V.A. & Jackson, M.B. (2002) cGMP and S-nitrosylation: two routes for modulation of neuronal excitability by NO. *Trends Neurosci*, **25**, 510-517.

Alderton, W.K., Cooper, C.E. & Knowles, R.G. (2001) Nitric oxide synthases: structure, function and inhibition. *Biochem J*, **357**, 593-615.

Alessi, D.R., James, S.R., Downes, C.P., Holmes, A.B., Gaffney, P.R., Reese, C.B. & Cohen, P. (1997) Characterization of a 3-phosphoinositide-dependent protein kinase which phosphorylates and activates protein kinase Balpha. *Curr Biol*, **7**, 261-269.

Antar, L.N., Li, C., Zhang, H., Carroll, R.C. & Bassell, G.J. (2006) Local functions for FMRP in axon growth cone motility and activity-dependent regulation of filopodia and spine synapses. *Molecular and cellular neurosciences*, **32**, 37-48.

Arnold, W.P., Mittal, C.K., Katsuki, S. & Murad, F. (1977) Nitric oxide activates guanylate cyclase and increases guanosine 3':5'-cyclic monophosphate levels in various tissue preparations. *Proc Natl Acad Sci U S A*, **74**, 3203-3207.

Ball, E.E. & Truman, J.W. (1998) Developing grasshopper neurons show variable levels of guanylyl cyclase activity on arrival at their targets. *J Comp Neurol*, **394**, 1-13.

Bamburg, J.R. (2003) Introduction to cytoskeletal dynamics and pathfinding of neuronal growth cones. *J Histochem Cytochem*, **51**, 407-409.

Bandtlow, C.E., Schmidt, M.F., Hassinger, T.D., Schwab, M.E. & Kater, S.B. (1993) Role of intracellular calcium in NI-35-evoked collapse of neuronal growth cones. *Science*, **259**, 80-83.

Bang, O.S., Park, E.K., Yang, S.I., Lee, S.R., Franke, T.F. & Kang, S.S. (2001) Overexpression of Akt inhibits NGF-induced growth arrest and neuronal differentiation of PC12 cells. *J Cell Sci*, **114**, 81-88.

Barnstable, C.J., Wei, J.Y. & Han, M.H. (2004) Modulation of synaptic function by cGMP and cGMP-gated cation channels. *Neurochem Int*, **45**, 875-884.

Bellamy, T.C. & Garthwaite, J. (2001) Sub-second kinetics of the nitric oxide receptor, soluble guanylyl cyclase, in intact cerebellar cells. *J Biol Chem*, **276**, 4287-4292.

Bellamy, T.C. & Garthwaite, J. (2002) The receptor-like properties of nitric oxide-activated soluble guanylyl cyclase in intact cells. *Molecular and cellular biochemistry*, **230**, 165-176.

Bellamy, T.C., Wood, J., Goodwin, D.A. & Garthwaite, J. (2000) Rapid desensitization of the nitric oxide receptor, soluble guanylyl cyclase, underlies diversity of cellular cGMP responses. *Proc Natl Acad Sci U S A*, **97**, 2928-2933.

Bentley, D. & Toroian-Raymond, A. (1986) Disoriented pathfinding by pioneer neurone growth cones deprived of filopodia by cytochalasin treatment. *Nature*, **323**, 712-715.

Berdan, R.C., Hauser, G. & Bulloch, A.G. (1990) Ultrastructure of an identified molluscan neuron in organ culture and cell culture following axotomy. *J Comp Neurol*, **296**, 437-446.

Berdan, R.C., Jones, P.G. & Bulloch, A.G. (1989) Modulation of neurite outgrowth: ultrastructure and physiology. In Bulloch, A.G. (ed.) *The cellular basis of neuronal plasticity: physiology, morphology, and biochemistry of molluscan neurons.* Manchester University Press, New York, pp. 97-128.

Berridge, M.J. (1995) Capacitative calcium entry. *Biochem J*, **312 (Pt 1)**, 1-11.

Berridge, M.J. (2005) Unlocking the secrets of cell signaling. *Annu Rev Physiol*, **67**, 1-21.

Berridge, M.J., Bootman, M.D. & Roderick, H.L. (2003) Calcium signalling: dynamics, homeostasis and remodelling. *Nature reviews*, **4**, 517-529.

Bicker, G. (1998) NO news from insect brains. *Trends Neurosci*, **21**, 349-355.

Bicker, G. (2005) STOP and GO with NO: nitric oxide as a regulator of cell motility in simple brains. *Bioessays*, **27**, 495-505.

Bicker, G. (2006) Pharmacological approaches to nitric oxide signalling during neural development of locusts and other model insects. *Arch Insect Biochem Physiol*, **64**, 43-58.

Bird, M.M. & Owen, A. (2000) The effect of calcium ionophore A23187 on neurites from embryonic mouse spinal cord explants in culture. *Journal of electron microscopy*, **49**, 379-386.

Bishop, A.L. & Hall, A. (2000) Rho GTPases and their effector proteins. *Biochem J*, **348 Pt 2**, 241-255.

Bolz, J., Uziel, D., Muhlfriedel, S., Gullmar, A., Peuckert, C., Zarbalis, K., Wurst, W., Torii, M. & Levitt, P. (2004) Multiple roles of ephrins during the formation of thalamocortical projections: maps and more. *J Neurobiol*, **59**, 82-94.

Bon, C.L. & Garthwaite, J. (2002) Adenosine acting on A1 receptors protects NO-triggered rebound potentiation and LTP in rat hippocampal slices. *J Neurophysiol*, **87**, 1781-1789.

Bondeva, T., Pirola, L., Bulgarelli-Leva, G., Rubio, I., Wetzker, R. & Wymann, M.P. (1998) Bifurcation of lipid and protein kinase signals of PI3Kgamma to the protein kinases PKB and MAPK. *Science*, **282**, 293-296.

Bonsall, J. & Rehder, V. (1999) Regulation of chick dorsal root ganglion growth cone filopodia by protein kinase C. *Brain Res*, **839**, 120-132.

Bossing, T. & Technau, G.M. (1994) The fate of the CNS midline progenitors in Drosophila as revealed by a new method for single cell labelling. *Development*, **120**, 1895-1906.

Boulo, V., Cadoret, J.P., Le Marrec, F., Dorange, G. & Miahle, E. (1996) Transient expression of luciferase reporter gene after lipofection in oyster (Crassostrea gigas) primary cell cultures. *Mol Mar Biol Biotechnol*, **5**, 167-174.

Bultynck, G., Rossi, D., Callewaert, G., Missiaen, L., Sorrentino, V., Parys, J.B. & De Smedt, H. (2001) The conserved sites for the FK506-binding proteins in ryanodine receptors and inositol 1,4,5-trisphosphate receptors are structurally and functionally different. *J Biol Chem*, **276**, 47715-47724.

Burrows, R.C., Wancio, D., Levitt, P. & Lillien, L. (1997) Response diversity and the timing of progenitor cell maturation are regulated by developmental changes in EGFR expression in the cortex. *Neuron*, **19**, 251-267.

Cafferty, P., Yu, L., Long, H. & Rao, Y. (2006) Semaphorin-1a functions as a guidance receptor in the Drosophila visual system. *J Neurosci*, **26**, 3999-4003.

Cantley, L.C. (2002) The phosphoinositide 3-kinase pathway. *Science*, **296**, 1655-1657.

Cantrell, D.A. (2001) Phosphoinositide 3-kinase signalling pathways. *J Cell Sci*, **114**, 1439-1445.

Carafoli, E. (2004) Calcium signaling: a historical account. *Biological research*, **37**, 497-505.

Cary, S.P., Winger, J.A. & Marletta, M.A. (2005) Tonic and acute nitric oxide signaling through soluble guanylate cyclase is mediated by nonheme nitric oxide, ATP, and GTP. *Proc Natl Acad Sci U S A*, **102**, 13064-13069.

Chen, H.L. & Panchision, D.M. (2007) Concise review: bone morphogenetic protein pleiotropism in neural stem cells and their derivatives--alternative pathways, convergent signals. *Stem cells (Dayton, Ohio)*, **25**, 63-68.

Chen, J., Tu, Y., Moon, C., Matarazzo, V., Palmer, A.M. & Ronnett, G.V. (2004) The localization of neuronal nitric oxide synthase may influence its role in neuronal precursor proliferation and synaptic maintenance. *Dev Biol*, **269**, 165-182.

Chen, T.J., Gehler, S., Shaw, A.E., Bamburg, J.R. & Letourneau, P.C. (2006) Cdc42 participates in the regulation of ADF/cofilin and retinal growth cone filopodia by brain derived neurotrophic factor. *J Neurobiol*, **66**, 103-114.

Cheng, A., Wang, S., Cai, J., Rao, M.S. & Mattson, M.P. (2003) Nitric oxide acts in a positive feedback loop with BDNF to regulate neural progenitor cell proliferation and differentiation in the mammalian brain. *Dev Biol*, **258**, 319-333.

Cheng, S., Geddis, M.S. & Rehder, V. (2002) Local calcium changes regulate the length of growth cone filopodia. *J Neurobiol*, **50**, 263-275.

Cheng, S., Mao, J. & Rehder, V. (2000) Filopodial behavior is dependent on the phosphorylation state of neuronal growth cones. *Cell Motil Cytoskeleton*, **47**, 337-350.

Cheng, T.P. & Reese, T.S. (1985) Polarized compartmentalization of organelles in growth cones from developing optic tectum. *J Cell Biol*, **101**, 1473-1480.

Cheung, W.S., Bhan, I. & Lipton, S.A. (2000) Nitric oxide (NO.) stabilizes whereas nitrosonium (NO+) enhances filopodial outgrowth by rat retinal ganglion cells in vitro. *Brain Res*, **868**, 1-13.

Chien, C.B., Rosenthal, D.E., Harris, W.A. & Holt, C.E. (1993) Navigational errors made by growth cones without filopodia in the embryonic Xenopus brain. *Neuron*, **11**, 237-251.

Clark, M.C., Dever, T.E., Dever, J.J., Xu, P., Rehder, V., Sosa, M.A. & Baro, D.J. (2004) Arthropod 5-HT2 receptors: a neurohormonal receptor in decapod crustaceans that displays agonist independent activity resulting from an evolutionary alteration to the DRY motif. *J Neurosci*, **24**, 3421-3435.

Clementi, E., Riccio, M., Sciorati, C., Nistico, G. & Meldolesi, J. (1996) The type 2 ryanodine receptor of neurosecretory PC12 cells is activated by cyclic ADP-ribose. Role of the nitric oxide/cGMP pathway. *J Biol Chem*, **271**, 17739-17745.

Cogen, J. & Cohen-Cory, S. (2000) Nitric oxide modulates retinal ganglion cell axon arbor remodeling in vivo. *J Neurobiol*, **45**, 120-133.

Cohan, C.S., Connor, J.A. & Kater, S.B. (1987) Electrically and chemically mediated increases in intracellular calcium in neuronal growth cones. *J Neurosci*, **7**, 3588-3599.

Cohan, C.S., Welnhofer, E.A., Zhao, L., Matsumura, F. & Yamashiro, S. (2001) Role of the actin bundling protein fascin in growth cone morphogenesis: localization in filopodia and lamellipodia. *Cell motility and the cytoskeleton*, **48**, 109-120.

Contestabile, A. (2000) Roles of NMDA receptor activity and nitric oxide production in brain development. *Brain Res Brain Res Rev*, **32**, 476-509.

Contestabile, A. & Ciani, E. (2004) Role of nitric oxide in the regulation of neuronal proliferation, survival and differentiation. *Neurochem Int*, **45**, 903-914.

Corvera, S. & Czech, M.P. (1998) Direct targets of phosphoinositide 3-kinase products in membrane traffic and signal transduction. *Trends in cell biology*, **8**, 442-446.

Craig, A.M., Wyborski, R.J. & Banker, G. (1995) Preferential addition of newly synthesized membrane protein at axonal growth cones. *Nature*, **375**, 592-594.

Cramer, K.S. & Sur, M. (1999) The neuronal form of nitric oxide synthase is required for pattern formation by retinal afferents in the ferret lateral geniculate nucleus. *Brain Res Dev Brain Res*, **116**, 79-86.

Craven, P.A. & DeRubertis, F.R. (1978) Restoration of the responsiveness of purified guanylate cyclase to nitrosoguanidine, nitric oxide, and related activators by heme and hemeproteins. Evidence for involvement of the paramagnetic nitrosyl-heme complex in enzyme activation. *J Biol Chem*, **253**, 8433-8443.

Currie, D.A., de Vente, J. & Moody, W.J. (2006) Developmental appearance of cyclic guanosine monophosphate (cGMP) production and nitric oxide responsiveness in embryonic mouse cortex and striatum. *Dev Dyn*, **235**, 1668-1677.

da Silva, J.S. & Dotti, C.G. (2002) Breaking the neuronal sphere: regulation of the actin cytoskeleton in neuritogenesis. *Nat Rev Neurosci*, **3**, 694-704.

Dargie, P.J., Agre, M.C. & Lee, H.C. (1990) Comparison of Ca2+ mobilizing activities of cyclic ADP-ribose and inositol trisphosphate. *Cell Regul*, **1**, 279-290.

Davenport, R.W., Dou, P., Rehder, V. & Kater, S.B. (1993) A sensory role for neuronal growth cone filopodia. *Nature*, **361**, 721-724.

Davenport, R.W. & Kater, S.B. (1992) Local increases in intracellular calcium elicit local filopodial responses in Helisoma neuronal growth cones. *Neuron*, **9**, 405-416.

Dawson, T.M., Sasaki, M., Gonzalez-Zulueta, M. & Dawson, V.L. (1998) Regulation of neuronal nitric oxide synthase and identification of novel nitric oxide signaling pathways. *Prog Brain Res*, **118**, 3-11.

De Flora, A., Guida, L., Franco, L., Zocchi, E., Pestarino, M., Usai, C., Marchetti, C., Fedele, E., Fontana, G. & Raiteri, M. (1996) Ectocellular in vitro and in vivo metabolism of cADP-ribose in cerebellum. *Biochem J*, **320 (Pt 2)**, 665-671.

Dehmelt, L. & Halpain, S. (2004) Actin and microtubules in neurite initiation: are MAPs the missing link? *J Neurobiol*, **58**, 18-33.

Dent, E.W., Barnes, A.M., Tang, F. & Kalil, K. (2004) Netrin-1 and semaphorin 3A promote or inhibit cortical axon branching, respectively, by reorganization of the cytoskeleton. *J Neurosci*, **24**, 3002-3012.

Dhand, R., Hiles, I., Panayotou, G., Roche, S., Fry, M.J., Gout, I., Totty, N.F., Truong, O., Vicendo, P., Yonezawa, K. & et al. (1994) PI 3-kinase is a dual specificity enzyme: autoregulation by an intrinsic protein-serine kinase activity. *The EMBO journal*, **13**, 522-533.

Diefenbach, T.J., Guthrie, P.B., Stier, H., Billups, B. & Kater, S.B. (1999) Membrane recycling in the neuronal growth cone revealed by FM1-43 labeling. *J Neurosci*, **19**, 9436-9444.

Ding, J.D., Burette, A. & Weinberg, R.J. (2005) Expression of soluble guanylyl cyclase in rat cerebral cortex during postnatal development. *J Comp Neurol*, **485**, 255-265.

Ditlevsen, D.K., Kohler, L.B., Pedersen, M.V., Risell, M., Kolkova, K., Meyer, M., Berezin, V. & Bock, E. (2003) The role of phosphatidylinositol 3-kinase in neural

cell adhesion molecule-mediated neuronal differentiation and survival. *J Neurochem*, **84**, 546-556.

Dmetrichuk, J.M., Carlone, R.L. & Spencer, G.E. (2006) Retinoic acid induces neurite outgrowth and growth cone turning in invertebrate neurons. *Dev Biol*, **294**, 39-49.

Dontchev, V.D. & Letourneau, P.C. (2002) Nerve growth factor and semaphorin 3A signaling pathways interact in regulating sensory neuronal growth cone motility. *J Neurosci*, **22**, 6659-6669.

Dontchev, V.D. & Letourneau, P.C. (2003) Growth cones integrate signaling from multiple guidance cues. *J Histochem Cytochem*, **51**, 435-444.

Downward, J. (1998) Mechanisms and consequences of activation of protein kinase B/Akt. *Curr Opin Cell Biol*, **10**, 262-267.

Doyle, K.P., Simon, R.P., Snyder, A. & Stenzel-Poore, M.P. (2003) Working with GFP in the brain. *Biotechniques*, **34**, 492-494.

Duronio, V., Scheid, M.P. & Ettinger, S. (1998) Downstream signalling events regulated by phosphatidylinositol 3-kinase activity. *Cell Signal*, **10**, 233-239.

Elliott, C.J. & Kleindienst, H.U. (1990) Photoinactivation of neurones in the pond snail, Lymnaea stagnalis: estimation of a safety factor. *Brain Res*, **524**, 149-152.

Elliott, C.J. & Susswein, A.J. (2002) Comparative neuroethology of feeding control in molluscs. *The Journal of experimental biology*, **205**, 877-896.

Empson, R.M. & Galione, A. (1997) Cyclic ADP-ribose enhances coupling between voltage-gated Ca2+ entry and intracellular Ca2+ release. *J Biol Chem*, **272**, 20967-20970.

Endo, M., Tanaka, M. & Ogawa, Y. (1970) Calcium induced release of calcium from the sarcoplasmic reticulum of skinned skeletal muscle fibres. *Nature*, **228**, 34-36.

Ernst, A.F., Gallo, G., Letourneau, P.C. & McLoon, S.C. (2000) Stabilization of growing retinal axons by the combined signaling of nitric oxide and brain-derived neurotrophic factor. *J Neurosci*, **20**, 1458-1469.

Ernst, A.F., Wu, H.H., El-Fakahany, E.E. & McLoon, S.C. (1999) NMDA receptor-mediated refinement of a transient retinotectal projection during development requires nitric oxide. *J Neurosci*, **19**, 229-235.

Escuin, S. & Georges-Labouesse, E. (2007) Adhesion-Induced Intracellular Mechanisms of Neurite Elongation. In de Curtis, I. (ed.) *Intracellular Mechanisms for Neuritogenesis*. Springer Science, New York, pp. 1-24.

Fain, G.L., Matthews, H.R., Cornwall, M.C. & Koutalos, Y. (2001) Adaptation in vertebrate photoreceptors. *Physiol Rev*, **81**, 117-151.

Fan, L. & Simard, L.R. (2002) Survival motor neuron (SMN) protein: role in neurite outgrowth and neuromuscular maturation during neuronal differentiation and development. *Human molecular genetics*, **11**, 1605-1614.

Finch, E.A., Turner, T.J. & Goldin, S.M. (1991) Calcium as a coagonist of inositol 1,4,5-trisphosphate-induced calcium release. *Science*, **252**, 443-446.

Flynn, K., Pak, C. & Bamburg, J.R. (2007) Regulation of Growth Cone Initiation and Actin Dynamics by ADF/Cofilin. In de Curtis, I. (ed.) *Intracellular Mechanisms for Neuritogenesis*. Springer Science, New York, pp. 25-56.

Forscher, P. & Smith, S.J. (1988) Actions of cytochalasins on the organization of actin filaments and microtubules in a neuronal growth cone. *J Cell Biol*, **107**, 1505-1516.

Franco, L., Bodrato, N., Moreschi, I., Usai, C., Bruzzone, S., Scarf i, S., Zocchi, E. & De Flora, A. (2006) Cyclic ADP-ribose is a second messenger in the lipopolysaccharide-stimulated activation of murine N9 microglial cell line. *J Neurochem*, **99**, 165-176.

Galione, A., White, A., Willmott, N., Turner, M., Potter, B.V. & Watson, S.P. (1993) cGMP mobilizes intracellular Ca2+ in sea urchin eggs by stimulating cyclic ADP-ribose synthesis. *Nature*, **365**, 456-459.

Garthwaite, J. (2005) Dynamics of cellular NO-cGMP signaling. *Front Biosci*, **10**, 1868-1880.

Garthwaite, J. & Boulton, C.L. (1995) Nitric oxide signaling in the central nervous system. *Annu Rev Physiol*, **57**, 683-706.

Garthwaite, J., Charles, S.L. & Chess-Williams, R. (1988) Endothelium-derived relaxing factor release on activation of NMDA receptors suggests role as intercellular messenger in the brain. *Nature*, **336**, 385-388.

Geddis, M.S., Tornieri, K., Giesecke, A. & Rehder, V. (2004) PLA2 and secondary metabolites of arachidonic acid control filopodial behavior in neuronal growth cones. *Cell Motil Cytoskeleton*, **57**, 53-67.

Gehler, S., Gallo, G., Veien, E. & Letourneau, P.C. (2004a) p75 neurotrophin receptor signaling regulates growth cone filopodial dynamics through modulating RhoA activity. *J Neurosci*, **24**, 4363-4372.

Gehler, S., Shaw, A.E., Sarmiere, P.D., Bamburg, J.R. & Letourneau, P.C. (2004b) Brain-derived neurotrophic factor regulation of retinal growth cone filopodial dynamics is mediated through actin depolymerizing factor/cofilin. *J Neurosci*, **24**, 10741-10749.

Gelperin, A. & Flores, J. (1997) Vital staining from dye-coated microprobes identifies new olfactory interneurons for optical and electrical recording. *J Neurosci Methods*, **72**, 97-108.

Gibbs, S.M., Becker, A., Hardy, R.W. & Truman, J.W. (2001) Soluble guanylate cyclase is required during development for visual system function in Drosophila. *J Neurosci*, **21**, 7705-7714.

Gibbs, S.M. & Truman, J.W. (1998) Nitric oxide and cyclic GMP regulate retinal patterning in the optic lobe of Drosophila. *Neuron*, **20**, 83-93.

Gibson, N.J. & Nighorn, A. (2000) Expression of nitric oxide synthase and soluble guanylyl cyclase in the developing olfactory system of Manduca sexta. *J Comp Neurol*, **422**, 191-205.

Gifondorwa, D.J. & Leise, E.M. (2006) Programmed cell death in the apical ganglion during larval metamorphosis of the marine mollusc Ilyanassa obsoleta. *Biol Bull*, **210**, 109-120.

Godfrey, E.W. & Schwarte, R.C. (2003) The role of nitric oxide signaling in the formation of the neuromuscular junction. *J Neurocytol*, **32**, 591-602.

Goldberg, J.I., Mills, L.R. & Kater, S.B. (1992) Effects of serotonin on intracellular calcium in embryonic and adult Helisoma neurons. *Int J Dev Neurosci*, **10**, 255-264.

Gomes, R.A., Hampton, C., El-Sabeawy, F., Sabo, S.L. & McAllister, A.K. (2006) The dynamic distribution of TrkB receptors before, during, and after synapse formation between cortical neurons. *J Neurosci*, **26**, 11487-11500.

Gomez, T.M., Robles, E., Poo, M. & Spitzer, N.C. (2001) Filopodial calcium transients promote substrate-dependent growth cone turning. *Science*, **291**, 1983-1987.

Gomez, T.M., Snow, D.M. & Letourneau, P.C. (1995) Characterization of spontaneous calcium transients in nerve growth cones and their effect on growth cone migration. *Neuron*, **14**, 1233-1246.

Gordon-Weeks, P.R. (1987) The cytoskeletons of isolated, neuronal growth cones. *Neuroscience*, **21**, 977-989.

Goshima, Y., Ito, T., Sasaki, Y. & Nakamura, F. (2002) Semaphorins as signals for cell repulsion and invasion. *The Journal of clinical investigation*, **109**, 993-998.

Goswami, C., Schmidt, H. & Hucho, F. (2007) TRPV1 at nerve endings regulates growth cone morphology and movement through cytoskeleton reorganization. *Febs J*, **274**, 760-772.

Greka, A., Navarro, B., Oancea, E., Duggan, A. & Clapham, D.E. (2003) TRPC5 is a regulator of hippocampal neurite length and growth cone morphology. *Nat Neurosci*, **6**, 837-845.

Grueber, W.B. & Truman, J.W. (1999) Development and organization of a nitric-oxide-sensitive peripheral neural plexus in larvae of the moth, Manduca sexta. *J Comp Neurol*, **404**, 127-141.

Gruenbaum, L.M. & Carew, T.J. (1999) Growth factor modulation of substrate-specific morphological patterns in Aplysia bag cell neurons. *Learn Mem*, **6**, 292-306.

Grynkiewicz, G., Poenie, M. & Tsien, R.Y. (1985) A new generation of Ca2+ indicators with greatly improved fluorescence properties. *J Biol Chem*, **260**, 3440-3450.

Gundersen, R.W. & Barrett, J.N. (1980) Characterization of the turning response of dorsal root neurites toward nerve growth factor. *J Cell Biol*, **87**, 546-554.

Guse, A.H. (2004) Biochemistry, biology, and pharmacology of cyclic adenosine diphosphoribose (cADPR). *Curr Med Chem*, **11**, 847-855.

Guse, A.H. (2005) Second messenger function and the structure-activity relationship of cyclic adenosine diphosphoribose (cADPR). *Febs J*, **272**, 4590-4597.

Haase, A. & Bicker, G. (2003) Nitric oxide and cyclic nucleotides are regulators of neuronal migration in an insect embryo. *Development*, **130**, 3977-3987.

Hadley, R.D., Wong, R.G., Kater, S.B., Barker, D.L. & Bulloch, A.G. (1982) Formation of novel central and peripheral connections between molluscan central neurons in organ cultured ganglia. *J Neurobiol*, **13**, 217-230.

Hagiwara, S. & Byerly, L. (1981) Calcium channel. *Annu Rev Neurosci*, **4**, 69-125.

Hall, C.N. & Garthwaite, J. (2005) Trans-Synaptic Signalling by Nitric Oxide. In Ludwig, M. (ed.) *Dendritic Neurotransmitter Release*. Springer Science, New York, pp. 283-300.

Hall, C.N. & Garthwaite, J. (2006) Inactivation of nitric oxide by rat cerebellar slices. *The Journal of physiology*, **577**, 549-567.

Hashii, M., Minabe, Y. & Higashida, H. (2000) cADP-ribose potentiates cytosolic Ca2+ elevation and Ca2+ entry via L-type voltage-activated Ca2+ channels in NG108-15 neuronal cells. *Biochem J*, **345 Pt 2**, 207-215.

Haydon, P.G. (1988) The formation of chemical synapses between cell-cultured neuronal somata. *J Neurosci*, **8**, 1032-1038.

Haydon, P.G., Cohan, C.S., McCobb, D.P., Miller, H.R. & Kater, S.B. (1985) Neuron-specific growth cone properties as seen in identified neurons of Helisoma. *J Neurosci Res*, **13**, 135-147.

Haydon, P.G., McCobb, D.P. & Kater, S.B. (1984) Serotonin selectively inhibits growth cone motility and synaptogenesis of specific identified neurons. *Science*, **226**, 561-564.

Haydon, P.G. & Zoran, M.J. (1989) Formation and modulation of chemical connections: evoked acetylcholine release from growth cones and neurites of specific identified neurons. *Neuron*, **2**, 1483-1490.

Henley, J. & Poo, M.M. (2004) Guiding neuronal growth cones using Ca2+ signals. *Trends in cell biology*, **14**, 320-330.

Hess, D.T., Matsumoto, A., Kim, S.O., Marshall, H.E. & Stamler, J.S. (2005) Protein S-nitrosylation: purview and parameters. *Nat Rev Mol Cell Biol*, **6**, 150-166.

Hess, D.T., Patterson, S.I., Smith, D.S. & Skene, J.H. (1993) Neuronal growth cone collapse and inhibition of protein fatty acylation by nitric oxide. *Nature*, **366**, 562-565.

Higashida, H., Hashii, M., Yokoyama, S., Hoshi, N., Asai, K. & Kato, T. (2001) Cyclic ADP-ribose as a potential second messenger for neuronal Ca2+ signaling. *J Neurochem*, **76**, 321-331.

Hindley, S., Juurlink, B.H., Gysbers, J.W., Middlemiss, P.J., Herman, M.A. & Rathbone, M.P. (1997) Nitric oxide donors enhance neurotrophin-induced neurite outgrowth through a cGMP-dependent mechanism. *J Neurosci Res*, **47**, 427-439.

Holt, C.E. (1989) A single-cell analysis of early retinal ganglion cell differentiation in Xenopus: from soma to axon tip. *J Neurosci*, **9**, 3123-3145.

Hong, K., Nishiyama, M., Henley, J., Tessier-Lavigne, M. & Poo, M. (2000) Calcium signalling in the guidance of nerve growth by netrin-1. *Nature*, **403**, 93-98.

Hua, S.Y., Tokimasa, T., Takasawa, S., Furuya, Y., Nohmi, M., Okamoto, H. & Kuba, K. (1994) Cyclic ADP-ribose modulates Ca2+ release channels for activation by physiological Ca2+ entry in bullfrog sympathetic neurons. *Neuron*, **12**, 1073-1079.

Huang, P.L., Dawson, T.M., Bredt, D.S., Snyder, S.H. & Fishman, M.C. (1993) Targeted disruption of the neuronal nitric oxide synthase gene. *Cell*, **75**, 1273-1286.

Huber, A.B., Kania, A., Tran, T.S., Gu, C., De Marco Garcia, N., Lieberam, I., Johnson, D., Jessell, T.M., Ginty, D.D. & Kolodkin, A.L. (2005) Distinct roles for secreted semaphorin signaling in spinal motor axon guidance. *Neuron*, **48**, 949-964.

Huber, A.B., Kolodkin, A.L., Ginty, D.D. & Cloutier, J.F. (2003) Signaling at the growth cone: ligand-receptor complexes and the control of axon growth and guidance. *Annual review of neuroscience*, **26**, 509-563.

Kaang, B.K. (1996a) Neuronal expression of reporter genes in the intact nervous system of *Aplysia*. *Molecules and Cells*, **6**, 285-295.

Kaang, B.K. (1996b) Parameters influencing ectopic gene expression in Aplysia neurons. *Neurosci Lett*, **221**, 29-32.

Kalil, K. & Dent, E.W. (2005) Touch and go: guidance cues signal to the growth cone cytoskeleton. *Curr Opin Neurobiol*, **15**, 521-526.

Kater, S.B. (1974) Feeding in *Helisoma trivolvis*: The morphological and physiological bases of a fixed action pattern. *Am Zool*, **14**, 1017-1036.

Kater, S.B. & Mills, L.R. (1991) Regulation of growth cone behavior by calcium. *J Neurosci*, **11**, 891-899.

Kater, S.B. & Rehder, V. (1995) The sensory-motor role of growth cone filopodia. *Curr.Opin.Neurobiol.*, **5**, 68-74.

Kelm, M. (1999) Nitric oxide metabolism and breakdown. *Biochim Biophys Acta*, **1411**, 273-289.

Kenwrick, S., Watkins, A. & De Angelis, E. (2000) Neural cell recognition molecule L1: relating biological complexity to human disease mutations. *Human molecular genetics*, **9**, 879-886.

Kiryushko, D., Berezin, V. & Bock, E. (2004) Regulators of neurite outgrowth: role of cell adhesion molecules. *Ann N Y Acad Sci*, **1014**, 140-154.

Kita, Y., Kimura, K.D., Kobayashi, M., Ihara, S., Kaibuchi, K., Kuroda, S., Ui, M., Iba, H., Konishi, H., Kikkawa, U., Nagata, S. & Fukui, Y. (1998) Microinjection of activated phosphatidylinositol-3 kinase induces process outgrowth in rat PC12 cells through the Rac-JNK signal transduction pathway. *J Cell Sci*, **111 (Pt 7)**, 907-915.

Knobel, K.M., Jorgensen, E.M. & Bastiani, M.J. (1999) Growth cones stall and collapse during axon outgrowth in Caenorhabditis elegans. *Development*, **126**, 4489-4498.

Kobayashi, S., Sadamoto, H., Ogawa, H., Kitamura, Y., Oka, K., Tanishita, K. & Ito, E. (2000) Nitric oxide generation around buccal ganglia accompanying feeding behavior in the pond snail, Lymnaea stagnalis. *Neuroscience research*, **38**, 27-34.

Koesling, D., Russwurm, M., Mergia, E., Mullershausen, F. & Friebe, A. (2004) Nitric oxide-sensitive guanylyl cyclase: structure and regulation. *Neurochem Int*, **45**, 813-819.

Koshiyama, H., Lee, H.C. & Tashjian, A.H., Jr. (1991) Novel mechanism of intracellular calcium release in pituitary cells. *J Biol Chem*, **266**, 16985-16988.

Kranenburg, O., Poland, M., Gebbink, M., Oomen, L. & Moolenaar, W.H. (1997) Dissociation of LPA-induced cytoskeletal contraction from stress fiber formation by differential localization of RhoA. *J Cell Sci*, **110 (Pt 19)**, 2417-2427.

Krasilnikov, M.A. (2000) Phosphatidylinositol-3 kinase dependent pathways: the role in control of cell growth, survival, and malignant transformation. *Biochemistry (Mosc)*, **65**, 59-67.

Kruk, P.J. & Bulloch, A.G. (1992) Axonal regeneration of an identified Helisoma neuron depends on the site of axotomy. *J Neurosci Res*, **31**, 401-412.

Kuhn, T.B., Brown, M.D., Wilcox, C.L., Raper, J.A. & Bamburg, J.R. (1999) Myelin and collapsin-1 induce motor neuron growth cone collapse through different pathways: inhibition of collapse by opposing mutants of rac1. *J Neurosci*, **19**, 1965-1975.

Kuhn, T.B., Williams, C.V., Dou, P. & Kater, S.B. (1998) Laminin directs growth cone navigation via two temporally and functionally distinct calcium signals. *J Neurosci*, **18**, 184-194.

Lankford, K.L. & Letourneau, P.C. (1989) Evidence that calcium may control neurite outgrowth by regulating the stability of actin filaments. *J Cell Biol*, **109**, 1229-1243.

Lansman, J.B. (1990) Blockade of current through single calcium channels by trivalent lanthanide cations. Effect of ionic radius on the rates of ion entry and exit. *J Gen Physiol*, **95**, 679-696.

Lardans, V., Boulo, V., Duclermortier, P., Serra, E., Mialhe, E., Capron, A. & Dissous, C. (1996) DNA transfer in a Biomphalaria glabrata embryonic cell line by DOTAP lipofection. *Parasitol Res*, **82**, 574-576.

Leamey, C.A., Ho-Pao, C.L. & Sur, M. (2001) Disruption of retinogeniculate pattern formation by inhibition of soluble guanylyl cyclase. *J Neurosci*, **21**, 3871-3880.

Lebrand, C., Dent, E.W., Strasser, G.A., Lanier, L.M., Krause, M., Svitkina, T.M., Borisy, G.G. & Gertler, F.B. (2004) Critical role of Ena/VASP proteins for filopodia formation in neurons and in function downstream of netrin-1. *Neuron*, **42**, 37-49.

Lee, H., Engel, U., Rusch, J., Scherrer, S., Sheard, K. & Van Vactor, D. (2004) The microtubule plus end tracking protein Orbit/MAST/CLASP acts downstream of the tyrosine kinase Abl in mediating axon guidance. *Neuron*, **42**, 913-926.

Lee, H.C. (2001) Physiological functions of cyclic ADP-ribose and NAADP as calcium messengers. *Annual review of pharmacology and toxicology*, **41**, 317-345.

Lee, H.C., Walseth, T.F., Bratt, G.T., Hayes, R.N. & Clapper, D.L. (1989) Structural determination of a cyclic metabolite of NAD+ with intracellular Ca2+-mobilizing activity. *J Biol Chem*, **264**, 1608-1615.

Li, H., Wallerath, T. & Forstermann, U. (2002) Physiological mechanisms regulating the expression of endothelial-type NO synthase. *Nitric Oxide*, **7**, 132-147.

Li, Y., Jia, Y.C., Cui, K., Li, N., Zheng, Z.Y., Wang, Y.Z. & Yuan, X.B. (2005) Essential role of TRPC channels in the guidance of nerve growth cones by brain-derived neurotrophic factor. *Nature*, **434**, 894-898.

Linden, D.J., Dawson, T.M. & Dawson, V.L. (1995) An evaluation of the nitric oxide/cGMP/cGMP-dependent protein kinase cascade in the induction of cerebellar long-term depression in culture. *J Neurosci*, **15**, 5098-5105.

Lopez-Ilasaca, M., Crespo, P., Pellici, P.G., Gutkind, J.S. & Wetzker, R. (1997) Linkage of G protein-coupled receptors to the MAPK signaling pathway through PI 3-kinase gamma. *Science*, **275**, 394-397.

Lu, M., Witke, W., Kwiatkowski, D.J. & Kosik, K.S. (1997) Delayed retraction of filopodia in gelsolin null mice. *J Cell Biol*, **138**, 1279-1287.

Luo, Y., Raible, D. & Raper, J.A. (1993) Collapsin: a protein in brain that induces the collapse and paralysis of neuronal growth cones. *Cell*, **75**, 217-227.

Lytton, J., Westlin, M. & Hanley, M.R. (1991) Thapsigargin inhibits the sarcoplasmic or endoplasmic reticulum Ca-ATPase family of calcium pumps. *J Biol Chem*, **266**, 17067-17071.

Maness, P.F. & Schachner, M. (2007) Neural recognition molecules of the immunoglobulin superfamily: signaling transducers of axon guidance and neuronal migration. *Nat Neurosci*, **10**, 19-26.

Marchenko, S.M. & Thomas, R.C. (2006) Nuclear Ca2+ signalling in cerebellar Purkinje neurons. *Cerebellum (London, England)*, **5**, 36-42.

Marsh, L. & Letourneau, P.C. (1984) Growth of neurites without filopodial or lamellipodial activity in the presence of cytochalasin B. *J Cell Biol*, **99**, 2041-2047.

Mashimo, H. & Goyal, R.K. (1999) Lessons from genetically engineered animal models. IV. Nitric oxide synthase gene knockout mice. *Am J Physiol*, **277**, G745-750.

Matarredona, E.R., Murillo-Carretero, M., Moreno-Lopez, B. & Estrada, C. (2005) Role of nitric oxide in subventricular zone neurogenesis. *Brain research*, **49**, 355-366.

Mattson, M.P. & Kater, S.B. (1987) Calcium regulation of neurite elongation and growth cone motility. *J Neurosci*, **7**, 4034-4043.

McCaig, C.D. (1989) Nerve growth in the absence of growth cone filopodia and the effects of a small applied electric field. *J Cell Sci*, **93 (Pt 4)**, 715-721.

McCobb, D.P., Haydon, P.G. & Kater, S.B. (1988) Dopamine and serotonin inhibition of neurite elongation of different identified neurons. *J Neurosci Res*, **19**, 19-26.

Medeiros, N.A., Burnette, D.T. & Forscher, P. (2006) Myosin II functions in actin-bundle turnover in neuronal growth cones. *Nat Cell Biol*, **8**, 215-226.

Meier, R. & Hemmings, B.A. (1999) Regulation of protein kinase B. *Journal of receptor and signal transduction research*, **19**, 121-128.

Mejia-Garcia, T.A. & Paes-de-Carvalho, R. (2007) Nitric oxide regulates cell survival in purified cultures of avian retinal neurons: involvement of multiple transduction pathways. *J Neurochem*, **100**, 382-394.

Menager, C., Arimura, N., Fukata, Y. & Kaibuchi, K. (2004) PIP3 is involved in neuronal polarization and axon formation. *J Neurochem*, **89**, 109-118.

Miller, J.D. & Hadley, R.D. (1991) Laminin-like immunoreactivity in the snail Helisoma: involvement of approximately 300 kD extracellular matrix protein in promoting outgrowth from identified neurons. *J Neurobiol*, **22**, 431-442.

Ming, G.L., Song, H.J., Berninger, B., Holt, C.E., Tessier-Lavigne, M. & Poo, M.M. (1997) cAMP-dependent growth cone guidance by netrin-1. *Neuron*, **19**, 1225-1235.

Minke, B. (2006) TRP channels and Ca2+ signaling. *Cell Calcium*, **40**, 261-275.

Mize, R.R. & Lo, F. (2000) Nitric oxide, impulse activity, and neurotrophins in visual system development(1). *Brain Res*, **886**, 15-32.

Mizuhashi, S., Nishiyama, N., Matsuki, N. & Ikegaya, Y. (2001) Cyclic nucleotide-mediated regulation of hippocampal mossy fiber development: a target-specific guidance. *J Neurosci*, **21**, 6181-6194.

Moncada, S. & Higgs, A. (1993) The L-arginine-nitric oxide pathway. *The New England journal of medicine*, **329**, 2002-2012.

Morita, K., Kitayama, T., Kitayama, S. & Dohi, T. (2006) Cyclic ADP-ribose requires FK506-binding protein to regulate intracellular Ca2+ dynamics and catecholamine release in acetylcholine-stimulated bovine adrenal chromaffin cells. *Journal of pharmacological sciences*, **101**, 40-51.

Moroz, L.L., Radbourne, S. & Winlow, W. (1995) The use of NO-sensitive microelectrodes for direct detection of nitric oxide (NO) production in molluscs. *Acta biologica Hungarica*, **46**, 155-167.

Mothet, J.P., Fossier, P., Meunier, F.M., Stinnakre, J., Tauc, L. & Baux, G. (1998) Cyclic ADP-ribose and calcium-induced calcium release regulate neurotransmitter release at a cholinergic synapse of Aplysia. *The Journal of physiology*, **507 (Pt 2)**, 405-414.

Mungrue, I.N., Bredt, D.S., Stewart, D.J. & Husain, M. (2003) From molecules to mammals: what's NOS got to do with it? *Acta physiologica Scandinavica*, **179**, 123-135.

Murphy, A.D. & Kater, S.B. (1978) Specific reinnervation of a target organ by a pair of identified molluscan neurons. *Brain Res*, **156**, 322-328.

Murphy, A.D. & Kater, S.B. (1980a) Differential discrimination of appropriate pathways by regenerating identified neurons in Helisoma. *J Comp Neurol*, **190**, 395-403.

Murphy, A.D. & Kater, S.B. (1980b) Sprouting and functional regeneration of an identified neuron in Helisoma. *Brain Res*, **186**, 251-272.

Neely, M.D. (1993) Role of substrate and calcium in neurite retraction of leech neurons following depolarization. *J Neurosci*, **13**, 1292-1301.

Nikonenko, I., Jourdain, P. & Muller, D. (2003) Presynaptic remodeling contributes to activity-dependent synaptogenesis. *J Neurosci*, **23**, 8498-8505.

Nishiyama, M., Hoshino, A., Tsai, L., Henley, J.R., Goshima, Y., Tessier-Lavigne, M., Poo, M.M. & Hong, K. (2003) Cyclic AMP/GMP-dependent modulation of Ca2+ channels sets the polarity of nerve growth-cone turning. *Nature*, **423**, 990-995.

Noguchi, N., Takasawa, S., Nata, K., Tohgo, A., Kato, I., Ikehata, F., Yonekura, H. & Okamoto, H. (1997) Cyclic ADP-ribose binds to FK506-binding protein 12.6 to release Ca2+ from islet microsomes. *J Biol Chem*, **272**, 3133-3136.

Ohbayashi, K., Fukura, H., Inoue, H.K., Komiya, Y. & Igarashi, M. (1998) Stimulation of L-type Ca2+ channel in growth cones activates two independent signaling pathways. *J Neurosci Res*, **51**, 682-696.

Ooashi, N., Futatsugi, A., Yoshihara, F., Mikoshiba, K. & Kamiguchi, H. (2005) Cell adhesion molecules regulate Ca2+-mediated steering of growth cones via cyclic AMP and ryanodine receptor type 3. *The Journal of cell biology*, **170**, 1159-1167.

Packer, M.A., Stasiv, Y., Benraiss, A., Chmielnicki, E., Grinberg, A., Westphal, H., Goldman, S.A. & Enikolopov, G. (2003) Nitric oxide negatively regulates mammalian adult neurogenesis. *Proc Natl Acad Sci U S A*, **100**, 9566-9571.

Patel, B.A., Arundell, M., Parker, K.H., Yeoman, M.S. & O'Hare, D. (2006) Detection of nitric oxide release from single neurons in the pond snail, Lymnaea stagnalis. *Analytical chemistry*, **78**, 7643-7648.

Peunova, N. & Enikolopov, G. (1995) Nitric oxide triggers a switch to growth arrest during differentiation of neuronal cells. *Nature*, **375**, 68-73.

Philippides, A., Husbands, P. & O'Shea, M. (2000) Four-dimensional neuronal signaling by nitric oxide: a computational analysis. *J Neurosci*, **20**, 1199-1207.

Phung, Y.T., Bekker, J.M., Hallmark, O.G. & Black, S.M. (1999) Both neuronal NO synthase and nitric oxide are required for PC12 cell differentiation: a cGMP independent pathway. *Brain Res Mol Brain Res*, **64**, 165-178.

Piiper, A., Dikic, I., Lutz, M.P., Leser, J., Kronenberger, B., Elez, R., Cramer, H., Muller-Esterl, W. & Zeuzem, S. (2002) Cyclic AMP induces transactivation of the receptors for epidermal growth factor and nerve growth factor, thereby modulating activation of MAP kinase, Akt, and neurite outgrowth in PC12 cells. *J Biol Chem*, **277**, 43623-43630.

Polleux, F., Morrow, T. & Ghosh, A. (2000) Semaphorin 3A is a chemoattractant for cortical apical dendrites. *Nature*, **404**, 567-573.

Posern, G., Saffrich, R., Ansorge, W. & Feller, S.M. (2000) Rapid lamellipodia formation in nerve growth factor-stimulated PC12 cells is dependent on Rac and PI3K activity. *Journal of cellular physiology*, **183**, 416-424.

Pyriochou, A. & Papapetropoulos, A. (2005) Soluble guanylyl cyclase: more secrets revealed. *Cell Signal*, **17**, 407-413.

Quinn, K.E., Castellani, L., Ondrias, K. & Ehrlich, B.E. (1998) Characterization of the ryanodine receptor/channel of invertebrate muscle. *Am J Physiol*, **274**, R494-502.

Raffioni, S. & Bradshaw, R.A. (1992) Activation of phosphatidylinositol 3-kinase by epidermal growth factor, basic fibroblast growth factor, and nerve growth factor in PC12 pheochromocytoma cells. *Proc Natl Acad Sci U S A*, **89**, 9121-9125.

Ramón y Cajal, S. (1999) *Texture of the nervous system of man and the vertebrates*. (P. Pasik & T. Pasik Trans.). Springer, Wien; New York.

Ramsey, I.S., Delling, M. & Clapham, D.E. (2006) An introduction to TRP channels. *Annu Rev Physiol*, **68**, 619-647.

Rees, R.P., Bunge, M.B. & Bunge, R.P. (1976) Morphological changes in the neuritic growth cone and target neuron during synaptic junction development in culture. *J Cell Biol*, **68**, 240-263.

Regulski, M., Stasiv, Y., Tully, T. & Enikolopov, G. (2004) Essential function of nitric oxide synthase in Drosophila. *Curr Biol*, **14**, R881-882.

Rehder, V. & Cheng, S. (1998) Autonomous regulation of growth cone filopodia. *J Neurobiol*, **34**, 179-192.

Rehder, V., Jensen, J.R. & Kater, S.B. (1992) The initial stages of neural regeneration are dependent upon intracellular calcium levels. *Neuroscience*, **51**, 565-574.

Rehder, V. & Kater, S.B. (1992) Regulation of neuronal growth cone filopodia by intracellular calcium. *J Neurosci*, **12**, 3175-3186.

Renteria, R.C. & Constantine-Paton, M. (1996) Exogenous nitric oxide causes collapse of retinal ganglion cell axonal growth cones in vitro. *J Neurobiol*, **29**, 415-428.

Reyes-Harde, M., Empson, R., Potter, B.V., Galione, A. & Stanton, P.K. (1999a) Evidence of a role for cyclic ADP-ribose in long-term synaptic depression in hippocampus. *Proc Natl Acad Sci U S A*, **96**, 4061-4066.

Reyes-Harde, M., Potter, B.V., Galione, A. & Stanton, P.K. (1999b) Induction of hippocampal LTD requires nitric-oxide-stimulated PKG activity and Ca2+ release from cyclic ADP-ribose-sensitive stores. *J Neurophysiol*, **82**, 1569-1576.

Rialas, C.M., Nomizu, M., Patterson, M., Kleinman, H.K., Weston, C.A. & Weeks, B.S. (2000) Nitric oxide mediates laminin-induced neurite outgrowth in PC12 cells. *Exp Cell Res*, **260**, 268-276.

Ridgway, R.L., Syed, N.I., Lukowiak, K. & Bulloch, A.G. (1991) Nerve growth factor (NGF) induces sprouting of specific neurons of the snail, Lymnaea stagnalis. *J Neurobiol*, **22**, 377-390.

Rizzuto, R., Bernardi, P. & Pozzan, T. (2000) Mitochondria as all-round players of the calcium game. *The Journal of physiology*, **529 Pt 1**, 37-47.

Robles, E., Huttenlocher, A. & Gomez, T.M. (2003) Filopodial calcium transients regulate growth cone motility and guidance through local activation of calpain. *Neuron*, **38**, 597-609.

Rodgers, E.E. & Theibert, A.B. (2002) Functions of PI 3-kinase in development of the nervous system. *Int J Dev Neurosci*, **20**, 187-197.

Roy, B. & Garthwaite, J. (2006) Nitric oxide activation of guanylyl cyclase in cells revisited. *Proc Natl Acad Sci U S A*, **103**, 12185-12190.

Sabo, S.L. & McAllister, A.K. (2003) Mobility and cycling of synaptic protein-containing vesicles in axonal growth cone filopodia. *Nat Neurosci*, **6**, 1264-1269.

Sanes, D.H., Reh, T.A. & Harris, W.A. (2000) Axon Growth and Guidance. *Development of the Nervous System*. Academic Press, San Diego, pp. 145-202.

Santacana, M., Uttenthal, L.O., Bentura, M.L., Fernandez, A.P., Serrano, J., Martinez de Velasco, J., Alonso, D., Martinez-Murillo, R. & Rodrigo, J. (1998) Expression of neuronal nitric oxide synthase during embryonic development of the rat cerebral cortex. *Brain Res Dev Brain Res*, **111**, 205-222.

Sarmiere, P.D. & Bamburg, J.R. (2004) Regulation of the neuronal actin cytoskeleton by ADF/cofilin. *J Neurobiol*, **58**, 103-117.

Sattelle, D.B. & Buckingham, S.D. (2006) Invertebrate studies and their ongoing contributions to neuroscience. *Invert Neurosci*, **6**, 1-3.

Sebok, A., Nusser, N., Debreceni, B., Guo, Z., Santos, M.F., Szeberenyi, J. & Tigyi, G. (1999) Different roles for RhoA during neurite initiation, elongation, and regeneration in PC12 cells. *J Neurochem*, **73**, 949-960.

Seidel, C. & Bicker, G. (2000) Nitric oxide and cGMP influence axonogenesis of antennal pioneer neurons. *Development*, **127**, 4541-4549.

Sethi, J.K., Empson, R.M. & Galione, A. (1996) Nicotinamide inhibits cyclic ADP-ribose-mediated calcium signalling in sea urchin eggs. *Biochem J*, **319 (Pt 2)**, 613-617.

Shi, S.H., Jan, L.Y. & Jan, Y.N. (2003) Hippocampal neuronal polarity specified by spatially localized mPar3/mPar6 and PI 3-kinase activity. *Cell*, **112**, 63-75.

Shim, S., Goh, E.L., Ge, S., Sailor, K., Yuan, J.P., Roderick, H.L., Bootman, M.D., Worley, P.F., Song, H. & Ming, G.L. (2005) XTRPC1-dependent chemotropic guidance of neuronal growth cones. *Nature neuroscience*, **8**, 730-735.

Soltoff, S.P., Carpenter, C.L., Auger, K.R., Kapeller, R., Schaffhausen, B. & Cantley, L.C. (1992a) Phosphatidylinositol-3 kinase and growth regulation. *Cold Spring Harbor symposia on quantitative biology*, **57**, 75-80.

Soltoff, S.P., Rabin, S.L., Cantley, L.C. & Kaplan, D.R. (1992b) Nerve growth factor promotes the activation of phosphatidylinositol 3-kinase and its association with the trk tyrosine kinase. *J Biol Chem*, **267**, 17472-17477.

Song, H., Ming, G., He, Z., Lehmann, M., McKerracher, L., Tessier-Lavigne, M. & Poo, M. (1998) Conversion of neuronal growth cone responses from repulsion to attraction by cyclic nucleotides. *Science*, **281**, 1515-1518.

Stamler, J.S., Simon, D.I., Osborne, J.A., Mullins, M.E., Jaraki, O., Michel, T., Singel, D.J. & Loscalzo, J. (1992) S-nitrosylation of proteins with nitric oxide: synthesis and characterization of biologically active compounds. *Proceedings of the National Academy of Sciences of the United States of America*, **89**, 444-448.

Stephens, L., Smrcka, A., Cooke, F.T., Jackson, T.R., Sternweis, P.C. & Hawkins, P.T. (1994) A novel phosphoinositide 3 kinase activity in myeloid-derived cells is activated by G protein beta gamma subunits. *Cell*, **77**, 83-93.

Stoyanov, B., Volinia, S., Hanck, T., Rubio, I., Loubtchenkov, M., Malek, D., Stoyanova, S., Vanhaesebroeck, B., Dhand, R., Nurnberg, B. & et al. (1995) Cloning and characterization of a G protein-activated human phosphoinositide-3 kinase. *Science*, **269**, 690-693.

Sung, Y.J., Walters, E.T. & Ambron, R.T. (2004) A neuronal isoform of protein kinase G couples mitogen-activated protein kinase nuclear import to axotomy-induced long-term hyperexcitability in Aplysia sensory neurons. *J Neurosci*, **24**, 7583-7595.

Sunico, C.R., Portillo, F., Gonzalez-Forero, D. & Moreno-Lopez, B. (2005) Nitric oxide-directed synaptic remodeling in the adult mammal CNS. *J Neurosci*, **25**, 1448-1458.

Suter, D.M. & Forscher, P. (2000) Substrate-cytoskeletal coupling as a mechanism for the regulation of growth cone motility and guidance. *J Neurobiol*, **44**, 97-113.

Taghert, P.H., Bastiani, M.J., Ho, R.K. & Goodman, C.S. (1982) Guidance of pioneer growth cones: filopodial contacts and coupling revealed with an antibody to Lucifer Yellow. *Dev Biol*, **94**, 391-399.

Tanaka, M., Yoshida, S., Yano, M. & Hanaoka, F. (1994) Roles of endogenous nitric oxide in cerebellar cortical development in slice cultures. *Neuroreport*, **5**, 2049-2052.

Tang, F., Dent, E.W. & Kalil, K. (2003) Spontaneous calcium transients in developing cortical neurons regulate axon outgrowth. *J Neurosci*, **23**, 927-936.

Temple, S. (2001) The development of neural stem cells. *Nature*, **414**, 112-117.

Thastrup, O., Cullen, P.J., Drobak, B.K., Hanley, M.R. & Dawson, A.P. (1990) Thapsigargin, a tumor promoter, discharges intracellular Ca2+ stores by specific inhibition of the endoplasmic reticulum Ca2(+)-ATPase. *Proc Natl Acad Sci U S A*, **87**, 2466-2470.

Thomas, J.M., Masgrau, R., Churchill, G.C. & Galione, A. (2001) Pharmacological characterization of the putative cADP-ribose receptor. *Biochem J*, **359**, 451-457.

Thorn, P., Gerasimenko, O. & Petersen, O.H. (1994) Cyclic ADP-ribose regulation of ryanodine receptors involved in agonist evoked cytosolic Ca2+ oscillations in pancreatic acinar cells. *The EMBO journal*, **13**, 2038-2043.

Threadgill, R., Bobb, K. & Ghosh, A. (1997) Regulation of dendritic growth and remodeling by Rho, Rac, and Cdc42. *Neuron*, **19**, 625-634.

Tornieri, K., Welshhans, K., Geddis, M.S. & Rehder, V. (2006) Control of neurite outgrowth and growth cone motility by phosphatidylinositol-3-kinase. *Cell Motil Cytoskeleton*, **63**, 173-192.

Tosney, K.W. & Landmesser, L.T. (1985) Growth cone morphology and trajectory in the lumbosacral region of the chick embryo. *J Neurosci*, **5**, 2345-2358.

Tranguch, S. & Huet-Hudson, Y. (2003) Decreased viability of nitric oxide synthase double knockout mice. *Mol Reprod Dev*, **65**, 175-179.

Trimm, K.R. & Rehder, V. (2004) Nitric oxide acts as a slow-down and search signal in developing neurites. *Eur J Neurosci*, **19**, 809-818.

Truman, J.W., De Vente, J. & Ball, E.E. (1996) Nitric oxide-sensitive guanylate cyclase activity is associated with the maturational phase of neuronal development in insects. *Development*, **122**, 3949-3958.

Tsukada, S., Keino-Masu, K., Masu, M. & Fukuda, J. (2002) Activation of protein kinase A by nitric oxide in cultured dorsal root ganglion neurites of the rat, examined by a fluorescence probe, ARII. *Neurosci Lett*, **318**, 17-20.

Tunwell, R.E., Wickenden, C., Bertrand, B.M., Shevchenko, V.I., Walsh, M.B., Allen, P.D. & Lai, F.A. (1996) The human cardiac muscle ryanodine receptor-calcium release channel: identification, primary structure and topological analysis. *Biochem J*, **318 (Pt 2)**, 477-487.

Turner, L.J., Nicholls, S. & Hall, A. (2004) The activity of the plexin-A1 receptor is regulated by Rac. *J Biol Chem*, **279**, 33199-33205.

Van Wagenen, S., Cheng, S. & Rehder, V. (1999) Stimulation-induced changes in filopodial dynamics determine the action radius of growth cones in the snail Helisoma trivolvis. *Cell Motil and Cytoskeleton*, **44**, 248-262.

Van Wagenen, S. & Rehder, V. (1999) Regulation of neuronal growth cone filopodia by nitric oxide. *J Neurobiol*, **39**, 168-185.

Van Wagenen, S. & Rehder, V. (2001) Regulation of neuronal growth cone filopodia by nitric oxide depends on soluble guanylyl cyclase. *J Neurobiol*, **46**, 206-219.

VanBerkum, M.F. & Goodman, C.S. (1995) Targeted disruption of Ca(2+)-calmodulin signaling in Drosophila growth cones leads to stalls in axon extension and errors in axon guidance. *Neuron*, **14**, 43-56.

Vanhaesebroeck, B. & Alessi, D.R. (2000) The PI3K-PDK1 connection: more than just a road to PKB. *Biochem J*, **346 Pt 3**, 561-576.

Vanhaesebroeck, B. & Waterfield, M.D. (1999) Signaling by distinct classes of phosphoinositide 3-kinases. *Exp Cell Res*, **253**, 239-254.

Vastrik, I., Eickholt, B.J., Walsh, F.S., Ridley, A. & Doherty, P. (1999) Sema3A-induced growth-cone collapse is mediated by Rac1 amino acids 17-32. *Curr Biol*, **9**, 991-998.

Vazquez-Martinez, O., Canedo-Merino, R., Diaz-Munoz, M. & Riesgo-Escovar, J.R. (2003) Biochemical characterization, distribution and phylogenetic analysis of Drosophila melanogaster ryanodine and IP3 receptors, and thapsigargin-sensitive Ca2+ ATPase. *J Cell Sci*, **116**, 2483-2494.

Verkhratsky, A. (2005) Physiology and pathophysiology of the calcium store in the endoplasmic reticulum of neurons. *Physiol Rev*, **85**, 201-279.

Verkhratsky, A. & Shmigol, A. (1996) Calcium-induced calcium release in neurones. *Cell Calcium*, **19**, 1-14.

Villalobo, A. (2006) Nitric oxide and cell proliferation. *Febs J*, **273**, 2329-2344.

Villani, L. (1999) Development of NADPH-diaphorase activity in the central nervous system of the cichlid fish, Tilapia mariae. *Brain Behav Evol*, **54**, 147-158.

Virdee, K., Xue, L., Hemmings, B.A., Goemans, C., Heumann, R. & Tolkovsky, A.M. (1999) Nerve growth factor-induced PKB/Akt activity is sustained by phosphoinositide 3-kinase dependent and independent signals in sympathetic neurons. *Brain Res*, **837**, 127-142.

Walseth, T.F. & Lee, H.C. (1993) Synthesis and characterization of antagonists of cyclic-ADP-ribose-induced Ca2+ release. *Biochim Biophys Acta*, **1178**, 235-242.

Wang, G.X. & Poo, M.M. (2005) Requirement of TRPC channels in netrin-1-induced chemotropic turning of nerve growth cones. *Nature*, **434**, 898-904.

Wang, S., Teschemacher, A.G., Paton, J.F. & Kasparov, S. (2006) Mechanism of nitric oxide action on inhibitory GABAergic signaling within the nucleus tractus solitarii. *Faseb J*, **20**, 1537-1539.

Weiss, G.B. (1974) Cellular Pharmacology of Lanthanum. *Annu Rev Pharmacol*, **14**, 343-354.

Welnhofer, E.A., Zhao, L. & Cohan, C.S. (1999) Calcium influx alters actin bundle dynamics and retrograde flow in Helisoma growth cones. *J Neurosci*, **19**, 7971-7982.

Welshhans, K. & Rehder, V. (2005) Local activation of the nitric oxide/cyclic guanosine monophosphate pathway in growth cones regulates filopodial length via protein kinase G, cyclic ADP ribose and intracellular Ca2+ release. *Eur J Neurosci*, **22**, 3006-3016.

Wen, Z., Guirland, C., Ming, G.L. & Zheng, J.Q. (2004) A CaMKII/calcineurin switch controls the direction of Ca(2+)-dependent growth cone guidance. *Neuron*, **43**, 835-846.

Wen, Z. & Zheng, J.Q. (2006) Directional guidance of nerve growth cones. *Curr Opin Neurobiol*, **16**, 52-58.

Williams, C.V., Nordquist, D. & McLoon, S.C. (1994) Correlation of nitric oxide synthase expression with changing patterns of axonal projections in the developing visual system. *J Neurosci*, **14**, 1746-1755.

Williams, D.K. & Cohan, C.S. (1994) The role of conditioning factors in the formation of growth cones and neurites from the axon stump after axotomy. *Brain Res Dev Brain Res*, **81**, 89-104.

Williams, D.K. & Cohan, C.S. (1995) Calcium transients in growth cones and axons of cultured Helisoma neurons in response to conditioning factors. *J Neurobiol*, **27**, 60-75.

Willmott, N., Sethi, J.K., Walseth, T.F., Lee, H.C., White, A.M. & Galione, A. (1996a) Nitric oxide-induced mobilization of intracellular calcium via the cyclic ADP-ribose signaling pathway. *J Biol Chem*, **271**, 3699-3705.

Willmott, N.J., Asselin, J. & Galione, A. (1996b) Calcium store depletion potentiates a phosphodiesterase inhibitor- and dibutyryl cGMP-evoked calcium influx in rat pituitary GH3 cells. *FEBS Lett*, **386**, 39-42.

Wong, E.V., Kerner, J.A. & Jay, D.G. (2004) Convergent and divergent signaling mechanisms of growth cone collapse by ephrinA5 and slit2. *J Neurobiol*, **59**, 66-81.

Wong, R.G., Barker, D.L., Kater, S.B. & Bodnar, D.A. (1984) Nerve growth-promoting factor produced in culture media conditioned by specific CNS tissues of the snail Helisoma. *Brain Res*, **292**, 81-91.

Wong, R.G., Hadley, R.D., Kater, S.B. & Hauser, G.C. (1981) Neurite outgrowth in molluscan organ and cell cultures: the role of conditioning factor(s). *J Neurosci*, **1**, 1008-1021.

Woo, S. & Gomez, T.M. (2006) Rac1 and RhoA promote neurite outgrowth through formation and stabilization of growth cone point contacts. *J Neurosci*, **26**, 1418-1428.

Wood, J. & Garthwaite, J. (1994) Models of the diffusional spread of nitric oxide: implications for neural nitric oxide signalling and its pharmacological properties. *Neuropharmacology*, **33**, 1235-1244.

Wu, H.H., Selski, D.J., El-Fakahany, E.E. & McLoon, S.C. (2001) The role of nitric oxide in development of topographic precision in the retinotectal projection of chick. *J Neurosci*, **21**, 4318-4325.

Wu, H.H., Williams, C.V. & McLoon, S.C. (1994) Involvement of nitric oxide in the elimination of a transient retinotectal projection in development. *Science*, **265**, 1593-1596.

Wymann, M.P. & Pirola, L. (1998) Structure and function of phosphoinositide 3-kinases. *Biochim Biophys Acta*, **1436**, 127-150.

Xu, L., Tripathy, A., Pasek, D.A. & Meissner, G. (1998) Potential for pharmacology of ryanodine receptor/calcium release channels. *Ann N Y Acad Sci*, **853**, 130-148.

Yamazaki, M., Chiba, K., Mohri, T. & Hatanaka, H. (2001) Activation of the mitogen-activated protein kinase cascade through nitric oxide synthesis as a mechanism of neuritogenic effect of genipin in PC12h cells. *J Neurochem*, **79**, 45-54.

Yamazaki, M., Chiba, K., Mohri, T. & Hatanaka, H. (2004) Cyclic GMP-dependent neurite outgrowth by genipin and nerve growth factor in PC12h cells. *Eur J Pharmacol*, **488**, 35-43.

Zhang, N., Beuve, A. & Townes-Anderson, E. (2005) The nitric oxide-cGMP signaling pathway differentially regulates presynaptic structural plasticity in cone and rod cells. *J Neurosci*, **25**, 2761-2770.

Zhang, Y., Zhang, J. & Zhao, B. (2004) Nitric oxide synthase inhibition prevents neuronal death in the developing visual cortex. *Eur J Neurosci*, **20**, 2251-2259.

Zheng, J.Q., Wan, J.J. & Poo, M.M. (1996) Essential role of filopodia in chemotropic turning of nerve growth cone induced by a glutamate gradient. *J Neurosci*, **16**, 1140-1149.

Zhou, F.Q. & Cohan, C.S. (2001) Growth cone collapse through coincident loss of actin bundles and leading edge actin without actin depolymerization. *J Cell Biol*, **153**, 1071-1084.

Zhou, F.Q., Waterman-Storer, C.M. & Cohan, C.S. (2002) Focal loss of actin bundles causes microtubule redistribution and growth cone turning. *J Cell Biol*, **157**, 839-849.

Zoran, M.J., Haydon, P.G. & Matthews, P.J. (1989) Aminergic and peptidergic modulation of motor function at an identified neuromuscular junction in Helisoma. *The Journal of experimental biology*, **142**, 225-243.